GLASILO SLOVENSKIH TEKSTILCEV • SLOVENE JOURNAL FOR TEXTILE AND CLOTHING TECHNOLOGY, DESIGN AND MARKETING

tekstilec

2/2018 • vol. 61 • 73–148
ISSN 0351-3386 (tiskano / printed)
ISSN 2350 - 3696 (elektronsko / online)
UDK 677 + 687 (05)

http://www.tekstilec.si

tekstilec (ISSN: 0351-3386 tiskano, 2350-3696 elektronsko) je znanstvena revija, ki podaja temeljne in aplikativne znanstvene informacije v fizikalni, kemijski in tehnološki znanosti, vezani na tekstilno tehnologijo. V prilogah znanstvenih reviji so v slovenskem jeziku objavljeni strokovni članki in prispevki o novostih v tekstilni tehnologiji iz Slovenije in sveta, prispevki s področja oblikovanja tekstilij in oblačil, informacije o raziskovalnih projektih ip**d.**

tekstilec *(ISSN: 0351-3386 printed, 2350-3696 online) the scientific journal gives fundamental and applied scientic information in the physical, chemical and engineering sciences related to the textile industry. In the appendices written in Slovene language, are published technical and short articles about the textile-technology novelties from Slovenia and the world, articles on textile and clothing design, information about research projects etc.*

Dosegljivo na svetovnem spletu/*Available Online at*
www.tekstilec.si

Tekstilec je indeksiran v naslednjih bazah/*Tekstilec is indexed in*
Emerging Sources Citation Index – ESCI/Clarivate Analytics
SCOPUS/Elsevier
Ei Compendex
DOAJ
WTI Frankfurt/TEMA® Technology and Management/TOGA® Textile Database
World Textiles/EBSCO Information Services
Textile Technology Complete/EBSCO Information Services
Textile Technology Index/EBSCO Information Services
Chemical Abstracts/ACS
ULRICHWEB – global serials directory
LIBRARY OF THE TECHNICAL UNIVERSITY OF LODZ
dLIB
COBISS (SICRIS: 1A4/Z1)SICRIS (1A4/Z1)

tekstilec

Ustanovitelja / *Founded by*
• Zveza inženirjev in tehnikov tekstilcev Slovenije /
Association of Slovene Textile Engineers and Technicians
• Gospodarska zbornica Slovenije – Združenje za tekstilno,
oblačilno in usnjarsko predelovalno industrijo /
Chamber of Commerce and Industry of Slovenia – Textiles, Clothing and Leather Processing Association

Revijo sofinancirajo / *Journal is Financially Supported*
• Univerza v Ljubljani, Naravoslovnotehniška fakulteta / *University of Ljubljana, Faculty of Natural Sciences and Engineering*
• Univerza v Mariboru, Fakulteta za strojništvo /
University of Maribor, Faculty for Mechanical Engineering
• Industrijski razvojni center slovenske predilne industrije /
Slovene Spinning Industry Development Centre – IRSPIN
• Javna agencija za raziskovalno dejavnost Republike Slovenije /
Slovenian Research Agency

Izdajatelj / *Publisher*
Univerza v Ljubljani, Naravoslovnotehniška fakulteta /
University of Ljubljana, Faculty of Natural Sciences and Engineering

Naslov uredništva/*Editorial Office Address*
Uredništvo Tekstilec, Snežniška 5, SI–1000 Ljubljana
Tel./*Tel.*: + 386 1 200 32 00, +386 1 200 32 24
Faks/*Fax*: + 386 1 200 32 70
E–pošta/*E–mail*: tekstilec@ntf.uni–lj.si
Spletni naslov/*Internet page*: http://www.tekstilec.si

Lektor za slovenščino / *Slovenian Language Editor* Milojka Mansoor
Lektor za angleščino / *English Language Editor* Tina Kočevar Donkov, Barbara Lustek Preskar
Oblikovanje platnice / *Design of the Cover* Tanja Nuša Kočevar
Oblikovanje / *Design* Vilma Zupan
Oblikovanje spletnih strani / *Website Design* Jure Ahtik

Tisk / *Printed by* PRIMITUS, d. o. o.

Revija Tekstilec izhaja štirikrat letno /
Journal Tekstilec appears quarterly
Revija je pri Ministrstvu za kulturo vpisana v razvid medijev pod številko 583.
Letna naročnina za člane Društev inženirjev in tehnikov tekstilcev je vključena v članarino.

Letna naročnina
za posameznike 38 €
za študente 22 €
za mala podjetja 90 €
za velika podjetja 180 €
za tujino 110 €
Cena posamezne številke 10 €

Na podlagi Zakona o davku na dodano vrednost sodi revija Tekstilec med proizvode, od katerih se obračunava DDV po stopnji 9,5 %.

Transakcijski račun 01100–6030708186
Bank Account No. SI56 01100–6030708186
Nova Ljubljanska banka d.d.,
Trg Republike 2, SI–1000 Ljubljana,
Slovenija, SWIFT Code: LJBA SI 2X.

tekstilec VOLUME 61 • TEKSTILEC 2 • 2018 ISSN 0351-3386 (tiskano / printed)
UDK 677 + 687 (05)

IZVIRNI ZNANSTVENI ČLANKI / *Original Scientific Articles*

Abu Naser Md. Ahsanul Haque[1], Manwar Hussain[2], Fahmida Siddiqa[1], Md. Mahbubul Haque[1], G M Nazmul Islam[3]
[1] Daffodil International University, Department of Textile Engineering, 102 Shukrabad, Mirpur Road, Dhanmondi, Dhaka-1207, Bangladesh
[2] Hanyang University Erica campus, Department of Chemical Engineering, 55 Hanyangdaehakro, Sangnok-gu Ansan-si, Gyeonggi-do 426-791, South Korea
[3] Wuhan Textile University, School of Textile Science and Engineering, Wuhan, Hubei, China

Adsorption Kinetics of Curcumin on Cotton Fabric
Kinetika adsorpcije kurkumina na bombažnem pletivu

Original Scientific Article/*Izvirni znanstveni članek*
Received/*Prispelo* 01-2018 • Accepted/*Sprejeto* 05-2018

Abstract
The adsorption kinetics study of curcumin on a cotton fabric was investigated at three different temperatures at neutral pH with 1 : 20 material liquid ratio and 1 g/L initial dye concentration. Pseudo first-order and pseudo second-order kinetics were approached to experimental data and the adsorption kinetics of curcumin on cotton fitted well with the pseudo second-order kinetic model. The activation energy was 71.96 kJ/mol, whereas enthalpy and entropy were 68.99 kJ/mol and –59.7 J/mol K, respectively. Dye adsorption declined with increasing temperature, which suggests that the process is exothermic and the negative value of entropy indicates the presence of interaction between the adsorbent and adsorbate.
Keywords: activation parameters, chemisorption, equilibrium, natural dye, turmeric

Izvleček
Na bombažnem pletivu je bila proučevana kinetika adsorpcije kurkumina pri treh različnih temperaturah v nevtralnem pH mediju s kopelnim razmerjem 1 : 20 in začetno koncentracijo barvila 1 g/L. Eksperimentalni podatki so se približali kinetikama psevdoprvega reda in psevdodrugega reda. Adsorpcijska kinetika kurkumina na bombažu ustreza kinetičnemu modelu psevdodrugega reda. Aktivacijska energija je bila 71,96 kJ/mol, entalpija in aktivacijska entropija pa sta znašali 68,99 kJ/mol oziroma –59,7 $Jmol^{-1}K^{-1}$. Adsorpcija barvila se je z naraščajočo temperaturo zmanjšala, kar kaže, da je proces eksotermen, negativna vrednost entropije pa kaže na prisotnost interakcij med adsorbensom in adsorbendom.
Ključne besede: kinetika, adsorpcija, bombaž, kurkumin, naravno barvilo, kurkuma

1 Introduction

Dyeing textile materials with natural dyes has a long past and had its presence already in the prehistorical ages [1]. However, since the discovery of synthetic dyes in 1856, the use of natural dyes decreased dramatically. Moreover, at the start of the twentieth century when the cost for synthetic dye manufacturing decreased substantially, natural dyes were almost ignored [2]. Nevertheless, due to its environment friendly nature, a keen interest has been gained back among the researchers to utilize natural dyes effectively especially onto natural fibres [3]. It has also been reported that in comparison with synthetic dyes, natural dyes are more biodegradable and highly compatible with environment along with their good UV-protection capability and antibacterial activity [4–6].

Turmeric, the most commonly used source of natural dyes for textiles [7], is obtained from the root of the plant *Curcuma longa*. It is rich in curcuminoids and belongs to the diaroylmethane group called diferuloylemethane [8]. The active colouring component in turmeric rhizome is curcumin, also called Natural Yellow 3 with the colour index number 75300 [9]. This dye is not only environment friendly

Corresponding author/*Korespondenčni avtor:*
Abu Naser Md. Ahsanul Haque
Telephone: +8801715580985
E-mail: anmahaque@gmail.com

but also famous for different health benefits [10–12]. Curcumin has the molecular formula $C_{21}H_{20}O_6$ and its molecular weight is 368.38 g/mol [13].

It has been found in different studies that curcumin can be used to dye cotton with or without mordants (commonly metallic salts that possess affinity towards both fibre and dye) but using mordants can help improve the dye exhaustion and colour fastness properties of curcumin [9, 14–15].

The kinetic study of curcumin dye was approached previously by researchers on the PLA fibre. It was reported that the rate of exhaustion was greater by increasing the temperature of dyeing and a similarity was reported in the dyeing mechanism of curcumin with disperse dyeing [16]. The dyeing with curcumin on a cotton fabric was reported by scientists, where different temperatures and time durations were experimented to obtain an optimized dyeing condition. It was revealed that the exhaustion of curcumin on cotton was at its best at 75 °C for 45–60 min. [14]. However, the kinetic modelling of curcumin is also important to describe the adsorption behaviour and understand the optimum dyeing conditions more thoroughly. Though kinetic studies on cotton were conducted with other natural dyes (lac) [17–18], there is no such report available that would study the kinetics of curcumin on cotton.

2 Experimental

2.1 Materials

A single jersey scoured-bleached cotton fabric used for the process was collected from Impress-Newtex Composite Textiles Ltd, Gorai, Mirzapur, Tangail, Bangladesh. The specifications of the fabric are listed in Table 1.

Table 1: Fabric specification

Parameter	Value
Type of yarn	Combed
Yarn count [tex]	21.09
Twists [cm^{-1}]	7.87
Twist direction	Z
Loop length [mm]	2.44
Course [cm^{-1}]	20.47
Wales [cm^{-1}]	15.75
Mass per unit area [g/m^2]	140

2.2 Extraction of curcumin dye

Turmeric powder was directly collected from Square Food and Beverage Limited, Meril road, Salgaria, Pabna, 6600, Bangladesh for this current work. The extraction process was carried out in deionized water at 95 °C and neutral pH for 90 min from 1 g/L powder.

2.3 Dyeing process

The dyeing was done in a Mathis Labomat lab dyeing machine, which has the programmed temperature controlling system by IR heating and a combined air-water cooling unit. The pre-mordanting process was performed with 0.5 g/L $FeSO_4$ at 70 °C for 10 min with 1 : 20 MLR. For the dyeing of cotton, three different temperatures (i.e. 70 °C, 85 °C and 100 °C) were approached at neutral pH in 1 : 20 MLR and continued for 100 min with a 1.0 ml dye solution removed in every 2 min interval for the first 20 min, 5 min interval for 20 to 40 min and 20 min interval for 40 to 100 min for the spectroscopic measurement.

2.4 Kinetic experiments

A UV-Visible spectrophotometer (UV 1800) was used for absorbance measurements with quartz cuvette cells of 1 cm path length. The dye concentrations were determined at time zero and at subsequent times from the absorbance values at λ_{max} 419 nm. The concentration of dye in liquor was calculated with the Beer-Lambert equation:

$$A = \varepsilon\, l\, c \qquad (1),$$

where A is absorbance, ε is dye extinction coefficient ($Lmg^{-1}cm^{-1}$), l is path length of light (cm) and c is concentration of dye solution (mg/L). The dye extinction coefficient was 0.01031 $Lmg^{-1}\,cm^{-1}$ and was obtained by calculating the slope of the calibration curve (c versus A) where the concentration values were known.

The amount of dye (mg/g) absorbed on cotton at any time q_t was calculated with the mass-balance relationship formula:

$$q_t = \frac{(C_0 - C_t)\mathrm{V}}{W} \qquad (2)$$

where C_0 is preliminary dye concentration (mg/L) and C_t is dye concentration after time, t, (mg/L). V is the volume of solution (mL) and W represents the weight of cotton fabric in gram.

3 Results and discussion

3.1 Effect of temperature on adsorption of curcumin on cotton

The initial dye adsorption rate (h_i) of curcumin on cotton was higher in the case of higher temperature before reaching the equilibrium. Figure 1 represents the results in the first 20 min. However, at the equilibrium time, the amount of dye adsorbed by cotton declined with increasing temperature which represented an exothermic process [17]. The time needed to reach the equilibrium was shorter at higher dyeing temperatures (25 min at 70 °C, 16 min at 85 °C and 12 min at 100 °C), which can be seen in Figure 2. These results are predictably very similar to the results of our previous work of curcumin on modal, which is also a cellulose (regenerated) fibre [19].

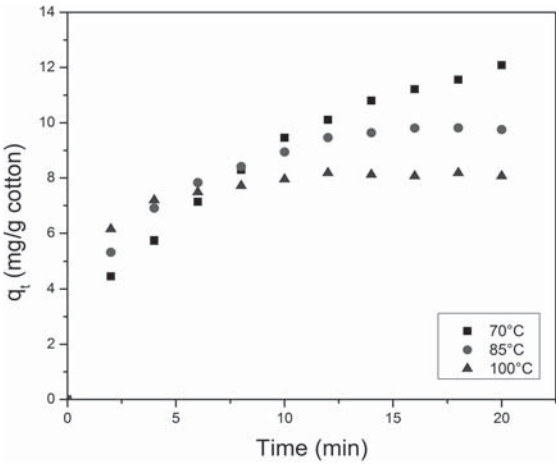

Figure 1: Effect of contact time and temperature of curcumin on cotton (0–20 min)

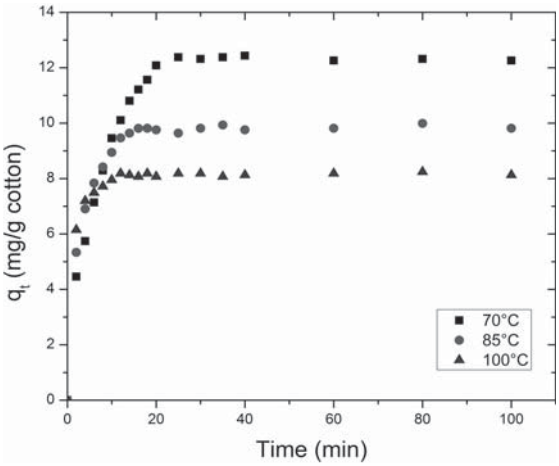

Figure 2: Effect of contact time and temperature of curcumin on cotton (0–100 min)

3.2 Kinetics of adsorption

Reactions can be treated as having a certain pseudo order under certain conditions, i.e. when the amount of one of the reactants is substantially greater than the amount of the other one, and can thus be regarded as a constant value and included in the rate constant. This is how the order of a reaction reduces and becomes a pseudo order. Despite no report on the kinetic study of curcumin on cotton exists, a report of a kinetic study of curcumin is available on a regenerated cellulose fibre, e.g. modal [19]. There are also available reports for other systems involving natural dye binding, e.g. lac dye on cotton and silk. In all cases, it was found out that a pseudo second-order kinetic law matched well with the experimental data [5, 17, 19].

In the current experiment, the pseudo first-order and second-order kinetic models were approached for the investigational data to represent the adsorption kinetics of curcumin dye on cotton. The linear form of the pseudo first-order equation, also known as the Lagergren equation, is as follows:

$$ln(q_e - q_t) = lnq_e - k_1 t \quad (3),$$

where k_1 is the rate constant of pseudo first-order adsorption (s^{-1}), and q_e and q_t are the amounts of dye adsorbed per gram of cotton (mg/g) at equilibrium and at a specific time, t. The first-order equation of Lagergren is likely to be applicable only over the preliminary stage of the adsorption and does not generally fit well for the whole range of contact times [20]. A linear plot of $ln\ (q_e - q_t)$ versus t indicates the applicability of the kinetic model to fit the investigational data. The rate constant, k_1, and equilibrium adsorption density, q_e, were calculated from the slope and intercept of the graph. The pseudo second-order kinetic model [20–21] based on the adsorption equilibrium can be expressed in a linear form as follows:

$$\frac{t}{q_t} = \frac{1}{k_2 q_e^2} + \frac{t}{q_e} \quad (4),$$

$$h_i = k_2 q_e^2 \quad (5),$$

where k_2 (g mg^{-1} min^{-1}) is the rate constant for pseudo second-order adsorption and where h_i [22] is the initial dye adsorption rate (mg $g^{-1}min^{-1}$). If the plot of (t/q_t) versus t shows a linear relationship, pseudo second-order kinetics is applicable.

The slope and intercept of (t/q_t) versus t were considered to calculate the pseudo second-order rate constant k_2 and q_e.

The overall range of adsorption of curcumin on cotton is likely to be matched with a chemisorption mechanism, which involves a chemical reaction between an absorbate and surface, and is usually categorized by higher values of enthalpy (80–240 kJ/mol) than the enthalpy of a physisorption mechanism (20–40 kJ/mol) [23].

The kinetic data obtained from curcumin adsorption in the current study was analysed using the pseudo first-order kinetic model (cf. Equation 3) as well as the pseudo second-order kinetic model (cf. Equation 4), and is shown in Figure 3 and Figure 4. The results are depicted in Table 2.

The data show that although the kinetics of adsorption is a first-order process in the initial stage (at times t < 20 min), it follows second-order kinetics at longer times (t > 25 min).

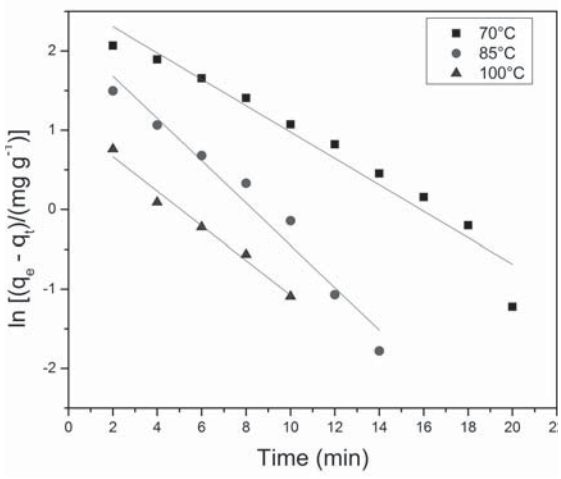

Figure 3: Plot of pseudo first-order equation at different temperatures for adsorption of curcumin on cotton

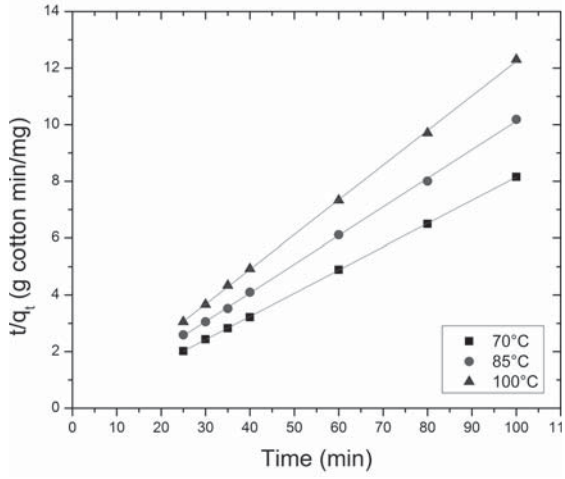

Figure 4: Plot of pseudo second-order equation at different temperatures for adsorption of curcumin on cotton

The correlation coefficients obtained from the pseudo second-order kinetic model were very close to 1 (more than 0.999) and also higher than that of the pseudo first-order kinetic model. This indicates that the adsorption of curcumin on cotton is unlikely to be a first-order reaction. The calculated q_e values were also relatively close to the experimental q_e. Therefore, the experimental data of curcumin dyeing on cotton fitted well with pseudo second-order kinetics.

3.3 Activation parameters

From the rate constant of pseudo second-order kinetics, k_2, (cf. Table 2), the activation energy, E_a, for the adsorption of curcumin dye on cotton was determined using the Arrhenius equation [24]:

$$lnk = lnA - \frac{E_a}{RT} \quad (6),$$

where A, E_a, T and R refer to the Arrhenius factor (temperature independent), the Arrhenius activation

Table 2: Comparison of pseudo first- and second-order adsorption rate constant of curcumin dyeing on cotton

Temperature [°C]	$q_{e,\,exp}$ [mg/g_{cotton}]	Pseudo first-order model		Pseudo second-order model			
		k_1 [min^{-1}]	R^2	k_2 [g_{cotton} mg^{-1} min^{-1}]	$q_{e,cal}$ [mg/g_{cotton}]	h_i [mg g_{cotton}^{-1} min^{-1}]	R^2
70	12.38	0.166	0.950	0.2196	12.22	32.79	1
85	9.81	0.266	0.966	0.2844	9.91	27.93	0.9996
100	8.29	0.217	0.981	1.7094	8.20	114.94	0.9998

energy (kJ/mol), absolute temperature (K) and the gas constant (8.314 J/mol K), respectively.
The Arrhenius plot of *ln k* against *1/T* for the adsorption of curcumin on cotton is shown in Figure 5 and the value of activation energy, which was calculated from the slope of the plot, is listed in Table 3.

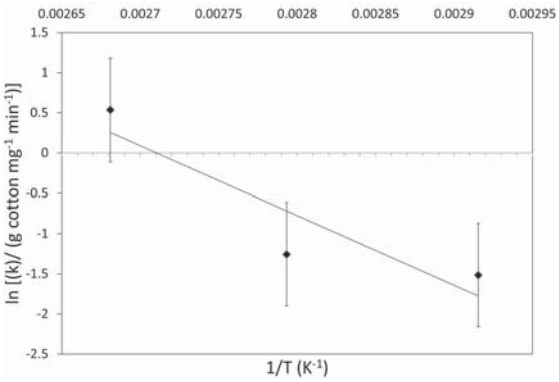

Figure 5: Arrhenius plot for adsorption of curcumin on cotton

The enthalpy ($\Delta H^{\ddagger}$) and entropy ($\Delta S^{\ddagger}$) of activation were calculated using the Eyring equation as follows:

$$ln(\frac{k}{T}) = ln(\frac{K_b}{h}) + \frac{\Delta S^{\ddagger}}{R} - \frac{\Delta H^{\ddagger}}{RT} \quad (7),$$

where K_b and h are the Boltzman's and Planck's constant. The standard enthalpy and entropy of dyeing were calculated from the slope and intercept of the plot (cf. Figure 6) $ln\ (k_2/T)$ versus $1/T$.
Gibbs energy of activation ($\Delta G^{\ddagger}$) was calculated with the following equation:

$$\Delta G^{\ddagger} = \Delta H^{\ddagger} - T\Delta S^{\ddagger} \quad (8)$$

The calculated values are listed in Table 3. The negative value of the activation entropy ($\Delta S^{\ddagger}$) supported the interaction between curcumin dye and cotton.

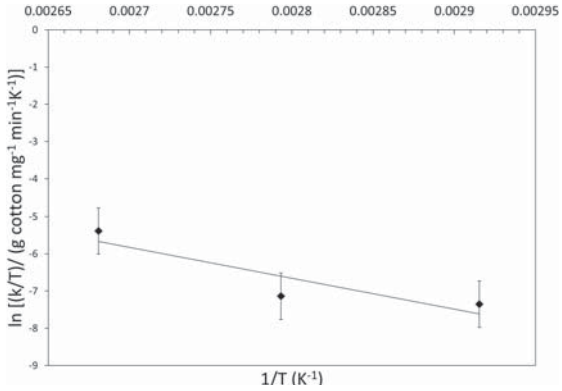

Figure 6: Eyring plot for adsorption of curcumin on cotton

4 Conclusion

The adsorption kinetics of curcumin on cotton suited with the pseudo second-order kinetic model. It was a kinetically controlled process as the initial dye adsorption rates (h_i) were higher at higher temperatures before the equilibrium time. The amount of dye adsorbed by cotton decreased with increasing temperature, which suggests that the process is exothermic. Furthermore, the positive value of free energy represents the strong affinity between the dye and substrate, and the negative value of entropy indicates the colour adsorbed more orderly on cotton with a certain interaction.

References

1. SIVA, Ramamoorthy. Status of natural dyes and dye-yielding plants in India. *Current Science*, 2007, **92**, 916–925.
2. SARAVANAN, P., CHANDRAMOHAN, G. Dyeing of silk with ecofriendly natural dye obtained from barks of *Ficus religiosa* L. *Universal Journal of Environment Research and Technology*, 2011, **1**(3), 268–273.

Table 3: Activation parameters for adsorption of curcumin on cotton

Temperature [°C]	k_2 [g_{cotton} mg^{-1} min^{-1}]	*Ea* [kJ/mol]	R^2	$\Delta H^{\ddagger}$ [kJ/mol]	$\Delta S^{\ddagger}$ [J/mol K]	$\Delta G^{\ddagger}$ [kJ/mol]	R^2
70	0.2196	71.96	0.825	68.99	–59.7	89.46	0.813
85	0.2844						
100	1.7094						

3. SAMANTA, Ashis Kumar, AGARWAL, Priti. Application of natural dyes on textiles. *Indian Journal of Fibre and Textile Research*, 2009, **34**(4), 384-399.
4. ADEEL, Shahid, BHATTI, Ijaz Ahmad, KAUSAR, Afifah, OSMAN, Eman. Influence of UV radiations on the extraction and dyeing of cotton fabric with Curcuma longa L. *Indian Journal of Fibre and Textile Research*, 2012, **37**(1), 87-90.
5. CHAIRAT, Montra, RATTANAPHANI, Saowanee, BREMNER, John B., RATTANAPHANI, Vichitr. An adsorption and kinetic study of lac dyeing on silk. *Dyes and Pigments*, 2005, **64**(3), 231-241, doi: 10.1016/j.dyepig.2004.06.009.
6. IBRAHIM, N. A., EL-GAMAL, A. R., GOUDA, M., MAHROUS, F. A new approach for natural dyeing and functional finishing of cotton cellulose. *Carbohydrate Polymers*, 2010, **82**(4), 1205-1211, doi: 10.1016/j.carbpol.2010.06.054.
7. SAMANTA, Ashis Kumar, KONAR, Adwaita. Dyeing of textiles with natural dyes. In *Natural Dyes*. Edited by E. A. Kumbasar. London : InTech, 2011, pp. 29–56.
8. RAVINDRAN, P. N., BABU, K. Nirmal, SIVARAMAN, Kandaswamy. *Turmeric: The genus Curcuma*. Boca Raton : CRC Press, 2007.
9. MULEC, Irena, GORJANC, Marija. The influence of mordanting on the dyeability of cotton dyed with turmeric extract. *Tekstilec*, 2015, **58**, 199-218, doi: 10.14502/Tekstilec2015.58.199–218.
10. BHATTI, Ijaz Ahmad, ADEEL, Shahid, JAMAL, M. Asghar, SAFDAR, Muhammad, ABBAS, Muhammad. Influence of gamma radiation on the colour strength and fastness properties of fabric using turmeric (Curcuma longa L.) as natural dye. *Radiation Physics and Chemistry*, 2010, **79**(5), 622-625, doi: 10.1016/j.radphyschem.2009.12.006.
11. EL-SHISHTAWY, Reda M., SHOKRY, G. M., AHMED, Nahed S. E., KAMEL, M. M. Dyeing of modified acrylic fibers with curcumin and madder natural dyes. *Fibers and Polymers*, 2009, **10**(5), 617-624, doi: 10.1007/s12221-010-0617-4.
12. JAYAPRAKASHA, Guddadarangavvanahally K., RAO, Lingamullu Jagan Mohan, SAKARIAH, Kunnumpurath K. Improved HPLC method for the determination of curcumin, demethoxycurcumin, and bisdemethoxycurcumin. *Journal of Agricultural and Food Chemistry*, 2002, **50**(13), 3668-3672, doi: 10.1021/jf025506a.
13. PRIYADARSINI, K. Indira. The chemistry of curcumin: from extraction to therapeutic agent. *Molecules*, 2014, **19**(12), 20091-20112, doi: 10.3390/molecules191220091.
14. HASAN, Md. Mahabub, HOSSAIN, Mohammad Billal, AZIM, Abu Yousuf Mohammad Anwarul, GHOSH, Nayon Chandra, REZA Md. Shamim. Application of purified curcumin as natural dye on cotton and polyester. *International Journal of Engineering & Technology*, 2014, **14**(5), 17–23.
15. MARGARETA, Sequin-Frey. The chemistry of plant and animal dyes. *Journal of Chemical Education*, 1981, **58**, 301–305.
16. WU, Jihong, GUO, Hui, KE, Jun, FAN, Jiangtao. Studies on kinetic and thermodynamic parameters of natural dye curcumin on PLA fibre. *Indian Journal of Fibre and Textile Research*, 2013, **38**(4), 424–426.
17. CHAIRAT, Montra, RATTANAPHANI, Saowanee, BREMNER, John B., RATTANAPHANI, Vichitr. Adsorption kinetic study of lac dyeing on cotton. *Dyes and Pigments*, 2008, **76**(2), 435-439, doi: 10.1016/j.dyepig.2006.09.008.
18. RATTANAPHANI, Sawanee, CHAIRAT, Mantra, BREMNER, John B., RATTANAPHANI, Vichitr. An adsorption and thermodynamic study of lac dyeing on cotton pretreated with chitosan. *Dyes and Pigments*, 2007, **72**(1), 88–96, doi: 10.1016/j.dyepig.2005.08.002.
19. HAQUE, Abu Naser Md Ahsanul, HUSSAIN, Manwar, SMRITI, Shamima Akter, SIDDIQA, Fahmida, FARZANA, Nawshin. Kinetic study of curcumin on modal fabric. *Tekstilec*, 2018, **61**(1), 27–32, doi: 10.14502/Tekstilec2018.61.27-32.
20. CHIOU, Ming-Shen, LI, Hsing-Ya. Equilibrium and kinetic modeling of adsorption of reactive dye on cross-linked chitosan beads. *Journal of Hazardous Materials*, 2002, **93**(2), 233-248, doi: 10.1016/S0304-3894(02)00030-4.
21. HO, Y. S., McKAY, G. Sorption of dye from aqueous solution by peat. *Chemical Engineering Journal*, 1998, **70**(2), 115-124, doi: 10.1016/S0923-0467(98)00076-1.
22. CHIOU, M. S., LI, H. Y. Adsorption behavior of reactive dye in aqueous solution on chemical cross-linked chitosan beads. *Chemosphere*, 2003, **50**(8), 1095-1105, doi: 10.1016/S0045-6535(02)00636-7.
23. XAMIDEA [online]. Adsorption [accessed 10.1.2018]. Available on World Wide Web: <https://www.xamidea.in/learning/chemistry/22/surface-chemistry/32 >.
24. DOGAN, Mehmet, ALKAN, Mahir. Adsorption kinetics of methyl violet onto perlite. *Chemosphere*, 2003, **50**(4), 517-528, doi: 10.1016/S0045-6535(02)00629-X.

Jana Vilman Proje[1], Matejka Bizjak[2]
[1]Folklordizajn, Jana Vilman Proje, s. p., Stara Fužina 134, 4265 Bohinjsko jezero, Slovenia
[2]University of Ljubljana, Faculty of Natural Sciences and Engineering, Aškerčeva 12, 1000 Ljubljana, Slovenia

Model for Designing Affiliated Clothes with Local Identity

Model oblikovanja pripadnostnih oblačil z lokalno identiteto

Original Scientific Article/*Izvirni znanstveni članek*
Received/*Prispelo* 03-2018 • Accepted/*Sprejeto* 05-2018

Abstract

The paper describes a new research methodology through design that has also proven relevant for the field of fashion design. According to some scientific opinions, the field of research in fashion design does not meet scientific standards, although that research produces original knowledge and products. The newly and artificially designed affiliated clothing image, which addresses the needs of tourism, found its inspiration in cultural heritage. The inspiration for the creation of symbolic signs and their application in individual garments was carefully selected from the story of local heritage. Newly designed clothing inspired by the story of local heritage should promote the recognition and acceptance of the affiliated clothing image as part of the identity of people from a particular region. This paper presents the definition and analysis of design processes for a known client, in this case a tourism organisation. The designer seeks practical and innovative solutions throughout the design process, from the definition of the local story to be interpreted, through collaboration with a client and the public, to the design of an affiliated symbol and its application in the clothing image, the production planning process and manufacturing, and finally the presentation of products to the public and the promotion of those products. An example of best practices in the designing of affiliated clothing for Bohinj is presented, where the design in question was tested in practice. In this process, the designer took into account the fact that design, as a process, is a form of cooperation, in which the members of the development team should be respected and understood.
Keywords: tourism, authenticity, fashion design, cultural heritage

Izvleček

Članek opisuje nov pristop raziskavanja s pomočjo oblikovanja, ki je pomemben tudi za področje modnega oblikovanja. V skladu z nekaterimi znanstvenimi mnenji, raziskovanje za potrebe modnega oblikovanja ne zadošča znanstvenim standardom, čeprav je produkt raziskav izvirno znanje oziroma originalni izdelki. Navdih za novooblikovana pripadnostna oblačila za potrebe turizma, izhaja iz kulturne dediščine. Osnova za oblikovanje simbolnih znakov in njihovo uporabo na posameznih oblačilih je bila skrbno izbrana lokalna dediščinska zgodba. Vizualizacija lokalne zgodbe v posamezne oblačilne kose spodbuja prepoznavnost področja in sprejetje nove pripadnostne oblačilne podobe kot del identitete lokalnih prebivalcev. V članku so opredeljeni in analizirani procesi pri oblikovanju za naročnika na primeru turistične organizacije. Oblikovalec išče praktične in inovativne rešitve skozi celoten proces oblikovanja, od definicije izhodiščne zgodbe, preko sodelovanja z naročnikom, vključevanja lokalnega prebivalstva, do oblikovanja in aplikacije simbolnih znakov v oblačilno podobo, priprave proizvodnje in izdelave ter predstavitve izdelkov javnosti. Predstavljen je primer dobre prakse oblikovanja pripadnostnih oblačil za Bohinj, s katerim je bil praktično preizkušen model oblikovanja. Oblikovalec v njem upošteva vodilo, da je oblikovanje kot proces oblika sodelovanja, v katerem spoštuje in razume člane razvojnega tima.
Ključne besede: turizem, avtentičnost, modno oblikovanje, kulturna dediščina

Corresponding author/*Korespondenčna avtorica:*
Assoc Prof dr. Mateja Bizjak
E-mail: mateja.bizjak@ntf.uni-lj.si

Tekstilec, 2018, ***61****(2), 82-92*
DOI: 10.14502/Tekstilec2018.61.82-92

1 Introduction

As a fashion designer, I was asked to design garments (*uniforms*) for a local tourism organisation in Bohinj. The new affiliated clothing design is to be used as a uniform for workers at tourist information centres. It should be the representative clothing of staff in their workplace, and of the local inhabitants when they present a particular destination, local products and services.

The story of that destination should be told through clothing, while its visual appearance should serve as a "clue" to the local stories that the destination would like to present. The visual appearance of clothing should at once evoke the traditional vibe of the destination, the theme of interpretation and the geographical characteristics of the region. A clothing image should also be consistent with the way customers dress, and be adapted to working conditions and job diversity, with a comfortable cut and materials that are easy to maintain. Staff should identify themselves with the clothing and feel good wearing it. The clothing must therefore allow for combining and individual accessories.

If we follow Knific, [1] who emphasises that numerous meanings are attached to a clothing image, which through its appearance completes a comprehensive visual image of the mythical stories that describe it, we can achieve all objectives through sound structural design. The primary challenge in design concerns the visual interpretation of selected heritage stories and the way they are applied in clothing, so that visitors will at once relate them to a particular destination, while local inhabitants will accept them as their own.

Tourism staff and representatives of Bohinj usually wear their own modern clothing. At the main Tourist Information Centre in Bohinj, where the staff are visitors' first contact with the destination, employees dress in work clothes (black trousers, a white blouse, a neckerchief and a red coat).

Local inhabitants understand the typical clothing of Bohinj to be the "Bohinj national costume" (i.e. a Bohinj version of the national costume) or semblances of the historical clothing image of Bohinj Alpine herdsmen. Generally, they are not acquainted with what is the "correct alpine herdsmen" or the "correct Bohinj costume" clothing image according to historical clothing heritage and affiliated costumes. They thus rely on stereotyped perceptions. Consequently, when they want to dress in a style typical of Bohinj (in Bohinj costume or Alpine herdsmen costume), they simplify cuts, search for cheap clothing solutions, and combine modern fashion that deviates significantly from the authentic presentation of historical clothing, which should be based on historical facts [1]. The feeling that something is authentic (even if it is not based on historical facts) is the key factor affecting the choice and recognition of elements of cultural heritage [2], and it is also the essential element for the holistic perception of the identity and style of a tourist area.

As Copeland and Hodges [3] determined, the clothing themes of the representatives and performers at festivals, and presentations of a destination play a key role in the perception of what is traditional or an interpretation of heritage. Affiliated clothing allows the community to be recognisable from the outside, and reinforces an essential identity communication between its members. Through a clothing image, both tourism workers and local inhabitants are able to convey a message within the community and to visitors, as well. By dressing "traditionally", members not only present an image, but also demonstrate their perception of local traditions [4]. This involves the aesthetic experience through which all senses are stimulated and garments serve as the medium of communication with a group, strengthening a certain aesthetic sense of belonging and presenting themselves [4].

Affiliated costumes can be considered a defining factor of a destination's image and local identity. Based on a practical example, we will attempt to answer the questions of how to find and interpret local stories, and how to apply newly designed symbols in affiliated clothing ("local costume"), so that it will be recognised as being an authentic reflection of Bohinj.

1.1 Cultural heritage and authenticity

Cultural heritage is closely related to the development of nationhood and countries. It represents the basis of the collective identity and the self-respect of an individual and society, as it answers the basic questions of who we are, where we come from and what we belong to [5]. A common cultural heritage connects the members of a group and excludes those who do not belong to the group. In order to be able to exclude "others", heritage cannot be universal. The main purpose of heritage is a subjective

pride in the history of a community that reveals its identity and glorifies its values [5]. As cultural heritage develops, history can be misinterpreted; it becomes a fabrication that in time, or because of its continuity over an extended period of time, can become an authentic memory of itself. Heritage can be recreated in order to make it attractive for modern times, and to adapt it to our image and wishes [6]. Bogataj synthesises the dimensions and the meaning of heritage into three concepts: continuity – memory; identity – reminder, and alternative – challenge [7]. The most important is continuity. The reappearance of elements of heritage over an extended period of time causes people to recognise these elements as local, original and authentic [1].

The perception and choice of cultural heritage is influenced by authenticity [2]. Authenticity is a problematic and insufficiently explored concept that hinders its practical application [8]. There are many types and meanings of authenticity, i.e. as an attribute of objects (object-based) and as an existential experience of the "true self" (existential authenticity) [8, 9]. The notion of authentic identifies something that is genuine, real, not invented or virtual, and something that is in accordance with broadly accepted, long-standing tradition and reflects the character of a certain time [6, 10], but is in fact a great part of the phenomena that are today understood as the tradition that we invented, or at least pieced together in a particular historical and social context [11].

The reality and experience of local inhabitants and visitors is shaped by various structural contrasts, i.e. distinctions between the modern and the primitive, the sacred and the shallow, insiders and outsiders, reality and show, tourists and intellectuals [12]. These can be associated with the concept of authenticity, which reflects the immense complexity of interactions involving a cultural conflict, an identity quest, the purpose of the use and various dialectical tensions that exist between tradition and change, reality and fictional history and contemporaneity, and culture and individuality [13]. The authenticity and historical meaning of an item are merely evaluated by the individual's opinion [14]; it is a socially and above all individually constructed and evaluated perception of experience [15].

The post-modernist tourist is an affection-driven, experience-seeking hedonist, who does not judge authenticity from an intellectual distance, but through emotional experience; an adventurer, who does not separate consumption from any other experience in life [16]. In terms of post-modernism, as mentioned above, authenticity is a socially and individually constructed and evaluated perception and experience, and can be influenced (claimed, presented, assured, authorised, and promoted) by tourism managers [15, 17].

The commercial presentation of cultural heritage or of culture itself has two different sides. Some authors cf. [18-20] claim that anything created and offered for commercial purposes automatically loses its authenticity (i.e. its natural meaning and value). Evidently, however, commercial presentation is often necessary for tourists to recognise the authenticity of cultural heritage [21], and often keeps traditional cultures and customs alive that would otherwise be lost [22]. The intent of the commodification of cultural heritage does not destroy its authenticity, but exposes its exchange value [23]. Tourism does, however, undoubtedly bring both positive and negative effects to the local economy and the integrity of heritage cf. [24, 25].

In our case, we are inventing new affiliated clothing that is supposed to become part of cultural heritage – authentic clothing from Bohinj. The interpretation of heritage – traditional stories – in a modern clothing image for tourism purposes may encompass both commercial presentation in a modern form and authentic content that should be recognised through affiliated symbols.

1.2 Affiliated dress

Dress, especially affiliated clothing, is a form of non-verbal communication – a means of interaction that conveys a message through symbolism. Affiliated clothing is a type of dress that facilitates the reception and promotion of ideas, and makes it easier for individuals and groups to identify the roles that they are to present through their clothes [1]. In the region involved in this study, expressing affiliation through a clothing image is mostly associated with affiliated costumes, which are understood to be costumes for special occasions [26]. The development of the regional affiliated costume began in the second half of 19th century, as a special means of manifesting identity through a clothing image [27]. To construct the regional affiliated costume, individual clothing pieces and accessories were taken from the clothing image of the peasantry. These components (parts of the

clothing image) conveyed a new and clear meaning because they were used to express regional identity before "others" (mostly through folklore programmes and the organisation of traditional events for tourists, where affiliated costumes and their various versions are presented). They became symbols that society associates with its roots, and identifies with and recognises "as its own". In this way, the clothing image and its individual parts gained the status of clothing heritage in the eyes of the members of the imagined community [1]. Therefore, the identity that is expressed through clothing should not only be sought in cultural heritage and its symbols, but also, and above all, in the recreated stereotypes that were asserted through clothing heritage.

According to Copeland and Hodges, modern forms of national costumes are in sharp visual contrast to traditional styles and performing traditions, as business and costume-making skills have been replaced by mass production. Transformations from individuality to uniformity and consequently to modifications based on one's own comfort level can also be observed. A shift in traditional dress styles has fostered a division between those who emphasise tradition and those who embrace the idea of the modernisation of traditional costumes [1, 3].

Under the influence of tourism, artificial constructs are emerging that falsely represent the clothing of the past and invented traditions. They also gain new images through repeated interpretations in traditional events, and over time they gain "recurrent authenticity" and are accepted as "authentic" by tourists and cultural producers [1, 28, 29].

The design of a clothing image for the Bohinj region is based on a similar premise – the artificial construction of a clothing image that seeks inspiration in cultural heritage and that will spread the notion of a "traditional" clothing heritage by repeated use at traditional events and tourist shows. Thus, the constructed clothing image should over time be recognised and become part of the identity of the people of Bohinj. The newly designed affiliated clothing should express the character of the region stylistically and visually. It should be in line with the guidelines of the tourist destination, encompass the elements of not only previous clothing practices and forms, but also current clothing fashions and, through subtly included affiliation symbols, it should also enable local inhabitants and visitors alike to identify the clothing as coming from Bohinj.

2 Methods and model development

The research methodology through design that has also proven relevant for the field of fashion design is, according to Findelie, the most relevant for design practice. However, it has also been pointed out that this research method does not meet scientific standards, although this project-grounded research approach produces original knowledge [30]. Because very few researchers are involved in scientific research for the needs of fashion [31], the scientific approach in design for, in and through fashion is deemed negligible.

A model of interpretation of cultural heritage in clothing has been developed in active research through design in two projects dealing with the design of affiliated clothing for tourism. One of them will be presented in the following chapter.

The projects were managed according to Borja de Mozota's [32] statements that design is an interdisciplinary field, where the active design process involves the following activities:

- problem solving,
- creation,
- systemisation,
- coordination, and
- cultural contribution.

Furthermore, design can be also equated with management, as it follows the systematic, logical and orderly process of problem solving. The designer assumes the function of the coordinator and is therefore involved in the entire design process as an innovator and trendsetter, an initiator of changes and someone who puts forth ideas [32] However, according to Borja de Mozota, the design process relies on the 4C theory [32]:

- creativity: something new that does not exist yet,
- complexity: integration / selection of various parameters and options,
- compromise: taking into account different influential parameters (costs, functionality, material, durability, etc.), and
- choice: choice between various options (from the basic concept to the smallest details in production).

Affiliated dress should become a symbol that community members can identify with. Its form should include the correct balance of fashion, trends, cultural aspects, aesthetics, comfort, durability and price

[33]. At the same time, it must include symbolic signs and elements from the past, as well as clothing practices that must be appropriately modified to create a new tradition. This is a phenomenon that can be contextualised by Hobsbawm's term [34] "invented traditions". These are created in contemporaneity, with the reiteration and implementation of certain rules that create allusions to continuity with the past [34].
The design process, in which cultural heritage is interpreted into affiliated clothing, first includes the definition of a platform, the meaning of a symbol/story/heritage, which relates to determining local characteristics and stereotypically recognisable signs, cultural heritage, past and contemporary dressing practices, the selection of local materials and various technological solutions, as well as cooperation, coordination and communication with the public and the client. This confirms the previously mentioned argument that a designer is a manager and coordinator who must identify all of the relevant facts of a project (complexity and compromise), while design is a process that involves creation and decision making (choice). Design, as an element of the entire process, plays a smaller but very important role, where design skills and good knowledge of cultural heritage is of a great importance. As it turned out in practice, a designer also requires the competences needed to manage a project: inventiveness, communication skills and a sense for details, as well as good knowledge of materials and technical solutions.

3 Discussion

A new model for transforming cultural heritage into a clothing image consists of five important and indispensable phases:

1. preparation/research – choice of a representative local story,
2. designing an affiliated symbol,
3. designing clothing with the application of that affiliated symbol,
4. the production planning process and manufacturing, and
5. the promotion and acceptance of clothing.

Table 1: Activities in process of designing affiliated clothing

Design process	Designing of affiliated clothing	Interaction with the 4C theory
Problem solving	Preparation/research – choice of a representative local story: *cooperation between a designer and an ethnologist, anthropologist and the local tourism organisation, local authorities and future users*	Complexity Compromise Choice
Creation	Design of an affiliated symbol: *design skills and good knowledge of local cultural heritage and traditions; dialog with local inhabitants, the client and future users*	Creativity Complexity Compromise Choice
Systemisation	Design of clothing pieces with the application of an affiliated symbol: *design skills in clothing, including all constrains (client requirements, future users' wishes, technological and cost performance limitations, etc.)*	Creativity Complexity Compromise Choice
Coordination	Production – the production planning process: *technical planning design, material selection, technology, management of the production process and timing, and cost and resource management*	Creativity Complexity Compromise Choice
Cultural contribution	Promotion and acceptance of clothing: *promotion of an idea, selected story, symbol and affiliated clothing via different media, cultural and other events, and tourism promotions*	Creativity Complexity Compromise Choice

3.1 Preparation/research – choice of a representative local story – inspiration

- Literature review: ethnological and historical records, cultural heritage and traditional crafts.
- Overview: tourism and local development strategies.
- Interview with local inhabitants: local traditions, living heritage stories, traditional crafts and skills.
- Clothing habits: past and contemporary clothing habits, communication with the client and representatives of the community.

In order to form a new group identity, the history, traditions, stereotypes, image of the region and development strategies must be reconstructed. A presentation story and symbols of the region must be extracted from it, thereby creating the inspiration for the creation of symbolic affiliation symbols and signs. It is difficult to define the story, as the identity of a certain (even national) region is not an unchangeable fact passively handed down from generation to generation, but is rather a series of interconnected trends that occasionally go in different directions. For this reason, each generation must decide which of these it will accept and build on them further [35]. In the Bohinj region, several authentic underlying topics can be found that are suitable for a presentational heritage story to serve as a basis for the formation of the symbolic signs of an affiliated clothing image. However, the chosen story must also be linked to the orientation of the tourism destination and, more importantly, the local inhabitants must identify themselves with that story.
In the *Strategy of the Development and Marketing of the Bohinj Tourist Destination 2012-2016,* the biodiversity of indigenous plants and wild flower meadows are highlighted as the main distinctive advantages of the region over other tourist areas. This is the reason why, in searching for an appropriate heritage story, the focus was on concepts relating to floral richness. Among these, living stories connected with the experience of local inhabitants and their personal involvement were most interesting. Lowenthal explains that only the traditions that we are touched by, and not those that we are taught, are those that we sense [5]. For the symbolic sign, we considered using the iris of Bohinj (Iris pallida subsp. Cengialti f. vochinensis), described as early as 1917 by the botanist Alfonz Paulin, who named it as an independent subspecies after Bohinj [36]. However, research conducted for the *Strategy of the Development and Marketing of the Bohinj Tourist Destination* found that local inhabitants do not identify themselves with it. Further searching leads to the article by Cvetek entitled "*Flora in the Storytelling of Bohinj*", which describes flowers that are close to the local inhabitants, as they connect it with their own experience and personal involvement. It also features a description of the "*Bohinj Bouquet*" and the symbolic meaning of its flowers: *"At the Cow's Ball, we can see how Alpine herdsmen and herdswomen drive cows decorated with an alpine bouquet on top. /…/ It had to include edelweiss, gentians, rhododendrons and nigritella*" [37]. The article also features interviews with older local inhabitants who discussed their attitudes towards the flowers in the bouquet. It also tells about gathering the flowers and why: *"We gave them as gifts to friends; if someone knew you were going to the mountains, they asked for them. It was a beautiful present from the mountains.*" [37]. The deciding factor for the choice of the story was the confirmation that these flowers are closely connected with the lives of the local inhabitants, and that tradition is still very much alive today. In this way, the Bohinj Bouquet symbolically represents that tradition and the flowers, as a very common theme, as an ideal starting point for stimulating personal emotions and storytelling that give added value to clothing. Given existing images, the choice of a symbol is not difficult to update and can also be recognised in a stylised form. In this way, the Bohinj Bouquet becomes a symbolic affiliation symbol.

3.2 Designing an affiliated symbol

- Search for the appearance/application of the symbol in the past.
- Graphic design of the symbol.
- Consideration of technological possibilities and limitations to application.
- Verification of whether the symbol is recognisable, and the exchange of views about it with the client and local inhabitants.

We approached the design process of the clothing image to express the identity of Bohinj using the "creative thinking" design method. This approach understands design as a process, a way of cooperation, where the designer is part of an interdisciplinary team and the design itself conforms to the understanding and vision of the individuals who will wear the clothing [38].

As a design inspiration, the chosen underlying story of the Bohinj Bouquet played an important role in the process of creative thinking. The creation of the symbol was carried out in two steps. The first step involved designing a symbol to be applied to individual affiliated garments. The symbol should facilitate the perception and identification of community members. In the second step, individual garments were designed, with the symbol applied to them. Based on the chosen story of the Bohinj Bouquet and old embroideries, a simple stylised symbol was designed, consisting of four alpine flowers: edelweiss (*Leontopodium alpinum*), gentian (*Gentiana clusii*), hairy alpenrose (*Rhododendron hirsutum*) and nigritella (*Nigritella nigra*).

Figure 1: Graphic design of the symbol "Bohinj Bouquet" [Photo: J. Vilman Proje] and knitted cardigan with the applied symbol [Photo: M. Sodja]

3.3 Designing clothing pieces with the applied affiliated symbol

- Croquis images of clothing.
- Selection of a production technology.
- Colour collection.
- Selection of fabrics.
- Preparation of motifs for technological application.
- Production of prototype garments.
- Evaluation of the collection of affiliated clothing with the client and potential wearers (representatives of the community – local inhabitants).

The newly designed symbol serves as the symbolic sign for both the identification and creation of the identity of the clothing image. The decision to make the most representative affiliated garment pieces using knitting techniques was closely linked to historical clothing habits. Hand-knitted pieces were essential in the past, in both the male and female wardrobe.

We presented the sketches and the idea of affiliated clothing, with a knitted cardigan as the central piece of the newly designed collection, first to the client (in this case representatives of the local tourism organisation) and then to the potential wearers (employees of the tourism organisation and members of the community). Some doubts were raised about the lack of a 'business look', with the knitted cardigan instead of a jacket. However, the majority expressed a positive opinion about the knitwear, especially in terms of comfort. The knitwear (cardigan) with the motif of the Bohinj Bouquet was recognised as the basic piece of the newly designed affiliated clothing image, which was agreed by tourism representatives and potential wearers alike.

The cardigan was produced using yarns (55% cotton and 45% acrylic) in speckled grey, burgundy and beige, forming the basis of the emerging clothing image. The complete design pattern for the women's cardigan derived from knitted samples, while a fitted cut was chosen, as it is suitable for different body types. Three versions of the cardigans with the same motif in different colour combinations were produced. Sample fabrics for other garments were chosen according to the colour combinations used for cardigans. These matched the style and rounded off the whole clothing image, and were presented to the client and potential wearers again.

3.4 Production –production planning process

- Evaluation of prototypes with the client and potential wearers, and corrections.
- Final selection of fabrics, colours, cuts and pattern.

- Production planning process: technical drawings of clothes, selection of manufacturers/contractors, cooperation with manufacturers and management.
- Graphic design of labels and packaging.

The complete design pattern for the women's cardigan derived from knitted prototypes. We chose a fitted cut for the cardigans, as it is suitable for different body types. The hems of the knitwear were finished with a wavy border. The shape of the men's cardigans followed the same concept as the women's – in the same colour combination of speckled grey and burgundy, but in a plain knitting technique, while the motif was much less prominent than on the women's cardigans, as the bouquet only appears in the striped pattern on the chest and collar. The chosen model of the men's cardigan was simple, with a ribbed welt at the bottom and on the sleeves, with a high collar, and a zipper.

The same knitting technique was also used for a belt, scarf and cap. We also added a destination logo on the cardigan sleeve, scarf edge and cap cuff.

The colour combination of speckled grey and burgundy were selected for the cardigan; a burgundy checked cotton fabric for the blouse; a beige cotton pique jersey fabric for T-shirts; and a dark blue light elastic denim for the skirt.

Besides the cardigans, other garments from the collection, according to selected sketches, were also produced: two versions of the skirt and two women's blouses (in plain and checked fabric), and men's and women's T-shirts made of jersey material. In the final phase of the design process, we presented all the prototype models and possible combinations to the client and employees of the local tourism organisation – future wearers of the affiliated garments. In the final selection of clothing pieces, the suggestions of community members (potential wearers) were considered, such as the possibility of wearing the tops with jeans, the cut of the skirt, colour combinations, etc. After the tourism organisation confirmed the whole collection, the chosen clothing pieces officially became the affiliated clothing with the identity of Bohinj.

The knitted women's and men's cardigans, and a scarf and cap in the same style are also sold in a souvenir shop. The items are sold in gift packages made of felt, to which a compact brochure is tied, describing the story of the Bohinj Bouquet.

Figure 2: Affiliated clothing image of the Bohinj region [Photo: U. Urbanc], scarf and cap with a gift package (sold in a gift shop) [Photo: M. Sodja]

3.5 Promotion and acceptance of affiliated clothing

- Promotion of the Bohinj Bouquet story and affiliated clothing via different media, events and tourist promotions.
- Expanding the recognition of the affiliated symbol – the Bohinj Bouquet motif – with application on a variety of products.
- Monitoring the sale of clothing pieces to local inhabitants and tourists.

We presented the newly-designed affiliated clothing at a fashion show during the opening ceremony of the International Wild Flower Festival in Bohinj, which is attended by many local inhabitants each year. The presentation of the affiliated clothing was highlighted in the invitation to the opening ceremony, and promoted in an article in the local newspaper, where the story of the Bohinj Bouquet was also retold. When announcing the fashion show featuring the affiliated clothing, the host told the story of the Bohinj Bouquet, associating it with the clothing and emphasising that "people in Bohinj will finally be dressed according to the identity of Bohinj". During the festival, the staff of the Tourist Information Centre, who are also members of the community, and those engaged in the design process wore the affiliated clothes and gave information to local inhabitants and visitors about the inspirational story and the possibilities of buying the items. They did so with enthusiasm, which further contributed to the recognisability of the clothes.

The anticipated positive effect of the design process led to the achievement of the main objective – local inhabitants recognised and accepted the affiliated dress with the applied heritage-based symbol. The possibility of being involved in the design process gave a special relevance to each individual, as well as a sense of belonging. Female members were much more passionately involved in the creation of the women's affiliated clothing image of Bohinj. Moreover, they did not take the task of spreading and strengthening the idea of affiliated clothing as an obligation, but as a pleasure. With that, we also fulfilled the desire to transform local heritage into a newly-made clothing image with a modern feel. With the transformation of the local traditional story into a symbol and comfortable affiliated clothing, individuals (such as tourist guides, vendors of local crafts, and employees of pubs and taverns) have the possibility of promoting the heritage of the community for commercial purposes, while at the same time subconsciously preserving their own heritage. With repeated use and a continuous presence, individuals could have a positive influence on the adoption of new affiliated clothing that could eventually become a trademark of the community.

4 Conclusion

The task of designing an affiliated clothing image extends beyond the field of fashion design. The key moment in the process is the definition and choice of a local heritage story that follows the development strategy, lifestyle and vibe of the destination, and the non-material heritage that is still alive among the local inhabitants and that identifies them.

The newly-designed affiliated clothing expresses the character of the region both stylistically and visually. Thanks to carefully-studied planning and its association with the story, the clothing is in line with the guidelines of the tourist destination, encompassing the elements of not only previous clothing practices and forms, but also current clothing fashions. Through a subtly applied affiliation symbol, it also enables local inhabitants and visitors alike to identify the clothing as coming from *Bohinj*.

Engaging the client and the future wearers of the affiliated clothing in the process of design is also an important factor, as they were in this way included in the decision-making process. This ensured a personal relationship between the users and the clothes, through which identification with the affiliated clothing image was achieved, while the clothing was also more effectively promoted. The individual pieces, especially the cardigans, are understood as a part of their own creation. Including the parties in the design process meant that the wearers became familiar with the story depicted on the garments. This information could thus be passed on to local inhabitants and visitors.

The artificially constructed affiliated clothing image seeks inspiration in cultural heritage that should spread the notion of "traditional" clothing heritage by the means of reiteration and use at tourist, traditional and business events. Thus, the constructed clothing image should be recognised over time as part of the identity of the inhabitants of Bohinj. It

facilitates the integration of local cultural heritage into modern life, and to the recreation of a story through which Bohinj can be identified, thus creating a new tradition.

References

1. KNIFIC, Bojan. *Folklornikom s(m)o vzeli noše: Kostumiranje folklornih skupin – med historično pričevalnostjo in istovetnostjo*. Ljubljana : ZRC, ZRC SAZU, 2010.
2. ČEPAITYTE GAMS, Ona Agota. *Preteklost, dediščina in vprašanje avtentičnosti: (re)konstrukcija dvorca velikih litovskih knezov v Vilni : magistrsko delo* . Univerza v Ljubljani, Filozofska fakulteta, Oddelek za sociologijo, 2012.
3. COPELAND, Raedene, HODGES, Nancy. Exploring masquerade dress at Trindade Carnival: bikinis, beads, and feathers and the emergence of the popular pretty mas. *Clothing and textilles Research journal,* 2014, **32**(3), 186–201, doi: 10.1177/0887302X14531452.
4. BAZIN, Yoann, AUBERT-TARBY, Clémence. Dressing preofessional, an aesthetic experience of professions. *Society and Business Review,* 2013, **8**(3), 251–268, doi: 10.1108/SBR-04-2013-0031.
5. LOWENTHAL, David. *The heritage crusade and the spoils of history*. Cambridge : Cambridge University Press, 1998.
6. LOWENTHAL, David . *The past is a foreign country-revisited*. Cambridge : Cambridge University Press, 2015.
7. BOGATAJ, Janez. *Sto srečanj z dediščino na Slovenskem*. Ljubljana : Prešernova družba, 1992.
8. WANG, Ning. Rethinking authenticity in tourism experience. *Annals of Tourism research,* 1999, **26**(2), 349–370, doi: 10.1016/s0160-7383-(98)00103-0.
9. STEINER, Carol J., REISINGER, Yvette. Understanding existential authenticity. *Annals of Tourism Research,* 2006, **33**(2), 299–318, doi: 10.1016/j.annals.2005.08.002.
10. KULEVIČIUS, Salvijus. Kulturos paveldo autentiškumas: reliatyvistine perspektyva. In *Lietuvos Did˛iosios Kunigaikštystės Valdovų rūmų atkūrimo byla. Vieno po˛iūrio likimas (serija „Lietuvos istorijos studijos", t. 4).* Edited by A. Bumblauskas. Vilnius : Vilniaus universiteto leidykla, 2006, 147–182.
11. HOBSBAWM, Erik John. *Nations and nationalism since 1780*. 2.ed. Cambridge : Cambridge University Press, 2012.
12. MACCANNELL, Dean. Staged authenticity: arrangements of social space in tourist settings. *The american Journal of Sociology,* 1973, **79**(3), 589–603.
13. COSTA, Janeen Arnold, BAMOSSY, Gary J. Le Parc Disney: creating an authentic@ American experience**.** In *NA - Advances in Consumer Research*, **28**. Edited by Mary C. Gilly and Joan Meyers-Levy. Valdosta, GA : Association for Consumer Research, 2001, pp. 398–402.
14. JOHNS, Nick, HOSEASON, Julian. Which way for heritage visitor attractions? In *Quality Issues in Heritage Visitor Attractions*. Edited by I. Jeoman, S. Drummond. Routledge, 2001, pp. 222–242.
15. KOLAR, Tomaž, ŽABKAR, Vesna. A consumer-based model of authenticity: An oxymoron or the foundation of cultural heritage marketing? *Tourism management,* 2010, **31**(5), 652–664, doi: 10.1016/j.tourman.2009.07.010.
16. JENSEN, Øystein, LINDBERG, Frank. The consumption of a tourist attraction: a modern, post-modern and existential encounter perspective. In *Interpretive consumer research: paradigms, methodologies & applications*. Edited by S. C. Beckmann, R. H. Elliott. København : Handelshøjskolens Forlag, 2000, pp. 213–238.
17. RYAN, Cris. Tourist experiences, phenomenographics analysis, post-positivism and neural network software. *International Journal of tourism Research,* 2000, **2**(2), 119–131, doi: 10.1002/(sici)1522-1970(200003/04)2:2<119::aid-jtr193>3.0.co;2-g.
18. HALEWOOD, Chris, HANNAM, Kevin. Viking heritage tourism: authenticity and commodification. *Annals of Tourism Research,* 2001, **28**(3), 565–580, doi: 10.1016/S0160-7383(00)00076-1.
19. SHEPHERD, Robert. Commodification, culture and tourism. *Tourist studies,* 2002, **2**(2), 183–201, doi: 10.1177/146879702761936653.
20. WAITT, Gordon. Consuming heritage: Perceived historical authenticity. *Annals of Tourism Research,* 2000, **27**(4), 835–862, doi: 10.1016/S0160-7383(99)00115-2.

21. NAOI, Taketo. Visitors' evaluation of a historical district: The roles of authenticity and manupulation. *Tourism and Hospitality Research,* 2004, **5**(1), 45–63, doi: 10.1057/palgrave.thr.6040004.
22. COHEN, Erik. Authenticity and commoditization in tourism. *Annals of Tourism Research,* 1988, **15**(3), 371–386, doi: 10.1016/0160-7383-(88)90028-x.
23. GOULDING, Christina. The commodification of the past, postmodern pastiche and the search for authentic experiences at contemporary heritage attractions. *European Journal of Marketing,* 2000, **34**(7), 835–853, doi: 10.1108/03090560010331298.
24. JENKINS, John Michael. Conservation. In *Encyclopedia of tourism*. Edited by J. Jafari. London : Routledge, 2000, pp.103–104.
25. VAN DER BORG, Jan, COSTA, Paolo, GOTTI, Giuseppe. Tourism in European heritage cities. *Annals of Tourism Research,* 1996, **23**(2), 306–321, doi: 10.1016/0160-7383(95)00065-8.
26. KNIFIC, Bojan. Slovenskost pripadnostnega kostumiranja Gorenjcev : Vizualna pričevanja o pripadnostnem kostumiranju Gorenjcev in nekaj misli o gorenjskosti »slovenske narodne noše«. In *Gorenjska. Etnologija in pokrajine na Slovenskem na primeru Gorenjske ali kaj lahko etnologi in kulturni antropologi doprinesemo h kulturni podobi in razumevanju pokrajin na Slovenskem*. Edited by T. Porenta, M. Tercelj Otorepec. Ljubljana : Slovenian Ethnological Society, 2012, pp. 211–240.
27. KNIFIC, Bojan. Vprašanje narodne noše na Slovenskem: njen razvoj od srede 19. stoletja do 2. svetovne vojne. *Etnolog,* 2003, **13**(64), 464–467.
28. MORGADO, Marcia, REILLY, Andrew. Funny kine clothes: The Hawaiian shirt as popular culture. *Paideusus-Journal for interdisciplinary and Cross-Cultural Studies,* 2012, **6**, D1–D24.
29. YOUNG, Patrick. Fashioning heritage: Regional costume and tourism in Brittany, 1890–1937. *Journal of Social History,* 2009, **42**(3), 631–656, doi: 10.1353/jsh.0.0164.
30. FINDELI, Alain. Research through design and transdisciplinarity a tentative contribution to the methodology of design research. In *FOCUSED – Current Design Research Projects and Methods, 4th Swiss Design Network Symposium*. Mount Gurten, Berne, Switzerland, 2008.
31. ECKERT, Claudia, STACEY, Martin. Sources of inspiration: a language of design. *Design Studies,* 2000, **21**(5), 523–538, doi: 10.1016/s0142-694x(00)00022-3.
32. BORJA DE MOZOTA, Brigitte. *Design management : Using Design to Build Brand Value and Corporate Innovation*. New York : Allworth Press, 2003.
33. ŠTERMAN, Sonja. Uniforme kot funkcionalno oblačilo z močjo komunikacije. *Tekstilec,* 2012, **55**(2), 140–147.
34. HOBSBAWM, Eric. Inventing Tradition. In *The invention of Tradition*. Edited by E. Hobsbawm, T. Ranger. Cambridge : Cambridge Univerity Press, 1983, pp.1–15.
35. KNEŽEVIĆ, Radule. *Politička kultura*. Podgorica : Crnogorska akademija nauka i umjetnosti, 2012.
36. SKOBERNE, Peter. Bohinjski šopek. In *Bohinjski zbornik II. Posvečeno 12-letnici muzejskega društva Žiga Zois Bohinj ter 20-letnici sodelovanja Bohinjcev v osamosvojitveni vojni*. Edited by M. Serajnik, I. Lapajne, K. Langus. Občina Bohinj; Turizem Bohinj : Tiskarna Medium Bohinj, 2012, pp. 23–27.
37. CVETEK, Marija. Rastlinski svet v bohinjskem folklornem pripovedništvu. In *Bohinjski zbornik II. Posvečeno 12-letnici muzejskega društva Žiga Zois Bohinj ter 20-letnici sodelovanja Bohinjcev v osamosvojitveni vojni*. Edited by M. Serajnik, I. Lapajne, K. Langus. Občina Bohinj; Turizem Bohinj : Tiskarna Medium Bohinj, 2012, pp. 28–41.
38. CUREDALE, Robert. *Design thinking: process and methodes manual.* Topanga, CA : Design Community College Inc., 2013.

Mohammad Neaz Morshed[1], Shamim Al Azad[2], Hridam Deb[1], Ashraful Islam[2], Xiaolin Shen[1]
[1] Wuhan Textile University, School of Textile Science and Engineering, State Key Laboratory for New Textile Materials and Application of Hubei Province, Wuhan, 430073, P. R. China
[2] Wuhan Textile University, College of Chemistry and Chemical Engineering, Wuhan, 430073, P. R. China

Eco-friendly UV Blocking Finishes Extracted from *Amaranthus viridis* and *Solanum nigrum*

Okolju prijazni apreturi iz izvlečkov Amaranthus viridis in Solanum nigrum za zaščito pred UV žarki

Original Scientific Article/*Izvirni znanstveni članek*
Received/*Prispelo* 01-2018 • Accepted/*Sprejeto* 05-2018

Abstract

This research work deals with a qualitative analysis of extracts from *Amaranthus viridis* and *Solanum nigrum* plants as eco-friendly ultraviolet (UV) blocking finishes. The presence of flavonoid and phenolic contents in the plant extracts and the influence of concentrations towards UV blocking was studied. The plant extracts were obtained through solvent (aqueous and methanolic) extraction and coated onto cotton fabrics with the pad-dry-cure method. UV-visible and CIELAB spectroscopy analysis were carried out for the quantitative measurement of UV blocking and sequential analysis. The results show that loading of selected extracts on the fabric samples results in a significant enhancement in UV blocking. The treated fabrics show exceptional UV blocking in both UV-A and UV-B region, where the highest anti-UV values were obtained when the fabrics were treated with methanolic extracts. Furthermore, a considerable influence on CIELAB coordinates was found inordinate for methanolic extracts treated fabric compared to aqueous extracts.

Keywords: *Amaranthus viridis*, *Solanum nigrum*, medicinal plants, UV blocking, natural finishes

Izvleček

Ta raziskava obravnava kvalitativno analizo izvlečkov iz rastlin Amaranthus viridis in Solanum nigrum kot okolju prijazne ultravijolične (UV) zaščitne apreture. Proučevana je bila prisotnost flavonoidnih in fenolnih snovi v rastlinskih izvlečkih ter vpliv koncentracije na UV zaščito. Z izvlečki, pridobljenimi z ekstrakcijami rastlin v topilih (v vodi in metanolu), so bile impregnirane bombažne tkanine. Na podlagi spektroskopskih meritev UV-vis in CIELAB je bila kvantitativno ocenjena UV zaščita in izdelana analiza. Rezultati kažejo, da prisotnost izbranih izvlečkov na vzorcih tkanin znatno izboljša UV zaščito. Obdelane tkanine imajo izjemno UV zaščito v obeh območjih, UV-A in UV-B, najvišje vrednosti UV zaščite pa so bile dobljene na tkanini, obdelani z metanolnimi izvlečki. Poleg tega je bila ugotovljena znatna razlika v CIELAB koordinatah med tkaninami, obdelanimi z metanolnimi izvlečki, v primerjavi s tkaninami, obdelanimi z vodnimi izvlečki.

Ključne besede: Amaranthus viridis, Solanum nigrum, zdravilne rastline, UV zaščita, naravne apreture

1 Introduction

UV radiations (UVR) that contain electromagnetic radiations can damage human skin and may result in chronic and non-chronic diseases [1]. Research shows that 90% of non-melanoma skin cancer is a consequence of the exposure to UV radiation. UVA can penetrate deeply into the skin and can damage

Corresponding author/*Korespondenčni avtor:*
Mohammad Neaz Morshed
E-mail: engr.neazmorshed@yahoo.com
ORCID: 0000-0003-2820-1333

the cells of DNA. An overdose of UVB radiations induces skin cancer, sun-burning, and cataracts, which have more serious effects than UVA [2]. The erythemal spectral effectiveness of UV radiation increases by 1000 times as the wavelength changes from UVA (315 nm) to UVB (300 nm) [3]. Wearing clothes is one of the protections recommended by physicians and medical experts to reduce or block the negative effects of UV radiation to human skin [4, 5].

Textiles can be used to provide protection to a product or wearer from UV radiation. To do so effectively, the textile requires the ability to resist UV transmission through the constituent fibres or the penetration of radiation through the fabric interstices. This means that the fibres themselves should be UV resistant and the fabric structure should have good breathability, yet low optical transparency.

Many physical and chemical factors are interrelated with the effectiveness of UV blocking [5, 6]. Various aspects are allied with the relative amount of radiation that is reflected, absorbed and transmitted through the fibre. They can include the type and selection of the fibre, smoothness of the fibre surface, surface area, presence of dyes and finishing, an incorporation of UV absorber [7]. To increase UV blocking, UV resistant particles can be applied as a finishing treatment. Often, such fabric finishes are a part of the dyeing process or an additional stage after the dyeing. They provide lustre and microscopic surface texture to reduce the UV penetration by reflecting, absorbing and/or scattering the radiation. Since last decades, different kinds of organic and metal oxide-based UV absorbers have been introduced to render the UV blocking property of textiles. Among them, titanium dioxide and zinc oxide-based finishing agents are widespread due to their effects on the UV blocking property [8]. Zinc oxide is always used with titanium dioxide in sunscreens because of its high refractive index [9]. However, the metal-based finishes tend to be non-biodegradable and they represent a threat during interaction with nature. The protection from UV radiations using plant-based natural finishing agents on textile materials is thus a potential solution with great benefits. UV protection has been imparted to fabrics using different types of extracts obtained from natural sources. These extracts are found mostly in ratanjot (*Onosma echioides*), annatto (*Bixa orellana*), manjistha (*Rubia cordifolia*), banana peel (*Musa, cv. Cavendish*) [10] and babool (Acacia Arabica) plants [11]. Silk and wool fabrics have been made to protect from UV radiations by having applied on them the extracts from neem and eucalyptus [12, 13]. Although several natural dyes have been studied with respect to UV protection and antibacterial properties [14], limited work has been reported on medicinal plant extracts for UV protection properties.

In this study, two medicinal plant extracts were tested as finishes for UV blocking. It was reported that flavonoids and phenolics present in Ray plants could shelter the plants from UV radiations [15]. However, with a thorough review of literature based on our best capabilities, we came to the conclusion that a UV blocking finish by using *Amaranthus viridis* and *Solanum nigrum* plant extracts is a nobel and sustainable approach.

2 Experimental

2.1 Materials

The cotton fabric used in this experiment was purchased from Guangdong overflow of textile co., Ltd (China). The average weight of the fabric was 200 g per square meter (GSM), thread density was 78 ends per inch (EPI) and 60 picks per inch (PPI), warp and weft count were 28 Ne. The mean ultraviolet protection factor (UPF) of the bleached fabric was 8.7. All the reagents used in this experiment were purchased from Sinopharm chemical reagent co., Ltd (China) of analytical grade and used as received without further purification. The water used throughout the experiment was purified using a Milli-Q Plus-185 water purification system (Millipore, Bedford, MA) with the resistivity higher than 18 MΩ cm.

2.2 Methods

Preparation of extracts

The plant leaves were collected and dried naturally at room temperature and powdered using an electric grinder. The powdered materials (100 g/l) were stirred with 95% methanol for 48 h at room temperature, blended with a continuous magnetic force stirrer as explained by Russo et al [16]. The aqueous extracts were prepared by wringing the dried plant powders (50 g/l) in distilled water for 30 mins, followed by heating at 95 °C for 40 min and vacuum extraction using standard filter paper. The extracts were filtered and concentrated to remove the solvents at 75 °C for 4 h and freeze-dried as the report in Nostro et al [17].

Determination of flavonoid and phenolic content

A diluted solution of plant extracts containing flavonoids was mixed with a requisite amount of 5% (w/w) $NaNO_2$ and 30% (v/v) ethanol for 5 min, and then a few drops of 10% $AlCl_3$ were added and mixed all together. A few minutes later, 5 ml of NaOH (1M) was added. The solution was then diluted to 25 ml with 30% (v/v) ethanol. After standing for 10 min, the absorbance of the solution was measured at 430 nm using a UV-visible spectrophotometer. The results were expressed in (quercetin/mg)/(dry-weight/g) by comparison with the quercetin standard curve, which was made under the same condition. On the other hand, the total phenolic content was determined using Folin-Ciocalteu reagents with the analytical grade gallic acid as the standard. Typically, 1 ml of extract or standard solution (0–500 mg/l) was added to deionized water (10 mL) and Folin-Ciocalteu phenol reagents (1.0 ml). After 5 minutes, 20% $NaCO_3$ (2.0 mL) was added to the mixture. After being kept in total darkness for 1 h, the absorbance was measured at 750 nm using a UV-visible spectrophotometer. The amounts of total phenolic contents were calculated using the gallic acid calibration curve. The results were expressed as gallic acid equivalents (GAE)g/g of dry plant matter as described in Kolasec et al and Gasemzadeh et al [18, 19].

Application of plant extracts on cotton fabric

Plant extracts were applied on a bleached cotton fabric by dispersing them in distilled water, followed by padding and drying on a laboratory scale padder and stenter machines according to the design of experiments explained by Huang et al (2010) and Wang et al (2006) [20, 21]. It was decided to treat the sample cotton fabric at different concentrations of extracts (1 g/l, 2 g/l, 4 g/l and 8 g/l). The padding pressure for all samples was 3.0 bars with 70% pick-up. The drying temperature of aqueous extracted finishes was 90 °C and 25 °C for methanolic extracted finishes.

Characterizations

The UV blocking of treated cotton fabrics and other UV-visible spectroscopic measurements were taken by using an Ultraviolet Transmittance Analyzer (HD902C, Nantong Hongda Experiment Instruments Co., Ltd, China) with integrating sphere according to corresponding standard methods. The ultraviolet protection factor (UPF) was computed as the ratio of ultraviolet radiation (UV-R) irradiance at the detector with no test sample to the UV-R irradiance at the detector with a test sample present as shown in equation 1 [22]:

$$UPF = \frac{\sum_{280\ nm}^{400\ nm} E_\lambda \times S_\lambda \times \Delta\lambda}{\sum_{280\ nm}^{400\ nm} E_\lambda \times S_\lambda \times T_\lambda \times \Delta\lambda} \quad (1)$$

The percentage of blocking in the UV-A and UV-B region was determined with equations 2 and 3:

$$UVA\ blocking = \frac{\sum_{315\ nm}^{400\ nm} \times T \times \Delta\lambda}{\sum_{315\ nm}^{400\ nm} \times T \times \Delta\lambda} \quad (2)$$

$$UVB\ blocking = \frac{\sum_{280\ nm}^{315\ nm} \times T \times \Delta\lambda}{\sum_{280\ nm}^{315\ nm} \times \Delta\lambda} \quad (3)$$

Where E_λ is relative erythemal spectral effectiveness, S_λ is solar spectral irradiance, T_λ is average spectral transmittance of the test sample, $\Delta\lambda$ is measured wavelength interval (nm) and T is average spectral transmission of the specimen.

The CIE whiteness values of samples were determined according to the AATCC 110-2005 methods by using Macbeth Color Eye 7000A (Gretag Macbeth Company, USA).

3 Results and discussion

3.1 Total flavonoid and phenolic contents in plant extracts

The quantity of the overall flavonoid and phenolic content present in extracts of plants is shown in Figure 1. The results indicate that the total flavonoid (mg QE/g) and phenolic (mg GAE/g) contents of *AV* aqueous extracts were 47 mg QE/g and 15 mg GAE/g, and of methanolic extracts 72 mg QE/g and 36 mg GAE/g, respectively. A similar scenario was noticed at *SN* extracts. The overall amount of flavonoid and phenolic content present in *AV* was higher than at *SN*. The analysis perceived that the flavonoid and phenolic contents were higher in methanolic extracts for both plants as contrasted to aqueous extracts. This may result from the fact that, water is not as effective as methanol in extracting flavonoid

or phenolic contents from these two plants, despite the inclusive yield of the powder extracted from the plants being higher in water compared to that in methanol.

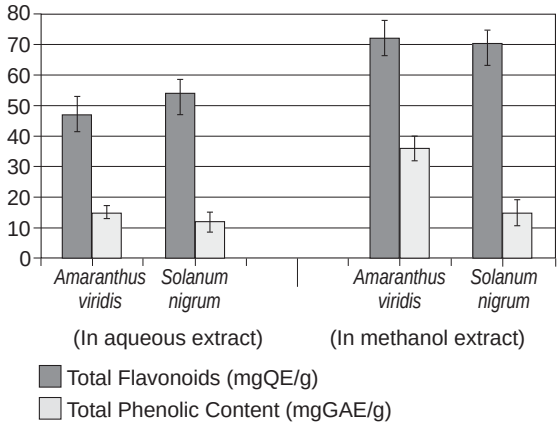

Figure 1: Total flavonoid and phenolic content present in extracts from Amaranthus viridis and Solanum nigrum

This may be explained by the improved solubility of flavonoid and phenolic contents in methanol and that of other plant contents in the aqueous solution. Such behaviour of both extracts results from the methanolic system containing more flavonoid and phenolic contents and other conjugated systems as compared to the aqueous system. So, the more is the system conjugated, the better is the UV protection (UPF) rating of a material.

3.2 UV blocking property of treated cotton fabric

The influence of extracts and their concentration on UPF is shown in Figure 2. The results show that the cotton fabric treated with both plant extracts maintained UV blocking capabilities. By comparing, contrasting and analysing the UPF value of untreated and treated fabric, it was seen that the UPF value increased with the increased concentration of the applied extract.

In the case of aqueous extracts of *AV,* the recorded UPF values were 10.6, 12.2, 18.8 and 36.2 against the concentration of extracts of 1, 2, 4 and 8 g/l respectively, which specifies that an increase in UPF can be achieved with an increase in concentration. For methanolic extracts, the UPF rating is significantly influenced by the concentration of extracts. In a typical run, the UPF values were 58.8, 125.2, 270.6 and 464.1 against the concentration of extracts of 1, 2, 4 and 8 g/l. A similar phenomenon was observed for *SN*. The highest UPF, i.e. 231, was found for 8 g/l of methanolic extracts of *SN*. Comparing the UPF rating between *AV* and *SN*, it can be seen that in the case of an aqueous extraction, there is no significant variation, whereas in the case of a methanolic extraction, *AV* gave the highest rating of 464.1 at 8 g/l, which is even more extraordinary than the highest yield of *SN*, i.e. 231. The fabric finished with both plant extracts rendered higher UVB than UVA protection (Figures 3 and 4).

The latter is also the main requirement of any UVR blocker, as UVB radiations cause greater erythemal damage and hence bear greater weight in calculating UPF. Comparing the UVA and UVB blocking of *AV* and *SN,* no significant difference was noticed between them, apart from the fact that *AV* showed much lower UVA blocking, i.e. 54.8%, at 1 g/l compared to *SN*. It became obvious that the fabrics treated with the methanolic extract show

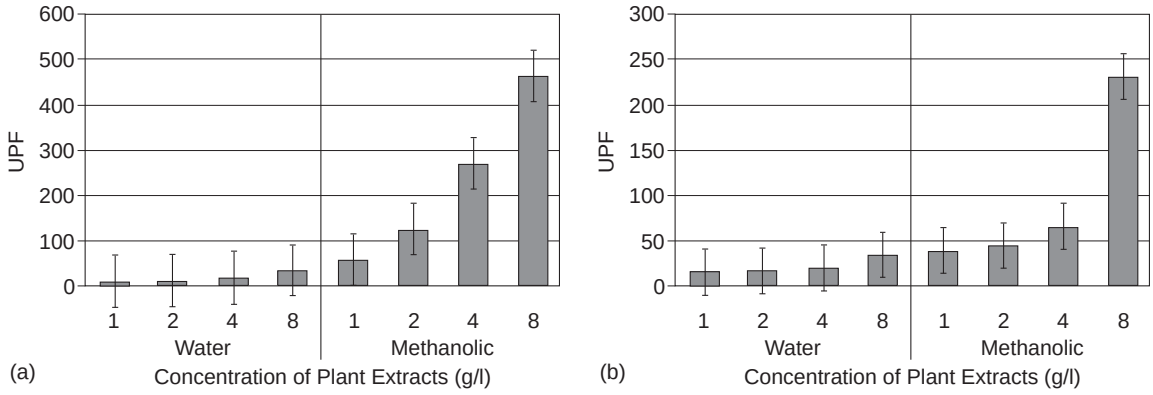

Figure 2: Mean ultraviolet protection factor (UPF) of cotton fabric treated with Amaranthus viridis (a) and Solanum nigrum (b) extracts

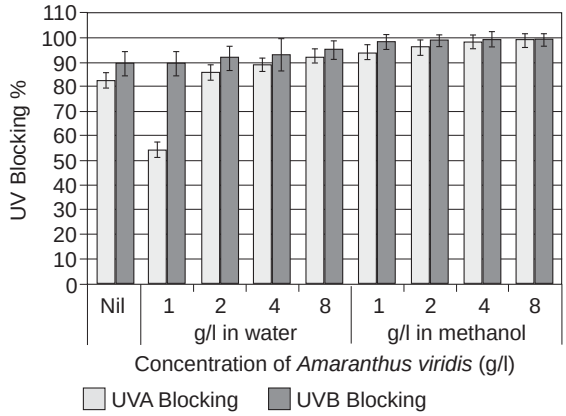

Figure 3: Blocking of UV radiations in UVA and UVB regions by different concentrations of Amaranthus viridis

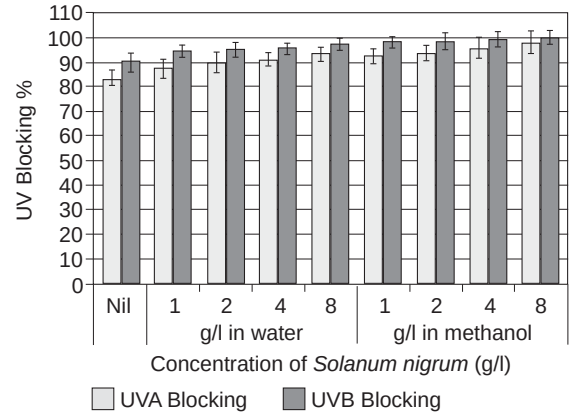

Figure 4: Blocking of UV radiations in UVA and UVB regions by different concentrations of Solanum nigrum

better results than the samples treated with the aqueous extract. The UV blocking properties of extracts could be attributed to the presence of total flavonoid and phenolic contents present in the methanolic extract. The UV blocking properties are better in the methanolic extract than in the aqueous extract, as the system responsible for a higher UPF rating is more conjugated in the methanolic extract.

3.3 CIELAB analysis of treated fabrics

The decrease in CIELAB analysis can be seen in Table 1.

CIELAB spectroscopic analysis of treated fabric has been compared and contrasted with untreated fabric. The L*, a*, and b* of the untreated fabric was measured 86,0.4, and 0.68, respectively. The CIELAB analysis indicates the presence of colouring

Table 1: CIELAB spectroscopic analysis of treated cotton fabric

Treatment	Extraction method	Conc. [g/l]	ΔL	Δa	Δb
Raw fabric	–		86	0.4	0.68
Treated with extracts of *Amaranthus viridis*	Aqueous	1	0.00	–0.14	1.09
		2	0.01	–0.15	1.83
		4	–0.136	–0.17	3.62
		8	–2.47	–0.11	5.49
	Methanolic	1	–2.24	–0.74	5.95
		2	–5.70	–2.55	11.34
		4	–6.44	–3.69	14.45
		8	–9.37	–4.14	18.75
Treated with extracts of *Solanum nigrum*	Aqueous	1	0.23	–0.34	1.67
		2	–0.35	–0.63	3.58
		4	–0.40	–0.73	3.82
		8	–2.00	–1.03	7.41
	Methanolic	1	–1.21	–1.07	4.77
		2	–1.69	–0.65	5.78
		4	–2.78	–1.70	9.57
		8	–4.42	–2.35	13.31

materials with the increased concentration. Methanolic extracts, when compared with aqueous extracts, were found to cause a higher influence in colour coordinates, which may be attributed to higher contents of flavonoids and phenolics, and subsequent UV blocking. The Δa and Δb coordinates of CIELAB were also influenced by different concentrations of extracts, thus reducing the brightness. However, Figures 3 and 4 show that both plants extract are able to impart superior UV blocking in the UV-A and UV-B region, which was proved by the UPF analysis. With a 4 g/l concentration of *SN* plant extracts, UPF increased from 8.7 to 19.9 (UPF rating 15–20 is considered as "good" according to the "Australian Radiation Protection and Nuclear Safety Agency" [5, 6]).

The increase in UPF mainly results from the components in extracts, which were successfully deposited on the cotton fabric. However, methanolic extracts, when applied on fabric samples, rendered exceptional UPF. The values close to 60 were achieved by using only 1 g/l of methanolic extracts; hence, concentrations much lower than that can be used. The methanolic extracts of *AV* showed excellent UPF.

At a minimum concentration of 2 g/l, the methanolic extracts of *SN* provided UPF of about 40, which is above the minimum UPF value considered "very good" UV protection by textile clothing. As methanolic extracts influence the CIELAB coordinates, this method can provide a sustainable solution, and the concentration of the plant extracts can be increased to obtain a much higher UPF. The use of fluorescent brightening agents may also be made in the combination with plant extracts to further optimize UPF as well as fabric whiteness [23]. The fastness of the applied finishes was measured for household laundry wash and it was noticed that the UPF values decreased adversely, which is a great drawback of natural finishes (Figure 5). Further experiments and analysis are needed to introduce sustainable fastness of the finishes.

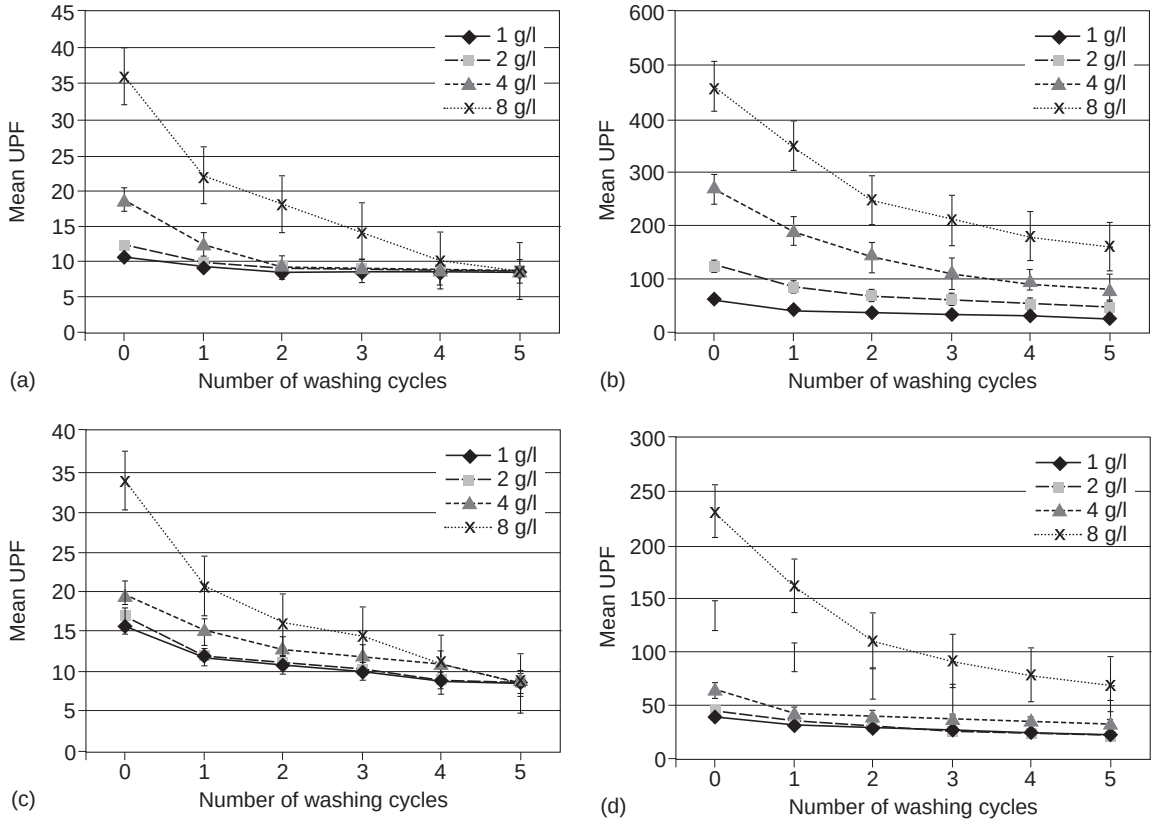

Figure 5: Fastness of applied finishes after household laundry wash treated with water (a) and methanolic (b) extracts of Amaranthus viridis, and water (c) and methanolic (d) extracts of Solanum nigrum

4 Conclusion

This work investigated and analysed a comparative performance of UV blocking of a cotton fabric treated with different natural finishes. Aqueous and methanolic extracts of two medicinal plants were applied on prepared bleached fabrics. About 99% of UVA and UVB rays were blocked. Methanolic extracts demonstrated better UV blocking property than aqueous extracts, causing a higher shade change in fabric color at the same time. This research is worthwhile for the preparation of a cost-effective and environmentally friendly material to formulate the UV blocking properties of textiles. Further research on the durability factor of extracted finishes and shade variation of the treated textile material is required to ensure a sustainable commercial application.

Acknowledgments

The authors wish to express their appreciation to the Hubei provincial department of education for providing support through the key project (no.: 20121701). They would also like to thank the staff of analysis and measurement centre as well as the technological institute of the Wuhan textile university for their help at handling the laboratory equipment.

References

1. ANDERSON, R. Rox, PARRISH, John A. The optics of human skin. *The Journal of Investigative Dermatology*, 1981, **77**(1), 13–19, doi: 10.1111/1523-1747.ep12479191.
2. REINERT, G., FUSO, F., HILFIKER., Rolf, SCHMIDT., E. UV-protecting properties of textile fabrics and their improvement. *Textile Chemist & Colorist*, 1997, **29**(12), 36–43.
3. VENTURA, Liliane, MASILI, Mauro, SCHIABEL, Homero. Ocular UV protection: revisiting safe limits for sunglasses standards. In *Proceedings of SPIE - The International Society for Optical Engineering* San Francisco, 2013, **8567**, doi : 10.1117/12.2000355.
4. DAVIS, S. G., CAPJACK, L., KERR, Nancy, FEDOSEJEVS, Robert. Clothing as protection from ultraviolet radiation: which fabric is most effective? *International Journal of Dermatology,* 1997, **36**(5), 374–379, doi: 10.1046/j.1365-4362.1997.00046.x.
5. KRIPKE, M. L. Sun and ultraviolet ray exposure. In *Cancer prevention*. Edited by V. T. DeVita, S. Hellman, S. A. Rosenberg. Philadelphia : Lippincott, 1989, pp. 1–18.
6. STANKOVIĆ, Snežana B., POPOVIĆ, Dušan, POPARIĆ, Goran B., BIZJAK, Mateja. An ultraviolet protection factor of gray-state plain cotton knitted fabrics. *Textile Research Journal*, 2009, **79**(11), 1034–1042, doi: 10.1177/0040517508102016.
7. AATCC 183 Transmittance or blocking of erythemally weighted ultraviolet radiation through fabrics, Appendix B. *AATCC Technical Manual*, 2012, **87**.
8. ACHWAL, W. B. Use of UV absorbers in textiles. *Colourage*, 1995, **10**, 44–45.
9. MORSHED, M. N., SHEN, X., DEB H., AZAD, S. A., ZHANG X., LI, R. Sonochemical fabrication of nanocryatalline titanium dioxide (TiO_2) in cotton fiber for durable ultraviolet resistance. *Journal of Natural Fibers* (2018), doi: 10.1080/15440478.2018.1465506.
10. GANTZ, G. M., SUMNER, W. G. Stable ultraviolet light absorbers. *Textile Research Journal*, 1957, **27**(3), 244–251, doi: 10.1177/004051755702700310.
11. CHATTOPADHYAY, S. N., PAN, N. C., ROY, A. K., SAXENA, S., KHAN, A. Development of natural dyed jute fabric with improved colour yield and UV protection characteristics. *The Journal of The Textile Institute*, 2013, **104**(8), 808–818, doi: 10.1080/00405000.2012.758352.
12. SAMANTA, K. Kartick, BASAK, Santanu, CHATTOPADHYAY, Sajal Kumar. Eco-friendly coloration and functionalization of textile using plant extracts. In *Roadmap to sustainable textiles and clothing*. 2014, pp. 263–287. Edited by Subramanian Senthilkannan Muthu. Singapore : Springer, doi: 10.1007/978-981-287-110-7_10.
13. VAIDEKI, K., JAYAKUMAR, S., NITHYA, E., RAJENDRAN, Radhai. Study on the effect of RF plasma pretreatment on the antimicrobial efficacy of neem leaf extract processed cotton fabric. *Science and Technology against Microbial Pathogens Research, Development and Evaluation*, 2011, 259–265, doi : 10.1142/9789814354868_0051.
14. MONGKHOLRATTANASIT, Rattanaphol, KRYŠTŮFEK, Jiří, WIENER, Jakub, VIKOVÁ, Martina. Dyeing, fastness, and UV protection properties of silk and wool fabrics dyed with eucalyptus

leaf extract by the exhaustion process. *FIBRES & TEXTILES in Eastern Europe*, 2011, **19**(3), 94–99, doi: 10.1080/00405001003722369.

15. VAIDEKI, K., JAYAKUMAR, S., RAJENDRAN, Radhai, THILAGAVATHI, G. Investigation on the effect of RF air plasma and neem leaf extract treatment on the surface modification and antimicrobial activity of cotton fabric. *Applied Surface Science*, 2008, **254**(8), 2472–2478, doi: 10.1016/j.apsusc.2007.09.088.
16. BURCHARD, P., BILGER, W., WEISSENBÖCK, G. Contribution of hydroxycinnamates and flavonoids to epidermal shielding of UV–A and UV–B radiation in developing rye primary leaves as assessed by ultraviolet–induced chlorophyll fluorescence measurements. *Plant, Cell & Environment*, 2000, **23**(12), 1373–1380, doi: 10.1046/j.1365-3040.2000.00633.x.
17. RUSSO, Alessandra, CARDILE, Venera, LOMBARDO, Laura, VANELLA, Luca, VANELLA, Angelo, GARBARINO, Juan Antonio. Antioxidant activity and antiproliferative action of methanolic extract of Geum quellyon Sweet roots in human tumor cell lines. *Journal of Ethnopharmacology*, 2005, **100**(3), 323–332, doi: 10.1016/j.jep.2005.03.032.
18. NOSTRO, Antonia, GERMANO, Maria Paola, D'ANGELO, V., MARINO, Andreana, CANNATELLI, M. A. Extraction methods and bioautography for evaluation of medicinal plant antimicrobial activity. *Letters in Applied Microbiology*, 2000, **30**(5), 379–384, doi: 10.1046/j.1472-765x.2000.00731.x.
19. KOSALEC, Ivan, BAKMAZ, Marina, PEPELJNJAK, Stjepan, VLADIMIR-KNEZEVIC, Sanda. Quantitative analysis of the flavonoids in raw propolis from northern Croatia. *ACTA Pharmaceutica,* 2004, **54**(1), 65–72.
20. GHASEMZADEH, Ali, JAAFAR, Hawa Ze, RAHMAT, Asmah. Antioxidant activities, total phenolics and flavonoids content in two varieties of Malaysia young ginger (Zingiber officinale Roscoe). *Molecules*, 2010, **15**(6), 4324–4333, doi: 10.3390/molecules15064324.
21. HUANG, Hsiu-Chen, SYU, Kai-Yang, LIN, J. G. Chemical composition of *Solanum nigrum* linn extract and induction of autophagy by leaf water extract and its major flavonoids in AU565 breast cancer cells. *Journal of agricultural and food chemistry*, 2010, **58**(15), 8699–8708, doi : 10.1021/jf101003v.
22. WANG, Xiuije, YUAN, Shulan, WANG, Jing, LIN, Ping, LIU, Guanjian, LU, Yanrong, ZHANG, Jie, WANG, Wendong, WEI, Yuquan. Anticancer activity of litchi fruit pericarp extract against human breast cancer in vitro and in vivo. *Toxicology and Applied Pharmacology*, 2006, **215**(2), 168–178, doi: 10.1016/j.taap.2006. 02.004.
23. COX CREWS, Patricia, HUSTVEDT, Gwendolyn. The ultraviolet protection factor of naturally-pigmented cotton. *The Journal of Cotton Science,* 2005, **9**, 47–55.
24. LANTER, J. Properties and evaluation of fluorescent brightening agents. *Journal of the Society of Dyers and Colourists,* 1966, **82**(4), 125–132. doi: 10.1111/j.1478-4408.1966.tb02708.x.

Xiaoxin Zuo, Ren-Cheng Tang
Soochow University, College of Textile and Clothing Engineering, National Engineering Laboratory for Modern Silk, 199 Renai Road, Suzhou 215123, China

Study of the Disperse Dyeing Properties of Low-Temperature Dyeable Polyesteramide Fibre

Raziskava lastnosti nizkotemperaturnega barvanja poliesteramidnih vlaken z disperznimi barvili

Original Scientific Article/*Izvirni znanstveni članek*
Received/*Prispelo* 01-2018 • Accepted/*Sprejeto* 05-2018

Abstract

Polyethylene terephthalate (PET) is the most important synthetic fibre, and is widely used in the textile industry. However, the disperse dyeing of PET fibre must be carried out at a high temperature and under high pressure. This leads to high energy consumption and damage to the wool in a PET/wool blend. Some copolyesters and novel polyesters that can be dyed under normal pressure have proven to be good alternatives to PET. In this work, the low-temperature dyeable polyesteramide fibre was used, and its disperse dyeing properties were studied in terms of adsorption isotherms, the temperature-dependence of uptake, uptake rate, migration ability, building-up property, and colour fastness of disperse dyes. The adsorption isotherms of disperse dyes on polyesteramide fibre followed the Nernst adsorption model. Disperse dyes exhibited high exhaustion at 100 °C, indicating the good dyeability of polyesteramide fibre under atmospheric pressure. The uptake of dyes by polyesteramide fibre was considerably faster than that of PET fibre, while the majority of dye uptake occurred in the temperature range of 70 to 90 °C. Azo disperse dyes exhibited higher adsorption saturation and better a building-up property than anthraquinone dyes. Disperse dyes had a good migration ability on polyesteramide fibre, and the colour fastness of the dyed polyesteramide fabrics was also satisfactory.

Keywords: dyeing under normal pressure, partition, adsorption, dyeing rates, energy saving

Povzetek

Polietilentereftalat (PET) je najpomembnejše sintetično vlakno, ki ga v tekstilni industriji uporabljajo za različne namene. Barvanje vlaken iz PET z disperzijskimi barvili poteka le pri visoki temperaturi in visokem tlaku, kar predstavlja visoko porabo energije ter povzroči poškodbe volne v mešanicah PET/volna. Nekatera kopoliestrska vlakna in vlakna iz novih tipov poliestrov, ki so obarvljiva pri normalnem tlaku, so se izkazala kot dobra alternativa vlaknom PET. V članku je predstavljeno nizkotemperaturno barvanje poliesteramidnih vlaken, raziskovane so bile adsorpcijske izoterme, temperaturna odvisnost navzemanja, hitrost navzemanja, sposobnost migracije in barvna obstojnost disperzijskih barvil. Adsorpcijske izoterme disperznih barvil na poliesteramidna vlakna sledijo Nernstonovemu adsorpcijskemu modelu. Disperzna barvila so pokazala visoko izčrpanje pri 100 °C, kar je razkrilo dobro obarvanje poliesteramidnih vlaken pri atmosferskem tlaku. Vlakna iz poliesteramida so veliko hitreje navzemala barvila kot vlakna iz PET, večina barvila se je adsorbirala v temperaturnem območju od 70 do 90 °C. Azo disperzijska barvila so dala višjo nasičenost in adsorpcijo kot antrakinonska barvila. Disperzna barvila so pokazala dobro sposobnost migracije v poliesteramidna vlakna. Tudi barvna obstojnost poliestramidnih pletiv je bila zadovoljiva.

Ključne besede: barvanje pri normalnem tlaku, porazdelitev, adsorpcija, hitrost barvanja, prihranek energije

Corresponding author/*Korespondenčni avtor:*
Prof. Dr. Ren-Cheng Tang
E-mail: tangrencheng@suda.edu.cn

Tekstilec, 2018, ***61****(2), 101-109*
DOI: 10.14502/TEKSTILEC2018.61.101-109

1 Introduction

Textile processing uses an enormous amount of electricity, fuel, water and chemicals, and produces a significant amount of contaminated effluent [1–4]. Reducing energy and water consumption, as well as hazardous industrial effluents, represents the biggest sustainability challenge for the textile industry. In order to reduce energy consumption, low-temperature scouring and dyeing, and emerging techniques have become part of the industry's strategy, and attracted a great deal of attention [1, 2, 5].

Polyethylene terephthalate (PET) is the most important synthetic fibre, and is predominant on the man-made fibre market [5]. PET fibre has been widely used in clothing, home textiles and other industries due to its numerous outstanding properties, such as high strength, good thermal and chemical stability, and excellent wrinkle resistance, as well as its relatively low price [6]. However, it also has some shortcomings, such as low moisture regain, poor antistatic properties and poor dyeability due to its high structural regularity and crystallinity, lack of reactive dyeing sites and polar groups, and high hydrophobicity [6]. The biggest disadvantage of the wet processing of PET fibre is that it must be dyed under a high pressure at 125–130 °C in a weakly acidic condition, or at about 110 °C in the presence of carriers. High- temperature dyeing not only consumes a great deal of energy, but also requires expensive dyeing equipment and causes potential risks. When used, most carriers are associated with toxicological issues [7]. In addition, the high-temperature dyeing of a PET/wool blend leads to the damage of the wool.

The low-temperature dyeing of PET is a very difficult task if conventional dyes and chemicals are used. One successful approach to address this issue is to modify PET fibre for enhanced dyeability. The introduction of third and fourth monomers during the stage of polyester synthesis is a basic strategy. The copolymerisation of PET with dimethyl 5-sulfoisophthalate sodium salt as the third monomer confers cationic dyeability to PET fibre [8]. The addition of the fourth monomer, such as polyethylene glycol, 1,3-propanediol, 2-methyl-1,3-propanediol, or 2,2-dimethyl-1,3-propanediol, further improves the dyeability of PET fibre at the boiling point under normal pressure [8]. Today, cationic dyeable polyester (CDP) is deemed an industrial success. On the other hand, the application of new polyester polymers, such as polytrimethylene terephthalate (PTT), polybutylene terephthalate (PBT) and polylactic acid (PLA), is also an effective method for obtaining low-temperature dyeable polyester fibres [1, 5, 9].

In recent years, a new type of polyesteramide copolymer has been developed as an alternative to PET [10, 11]. Polyesteramide copolymer can be synthesised through the polycondensation reaction of ethylene glycol terephthalate and aliphatic amide [10, 11], and has both ester and amide blocks on its backbone. Polyesteramide fibre can be manufactured by using the melting spinning of polyesteramide chips. Previous researchers have found that while polyesteramide fibre has a lower tensile strength and whiteness than PET fibre [10–12], it possesses better dyeability, softness and anti-pilling properties [13, 14]. Very importantly, the incorporation of amide groups into an ester main chain results in a decrease in structural regularity and an increase in the amorphous region of the fibre. The glass transition and melting temperatures of polyesteramide fibre are 68–72 °C and 235 °C, respectively, which are lower than those of PET fibre [13]. These factors make polyesteramide fibre dyeable using disperse dyes at the boiling point under normal pressure.

The development of polyesteramide fibre provides the possibility of manufacturing pure polyester textiles as well as natural fibre (e.g. wool, silk and cotton) blends using a low-temperature dyeing technique, with the added advantage of energy savings. Although preliminary studies demonstrated the disperse dyeability of polyesteramide fibre [13, 14], more detailed dyeing properties need to be studied with the aim of better understanding the mechanism of disperse dyeing, and providing assistance in the selection of dyes and the determination of dyeing conditions. In this work, the adsorption isotherms of disperse dyes on polyesteramide fibre were studied in order to understand the mechanisms of dyeing, and the temperature-dependence of uptake, uptake rate, migration ability, build-up property and colour fastness of disperse dyes on polyesteramide fibre were assessed.

2 Materials and methods

2.1 Materials

Polyesteramide knitted fabric (178 g/m^2) was supplied by Sinopec Yizheng Chemical Fibre Co. Ltd.,

Table 1: Characteristics of disperse dyes

Trade name	C.I. disperse	Energy level	Structure class
Disperse Yellow Brown S-2RFL	Orange 30	High	Azobenzene
Disperse Scarlet S-BWFL	Red 74	High	Azobenzene
Longsperse Blue SE-2R	Blue 183	Medium	Azobenzene
Disperse Navy H-GL	Blue 79	High	Azobenzene
Disperse Brown 3R	Brown 1	High	Azobenzene
Disperse Red 3B	Red 60	Low	Anthraquinone
Terasil Pink 4BN	Red 11	Low	Anthraquinone
Disperse Violet HRFL	Violet 31	High	Anthraquinone
Disperse Blue 2BLN	Blue 56	Low	Anthraquinone

China. Fine denier PET knitted fabric (182 g/m^2) was obtained from Suzhou TA&A Ultra Clean Technology Co. Ltd., China. In order to remove the finish oils added to the fibres during the spinning process, the fabrics were treated in a scouring bath containing 4 g/L sodium carbonate and 2g/L Leveler O at 50 °C for 60 minutes. After scouring, the fabrics were thoroughly rinsed in distilled water and allowed to dry in the open air.

Disperse dyes were selected based on their chemical structures, energy levels, colours and applicability. The characteristics of the dyes are summarised in Table 1. Longsperse and Terasil dyes were provided by Zhejiang Longsheng Group Co. Ltd., China, and Huntsman International LLC (Shanghai Division), respectively, while other dyes were obtained from Zhejiang Runtu Co. Ltd., China. Sodium carbonate, citric acid, disodium hydrogen phosphate, sodium hydrosulfite and acetone were of analytical grade. Dispersant NNO was an industrial product from Anyang Double Circle Auxiliary Co. Ltd., China. Leveler O (polyoxyethylene alkyl ether) was provided by Jiangsu Hai'an Petrochemical Plant, China.

2.2 Dyeing methods

All dyeing processes were carried out in a laboratory using an infrared dyeing machine (FAD-7-18P; Yabo Textile Machinery Co. Ltd., Wuxi, China). The weight of the fabrics used for dyeing was 1 g, and the liquor ratio was 50:1. The dye solutions consisted of dyes, buffer and Dispersant NNO (1 g/L). The pH of the dyeing bath was adjusted to 5 by adding a McIlvaine buffer (citric acid and disodium hydrogen phosphate). At the end of dyeing process, polyesteramide fabrics were rinsed with distilled water and then dried in the open air.

Adsorption isotherm. Polyesteramide fabrics were dyed in solutions containing 0.5–12% owf (on the weight of fabric) dyes. The temperature was raised at the rate of 1.5 °C/minute from 30 to 80 °C prior to the addition of fabric samples, and then raised to 100 °C at the rate of 3 °C/minute. The dyeing process was continued at 100 °C for 150 minutes until the dye adsorption reached the equilibrium state.

Dyeing temperature. In order to study the temperature effect of dye uptake, the dyeing process was carried out according to the procedure illustrated in Figure 1. The dyeing solutions contained 2% owf dyes, 1 g/L Dispersant NNO and a buffer. The time for the dipping of each fabric in the dye solution was 120 minutes.

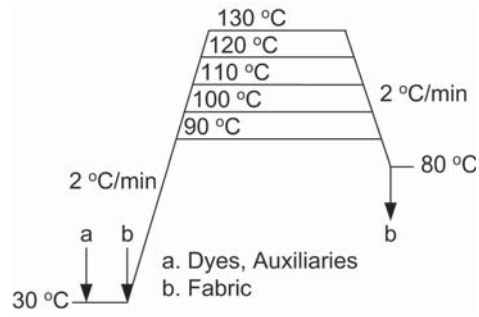

Figure 1: Dyeing profile for polyesteramide fabric at various temperatures

Dyeing rate. The dyeing rates of polyesteramide fibre were characterised by the uptake rates of Disperse Orange 30 for polyesteramide fibre in the conditions of 2% owf dyes, 1 g/L Dispersant NNO and pH 5. Two heating rates (2 °C/minute and 1 °C/minute) and two final holding temperatures (120 °C and 100 °C) were used. For the purpose of comparison, the uptake rate

of Disperse Orange 30 for PET fibre was also determined.

Building-up properties. The building-up properties of various dyes on polyesteramide fabrics were measured in a dye concentration range from 0.5% to 8% owf. The dyeing process was carried out at 100 °C for 80 minutes according to the profile illustrated in Figure 1.

2.3 Measurements

Exhaustion and adsorption of disperse dyes. The absorbance of dye solutions was measured using a Shimadzu UV-1800 UV–Vis spectrophotometer (Shimadzu Co. Ltd., Japan). The exhaustion of disperse dyes was assessed using the colourimetric method. Due to the poor water solubility of disperse dyes, a mixture of aqueous dye solution and acetone at a ratio of 30:70 (v/v) was prepared before the colourimetric analysis. The exhaustion percentage (E) of disperse dyes was calculated using equation 1:

$$E = \frac{A_0 - A_1}{A_0} \times 100\ (\%) \qquad (1),$$

where A_0 and A_1 are the absorbance at the maximum absorption wavelength of the dye solution before and after exhaustion, respectively.

The quantity of disperse dyes (C_f) on polyesteramide fibre was calculated using the exhaustion percentage of dyes, the initial dye concentration and the weight of the fabric using equation 2:

$$C_f = \frac{W_d \times E}{W_f} \times 1000\ (\text{mg/g}) \qquad (2),$$

where W_d is the initial dye weight (g) determined by fabric weight (1 g) and dye dosage (% owf) and W_f is the fabric weight (1 g).

The quantity of disperse dyes (C_s) in the solution after dyeing was calculated using equation 3:

$$C_s = \frac{W_d \times (1 - E)}{V}\ (\text{g/L}) \qquad (3),$$

where V is the volume of the dye bath (L).

Migration properties. Two undyed fabrics (A and B) with the same weight were prepared. Sample B was dyed with 2% owf dyes at 100 and 120 °C. Afterwards, dyed sample B and undyed sample A, at a liquor ratio of 50:1, were immersed in a blank dyeing bath that consisted of 1 g/L Dispersant NNO and a buffer, without the addition of dyes. In order to carry out the dye migration test, the temperature was raised at a rate of 2 °C /minute from 30 to 100 and 120 °C. At this temperature, the dye migration was continued for 60 minutes, after which the temperature was lowered to 80 °C. The migration rate was calculated using equation 4:

$$Migration = \frac{\left(\frac{K}{S}\right)_A}{\left(\frac{K}{S}\right)_B} \times 100\ (\%) \qquad (4),$$

where $(K/S)_A$ and $(K/S)_B$ are the colour depth values of samples A and B, respectively after the migration test.

Colour characteristics. The colour depth (K/S value) of each dyed sample was measured using a HunterLab UltraScan PRO reflectance spectrophotometer at the maximum absorption wavelength. A D65 illumination and 10° standard observer were used. Each sample was folded twice to give it a thickness of four layers.

Colour fastness. Prior to the assessment of colour fastness, the polyesteramide fabrics dyed with 3% owf dyes at 100 °C were subjected to reduction cleaning in a solution containing 2g/L sodium hydrosulfite and 1g/L sodium carbonate at 60 °C for 15 minutes. The wash fastness test was carried out in a WashTec-P fastness tester (Roaches International, UK), and the fastness level was accessed using a standard ISO 105-C06 test method. The fabrics were exposed to a xenon arc lamp for 35 hours in an Atlas XenoTest Alpha (SDL Atlas, USA) light fastness tester in standard testing conditions, and colour fastness to light was assessed according to ISO 105-B02. The sublimation fastness was measured on a sublimation fastness tester Model No. 620 (James H. Heal, UK) according to ISO 105-X11.

3 Results and discussion

3.1 Adsorption isotherm of disperse dyes on polyesteramide fibre

The adsorption isotherms of disperse dyes can be described by the relationship between the adsorption quantity of dyes on polyesteramide fibre (C_f) and the concentration of dyes in a solution (C_s) at equilibrium. Figure 2 shows the adsorption isotherms of two azo dyes and two anthraquinone dyes. There was a clear linear relationship between C_f and C_s, suggesting that the adsorption of disperse

dyes on polyesteramide fibre follows the Nernst model, and hydrogen bonding and the van der Waals forces between dyes and fibres contribute to Nernst adsorption. This observation is inconsistent with the mechanism of the distribution of disperse dyes on PET and the aqueous phase [15]. Moreover, it is evident from Figures 2a and 2b that azo dyes (Disperse Orange 30 and Red 74) did not exhibit a saturation adsorption in the range of the used dye concentration, while the adsorption saturation of the two anthraquinone dyes (Disperse Red 11 and Violet 31) approached the range of 50–60 mg/g. It is apparent that azo dyes had much higher adsorption saturation than anthraquinone dyes.

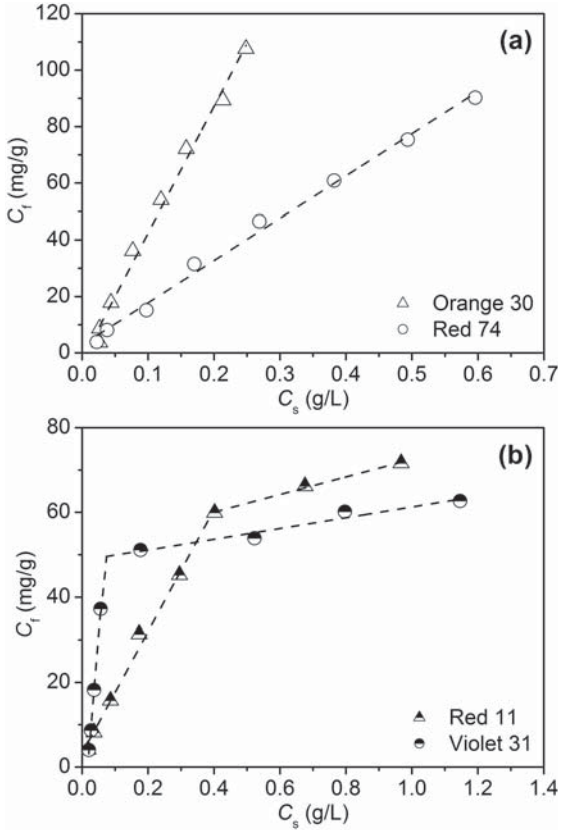

Figure 2: Adsorption isotherms of (a) azo and (b) anthraquinone disperse dyes on polyesteramide fibre at 100 °C

3.2 Dyeing temperature of polyesteramide fibre

It is a well-known fact that dyeing temperature plays a key role in the disperse dyeing of PET fibre because it affects the exhaustion, uptake rate, migration and diffusion of dyes, the colour depth and colour fastness of dyeing, and the efficiency of the dyeing process. High-temperature dyeing is typically used to achieve the high uptake of disperse dyes and the high colour depth of PET fibre because of the higher kinetic energy of dye molecules and the greater segmental mobility of the less-ordered regions within the fibre [16]. Polyesteramide fibre has lower glass transition and melting temperatures than PET fibre [13], and thus a lower dyeing temperature is to be expected.

Figure 3 shows the effect of dyeing temperature on the uptake of disperse dyes by polyesteramide fibre. The exhaustion of the five disperse dyes increased with the raising of the temperature, and almost reached the maximum rate at 100 °C, irrespective of their energy level or structure class. A further increase in dyeing temperature did not improve the exhaustion of dyes, with the exception of Disperse Red 74. This finding shows that the dyeing of polyesteramide fibre can be carried out under normal pressure. The good dyeing property of polyesteramide fibre is attributable to the fact that the incorporation of amide backbones into the polyester chain decreases the structural regularity of the fibre, as well as the glass transition temperature of the fibre [13]. This study implies that the low-temperature dyeability of polyesteramide fibre, as a novel synthetic fibre, has tremendous advantages in terms of energy consumption and dyeing efficiency.

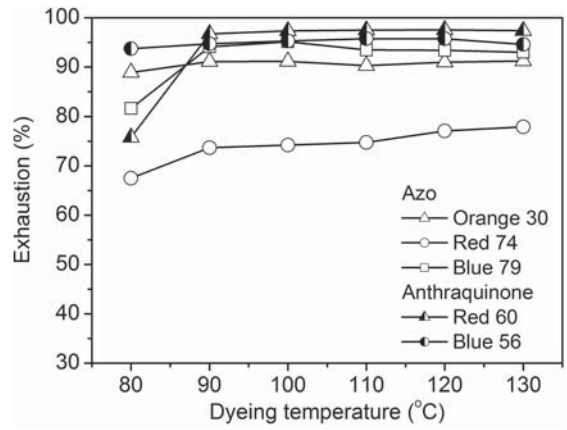

Figure 3: Uptake of disperse dyes by polyesteramide fibre at various temperatures

3.3 Dyeing rate of polyesteramide fibre

It is also a well-known fact that there are four fundamental steps involved in the uptake of dyes by textile fibres: the diffusion of dyes in the external water phase toward the diffusional boundary layer

on the fibre surface, the diffusion of dyes through the diffusional boundary layer, the adsorption of dyes onto the fibre surface and the diffusion of dyes into the fibre interior [17]. Of the four steps listed above, the diffusion of dyes in the fibre interior is the step that has the greatest impact on the dyeing rate of fibres. Based on this, it is interesting to study the dyeing rate of polyesteramide fibre.

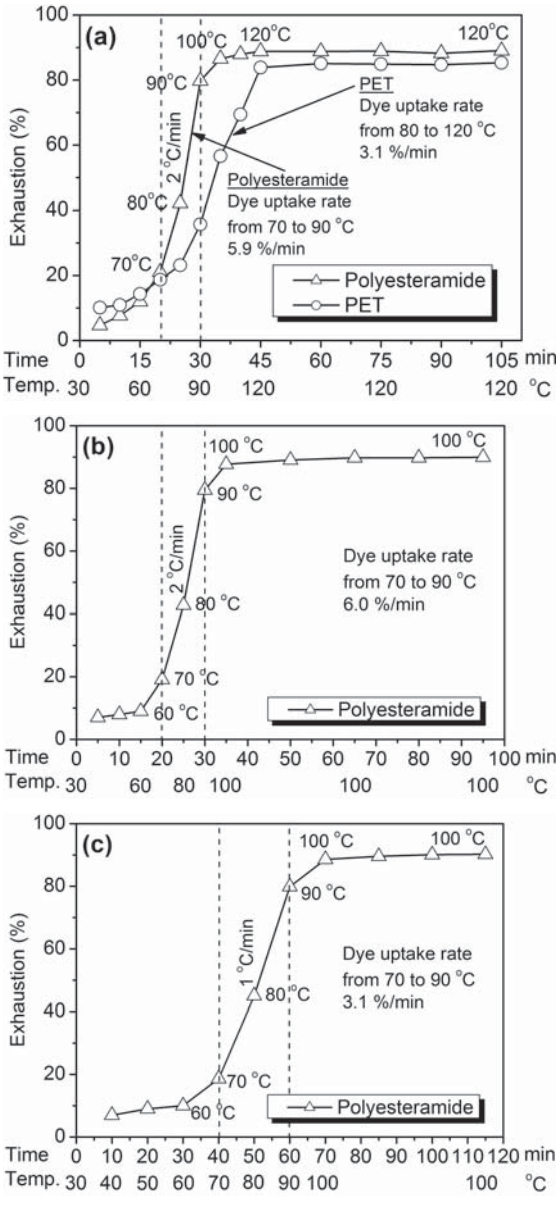

Figure 4: Uptake rates of Disperse Orange 30 for polyesteramide fibre: (a) polyesteramide and PET fibres, 120 °C, 2 °C/minute, (b) polyesteramide fibre, 100 °C, 2 °C/minute and (c) polyesteramide fibre, 100 °C, 1 °C/minute

Figure 4a shows the uptake rates of Disperse Orange 30 for polyesteramide and PET fibres at a holding temperature of 120 °C and a heat rate of 2 °C/minute. The rapid uptake of Orange 30 by polyesteramide fibre clearly occurred in the range of 70 to 90 °C, while the rapid dyeing temperature range for PET fibre was between 80 and 120 °C. Moreover, the uptake rates of Orange 30 for polyesteramide and PET fibres were 5.9 and 3.1%/minute, respectively in the temperature range for the rapid uptake of Orange 30. The dyeing rate of polyesteramide fibre was almost twice as high as that of PET fibre.

Figure 4b shows the uptake rate of Disperse Orange 30 for polyesteramide fibre at a holding temperature of 100 °C and a heat rate of 2 °C/minute. It is evident from Figure 4b that polyesteramide fibre displayed a rapid dyeing temperature range, dyeing rate and final uptake rate of dyes similar to those in Figure 4a. Figures 4a and 4b show that polyesteramide fibre exhibits a faster dyeing rate than PET fibre, which can be explained by the lower glass transition temperature of polyesteramide fibre.

Although polyesteramide fibre exhibits good low-temperature dyeability, its high dyeing rate would lead to poor dyeing levelness. Certain special measures should therefore be taken to improve the dyeing levelness of polyesteramide fibre. To that end, the most effective method is to decrease the uptake rate of disperse dyes in the faster dye-uptake temperature range or the critical temperature range (where 80% of adsorption takes place) by reducing the rate at which the temperature is raised [18]. Figure 4c shows the uptake rate of Disperse Orange 30 for polyesteramide fibre at a holding temperature of 100 °C and a heat rate of 1 °C/minute. When comparing Figures 4b and 4c, it is evident that using a heat rate of 1 °C/minute resulted in a decrease in the uptake rate of Disperse Orange 30 to 3.1%/minute from 6.0%/minute at a heat rate of 2 °C/minute. It can be suggested from this study that the dyeing of polyesteramide fibre should be carried out at a low heating rate to provide a dyeing levelness effect.

3.4 Migration ability of disperse dyes on polyesteramide fibre

The dyeing levelness of textile materials is dependent on the migration ability of dyes [18], which in turn are affected by many factors, such as fibre and dye structures, dyeing temperature and time, and

the dyeing auxiliaries used in the dye solution. The good migration ability of dyes is beneficial for dyeing levelness. Figure 5 shows the migration ability of three different disperse dyes on polyesteramide fibre at 100 and 120 °C. All three of the disperse dyes exhibited a high migration rate at 120 °C. Disperse Orange 30 and Red 74 also exhibited a high migration rate at 100 °C. However, Red 60 displayed a much lower migration rate at 100 °C than at 120 °C. Nevertheless, the migration rate of Red 60 reached 66%. Overall, the good migration ability of disperse dyes on polyesteramide fibre can be exploited to improve the dyeing levelness of polyesteramide textiles and to correct uneven dyeing.

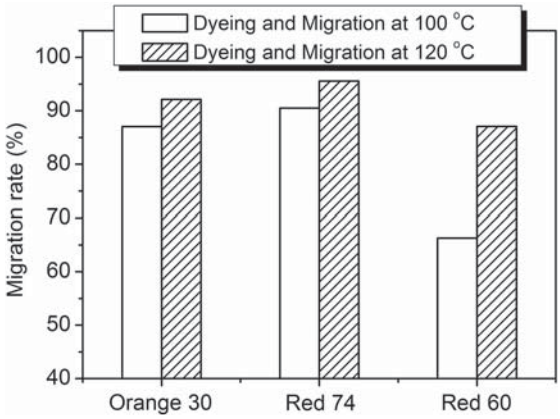

Figure 5: Migration ability of disperse dyes on polyesteramide fibre

3.5 Building-up property of disperse dyes on polyesteramide fibre

The building-up property of dyes is of great importance for practical application. Disperse dyes with a good building-up property can impart dark shades to polyesteramide fibre. The building-up property of disperse dyes primarily depends on the dye and fibre structures, the affinity of dyes to fibres and dyeing temperature. The building-up properties of azo and anthraquinone dyes on polyesteramide fibre are illustrated in Figure 6. In the case of azo dyes, the colour depth of the polyesteramide fabrics dyed with Disperse Red 74 and Blue 183 continually increased as the dye concentration in all of the dye concentration ranges was increased, while the same trend was identified for the fabrics dyed with Disperse Orange 30 and Brown 1, where dye concentrations in the range of 1% to 6% owf were used. In the case of anthraquinone dyes, the dyed fabrics displayed continually increasing colour depth when the concentrations of Disperse Red 11 and Violet 31 were less than 4% and 6% owf, respectively. Furthermore, the fabrics dyed with azo dyes exhibited higher colour depth than anthraquinone dyes. On the whole, azo dyes demonstrated a better building-up property than anthraquinone dyes. This finding is supported by the fact that azo dyes have a much higher adsorption saturation than anthraquinone dyes, as mentioned in subchapter 3.1.

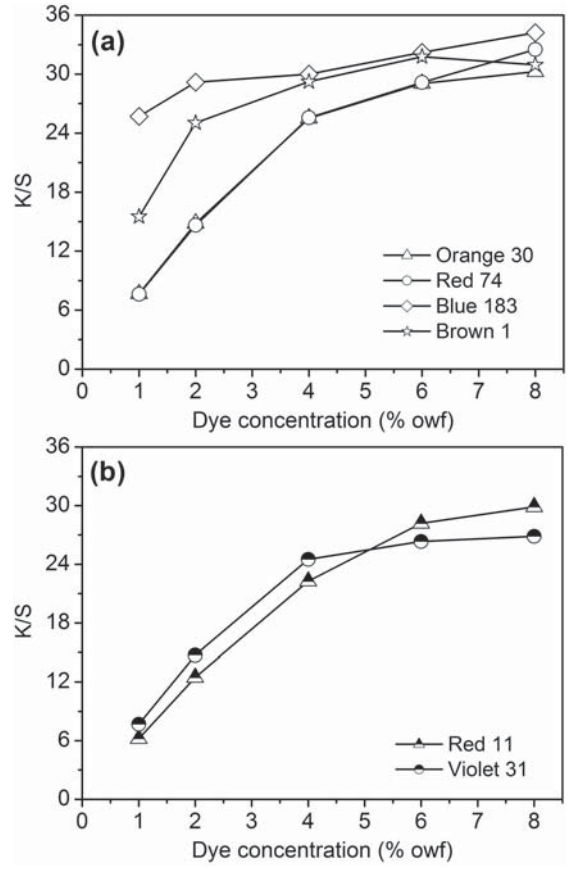

Figure 6: Building-up properties of (a) azo and (b) anthraquinone disperse dyes on polyesteramide fibre at 100 °C

3.6 Colour fastness of dyed polyesteramide fabrics

In order to assess the colour fastness of dyed polyesteramide fabrics, the dyeing process was carried out with widely used trichromatic disperse dyes at a concentration of 3% owf. Reduction cleaning was then carried out to remove loose colours. The wash, sublimation, and light fastness ratings of the dyed polyesteramide fabrics are presented in Table 2. The

Table 2: Colour fastness of dyed polyesteramide knitted fabrics

Dyes	Wash fastness			Sublimation fastness		Light fastness
	Colour change	Staining		Colour change	Staining	
		Polyester	Cotton		Cotton	
Orange 30	4–5	4–5	4–5	4	4–5	4–5
Red 74	4	4	4	3–4	3–4	3
Blue 79	4	4	4–5	4	4–5	4

fabrics dyed with Disperse Orange 30 and Blue 79 exhibited high wash, sublimation and light fastness levels. Good wash fastness was also identified for the fabric dyed with Disperse Red 74, while its sublimation and light fastness ratings were fair, at 3–4 and 3, respectively. According to GB 18401–2010: National General Safety Technical Code for Textile Products (Chinese National Standards for Textiles) [19], wash colour fastness ratings greater than or equal to 3–4 for baby/children products, and 3 for products that come into direct and indirect contact with skin are defined as "acceptable". Thus, the fabrics dyed with three disperse dyes were found to meet GB 18401–2010 in terms of acceptable colour fastness to washing. On the whole, the dyed polyesteramide fabrics exhibited good fastness properties that meet the requirements of consumers.

4 Conclusion

This study presented the dyeing properties of low-temperature dyeable polyesteramide fibre. The high exhaustion of disperse dyes at 100 °C revealed the good dyeability of polyesteramide fibre under atmospheric pressure. The Nernst adsorption isotherms of disperse dyes indicated a dyeing mechanism of polyesteramide fibre similar to that of PET fibre. The higher adsorption saturation and better building-up property of azo disperse dyes compared with anthraquinone dyes made the former a good selection for dark shades. The rapid uptake of dyes by fibres in the temperature range of 70 to 90 °C suggested that raising the temperature slowly was important for the improved dyeing levelness of polyesteramide textiles. The good migration of dyes on polyesteramide fabric can also be used to improve dyeing levelness. The good colour fastness properties of the dyed polyesteramide fabrics met the requirements of consumers. In summary, polyesteramide fibre can be used as an alternative to PET fibre to develop textile products, with regard to dyeing properties.

Acknowledgement
This study was funded by the Priority Academic Program Development (PAPD) of Jiangsu Higher Education Institutions (No. 2014-37).

References

1. DAWSON, Tim. Progress towards a greener textile industry. *Coloration Technology*, 2012, **128**(1), 1–8, doi: 10.1111/j.1478-4408.2011.00346.x.
2. HASANBEIGI, Ali, PRICE, Lynn. A technical review of emerging technologies for energy and water efficiency and pollution reduction in the textile industry. *Journal of Cleaner Production*, 2015, **95**, 30–44, doi: 10.1016/j.jclepro.2015.02.079.
3. OZTURK, Emrah, KOSEOGLU, Hasan, KARABOYACI, Mustafa, YIGIT, Nevzat O., YETIS, Ulku, KITIS, Mehmet. Sustainable textile production: cleaner production assessment/eco-efficiency analysis study in a textile mill. *Journal of Cleaner Production*, 2016, **138**, 248–263, doi: 10.1016/j.jclepro.2016.02.071.
4. XU, Suxin, CHEN, Jiangang, WANG, Bijia, YANG, Yiqi. An environmentally responsible polyester dyeing technology using liquid paraffin. *Journal of Cleaner Production*, 2016, **112**, 987–994, doi: 10.1016/j.jclepro.2015.08.114.
5. HUSSAIN, Tanveer, TAUSIF, Muhammad, ASHRAF, Munir. A review of progress in the dyeing of eco-friendly aliphatic polyester-based polylactic acid fabrics. *Journal of Cleaner Production*, 2015, **108**, 476–483, doi: 10.1016/j.jclepro.2015.05.126.

6. ZHAO, Ming-Liang, LI, Fa-Xue, YU, Jian-Yong, WANG, Xue-Li. Preparation and characterization of poly(ethylene terephthalate) copolyesters modified with sodium-5-sulfo-bis-(hydroxyethyl)-isophthalate and poly(ethylene glycol). *Journal of Applied Polymer Science*, 2014, **131**(3), d*oi: 10.1002/app.39823.*
7. WANG, Jun, LI, Xiaoyan, GE, Fengyan, CAI, Zaisheng, GU, Lixia. Carrier-free and low-temperature ultradeep dyeing of poly(ethylene terephthalate) copolyester modified with sodium-5-sulfobis(hydroxyethyl)-isophthalate and 2-methyl-1,3-propanediol. *ACS Sustainable Chemistry and Engineering*, 2016, **4**(6), 3285–3291, doi: 10.1021/acssuschemeng.6b00338.
8. FU, Changfei, GU, Lixia. Structures and properties of easily dyeable copolyesters and their fibres respectively modified by three kinds of diols. *Jounal of Applied Polymer Science*, 2013, **128**(6), 3964–3973, doi: 10.1002/app.38633.
9. KLANČNIK Maja. Dyeability of new polyesters. *Coloration Technology*, 2006, **122**(6), 334–337, doi: 10.1111/j.1478-4408.2006.00048.x.
10. CHEN, Pei, ZHAO, Fuping, SUN, Huaping, CHEN, Xiaohong. *Modified polyesteramide short fibre and preparation method thereof, CN patent no. 103952788 (B)*, 2016-09-14.
11. GONG, Liuliu, CAI, Xiudi, ZHOU, Qiong, SHI, Limei. *Flexible polyesteramide fibre and preparation method thereof. CN patent no. 103952787 (B),* 2016-05-25.
12. LIANG, Bichao, HAN, Chunyan, JI, Xuan, WEI, Qing, ZHAO, Jiongxin, WANG, Jianqing. Discoloration of Yilon fibre products. S*ynthetic Technology and Application*, 2015, **30**(3), 9–12. In Chinese.
13. LIU, Tian-tao, LIAN, Zhi-jun, WANG, Jianming. Dyeing properties of polyester/polyamide block copolymer fibre. *Dyeing and Finishing*, 2012, **38**(10), 1–4. In Chinese.
14. LIU, Tian-tao, LIAN, Zhi-jun, WANG, Jianming. Dyeing properties of polyester/polyamide and its cotton blended fabrics. *Journal of Textile Research*, 2013, **34**(10), 90–95. In Chinese.
15. BURKINSHAW, Stephen M. *Physico-chemical aspects of textile coloration*. 1st ed. West Sussex : Wiley, 2016, pp. 370–375.
16. BURKINSHAW Stephen M. *Chemical principles of synthetic fibre dyeing.* 1st ed. London [etc.] : Blackie Academic & Professional, 1995, pp. 61–62.
17. ETTERS, J. N. Kinetics of dye sorption: effect of dyebath flow on dyeing uniformity. *American Dyestuff Reporter*, 1995, **84**(1), 38–43.
18. CUNNINGHAM, Alan D. Identifying critical machinery and dye parameters for successful rapid dyeing of polyester. *Textile Chemist and Colorist*, 1996, **28**(2), 23–31.
19. *GB 18401-2010 National general safety technical code for textile products.*

Katja Kavkler[1], Nina Gunde Cimerman[2, 3], Polona Zalar[2], Andrej Demšar[4]
[1] Institute for the Protection of Cultural Heritage of Slovenia, Poljanska cesta 40, 1000 Ljubljana, Slovenia
[2] University of Ljubljana, Biotechnical Faculty, Jamnikarjeva 101, 1000 Ljubljana, Slovenia
[3] Centre of Excellence for Integrated Approaches in Chemistry and Biology of Proteins (CIPKeBiP), Jamova 39, 1000, Ljubljana, Slovenia
[4] University of Ljubljana, Faculty of Natural Sciences and Engineering, Aškerčeva 12, 1000 Ljubljana

FT-Raman Analysis of Cellulose based Museum Textiles: Comparison of Objects Infected and Non-infected by Fungi

FT-Ramanska analiza celuloznih muzejskih tekstilij: primerjava neokuženih in okuženih z glivami

Original Scientific Article/*Izvirni znanstveni članek*
Received/*Prispelo* 03-2018 • Accepted/*Sprejeto* 06-2018

Abstract

It is well-known fact that the supermolecular structure of museum textiles changes during aging and biodeterioration. These structural changes can be observed by different spectroscopic methods such as FT-IR, FT-Raman, and dispersive Raman spectroscopy. The purpose of the presented research is to present the usability of FT-Raman spectroscopy method for the analysis of the cellulose structure of the biodeteriorated historical textile fibers. Although historical textiles have already been analyzed using FT-Raman spectroscopy the method has been rarely used to analyze the changes of supermolecular structure of the biodeteriorated historical textiles attacked by microorganisms. In the research, cellulose textile samples from different museums and religious institutions were analyzed. Contemporary and historical cellulose textiles were scanned by FT-Raman spectra of reference and compared to determine the supermolecular cellulose fiber structure of each material. It has been shown that structural changes such as depolymerization and crystallinity changes can be detected using FT-Raman spectroscopy. The supermolecular changes of the cellulose fiber structure have been detected in biodeteriorated as well as in historical objects not infected by microorganisms. In the spectra of biodeteriorated objects, more intensive changes of spectral features were observed compared to spectra of non-infected samples. The changes were more pronounced at the museum objects made of flax. It can be concluded that biodeterioration causes more intensive structural changes than aging. On the basis of the research work, it has been shown that FT-Raman spectroscopy method can be used for the analysis of supermolecular structure changes of cellulose textiles.
Keywords: historical textiles, cellulose, biodeterioration

Izvleček

Dobro znano dejstvo je, da se nadmolekulska struktura muzejskih tekstilij med staranjem in biorazgradnjo spreminja. Strukturne spremembe opazujemo z različnimi spektroskopskimi metodami, npr. s FT-IR, FT-ramansko in disperzno ramansko spektroskopijo. Namen predstavljene raziskave je prikazati uporabnost FT-ramanske spektroskopske metode za analizo strukture celuloze biorazgrajenih zgodovinskih tekstilnih vlaken. Čeprav so bile zgodovinske tekstilije v preteklosti že analizirane z uporabo FT-ramanske spektroskopije, pa je bila metoda redko uporabljena za analizo sprememb v nadmolekulski strukturi biorazgrajenih zgodovinskih tekstilij, ki so jih napadli mikroorganizmi. V raziskavi smo analizirali celulozne tekstilne vzorce iz različnih muzejev in verskih ustanov. Zgodovinske celulozne tekstilije smo primerjali s sodobnimi referencami, da bi identificirali nadmolekulsko strukturo vsakega materiala. Pokazali smo, da lahko depolimerizacijo in spremembe kristalinosti detektiramo z uporabo FT-ramanske spektroskopije. Spremembe

Corresponding author/*Korespondenčna avtorica:*
Dr. Katja Kavkler
E-mail: katja.kavkler@rescen.si

Tekstilec, 2018, ***61****(2), 110-123*
DOI: 10.14502/TEKSTILEC2018.61.110-123

nadmolekulske strukture celuloznih vlaken smo opazili tako v biorazgrajenih kot tudi v neokuženih zgodovinskih vlaknih. V spektrih biorazgrajenih predmetov smo opazili intenzivnejše spremembe kot v neokuženih vzorcih. Spremembe so bile izrazitejše na zgodovinskih tekstilijah, izdelanih iz lanu. Zato lahko sklepamo, da biorazgradnja povzroči izrazitejše spremembe kot staranje. Na podlagi raziskovalnega dela smo pokazali, da s FT-ramansko spektroskopijo lahko analiziramo spremembe nadmolekulske strukture celuloznih tekstilij.
Ključne besede: zgodovinske tekstilije, celuloza, biorazgradnja

1 Introduction

The aim of all institutions dealing with cultural heritage is to preserve objects from the past for future generations. Among the most susceptible materials to be preserved are textiles. Materials produced from cellulosic (plant) fibers which consist mainly of cellulose (cotton more than 90%, flax 60-70%, and hemp up to 77%) represent an important part of textile materials in museums. In flax and hemp fibers, the main accompanying materials to cellulose are hemicelluloses (17%) and lignin (2–3%) [1]. Cellulose supermolecular structure in plant fibers is semi-crystalline which means that a certain part of cellulose fibers is ordered, i.e. crystalline, and a certain part is non-ordered, i.e. amorphous. The ratio between the crystalline and the amorphous phase differs between different plant types and depends on growth conditions, processing, use, and storing conditions. Features of the inner structure of cellulose fibers can be detected by spectroscopic methods. External influences, e.g. physical, chemical, or biological agents, cause changes of the textile fiber inner (supermolecular) structure as well as changes of appearance (fading of dyes and yellowing) [2]. The changes of inner structure of textile fibers cause changes of material mechanical properties. Textile fibers and textile materials become more fragile and prone to mechanical damages. Additionally, changes in the inner structure of textile fibers enable easier penetration of enzymes, produced by different types of living organisms into the structure [3, 4]. This is the case especially with fungi, which are among the most severe deteriorating agents of textiles [5] and which attack mainly pre-degraded fibers. Since fungi can cause changes in the supermolecular structure of textile fibers [6–11], an analysis of infected materials is of crucial importance. Such an analysis allows us to see the level of structural changes caused by aging processes or/and fungi attack and to decide what measures need to be taken to prevent further deterioration or even destruction of the historical objects. Biodeterioration of historical textile objects is usually investigated from the point of the infesting microorganisms [12, 13] and only rarely from the viewpoint of structure and properties of the attacked material(s). The latter were mainly analyzed on the buried contemporary samples [6, 14, 15].

Supermolecular structure of materials can be analyzed by different analytical methods, e.g. infrared and Raman spectroscopy, x-ray diffraction, etc. With the results obtained by the above-mentioned methods and their correlation with other visible and mechanical properties, it is possible to understand the changes and the plan of further treatment of historical objects. Spectroscopic techniques present a widely accepted approach for the analysis of historical objects. For the analysis of organic materials, infrared spectroscopy has proved to be a reliable and effective method [16]. Raman spectroscopy, on the other hand, can cause several problems when analyzing degraded organic materials. The research of historical textiles with dispersive Raman spectrometer using the visible laser wavelength 785 nm has already been presented by the authors of this paper [17]. Those problems can, to a certain extent, be solved by drench quenching (photobleaching), a prolonged exposition to a reduced laser power [18]. This method takes a long time to obtain spectra, sometimes more than a single working day. On the other hand, FT-Raman spectroscopy has proved to be a reliable tool when analyzing historical materials of organic origin [19, 20]. The near-infrared laser with 1064 nm wavelength should allow the analyst to obtain spectra with reduced luminescent background and enhanced Raman signal. The method was invented in 1986 as a response to high fluorescence in Raman spectra of certain types of materials [21].

The present study is a part of a broader research on the influence of different fungal species on structure of different natural fibers, being part of historical objects. The aim of the present study is twofold. Firstly,

to analyze historical textile materials infected by fungi using FT-Raman spectroscopy method and to detect whether fungi cause additional structural changes to natural aging, and, secondly, to compare the usefulness of different spectroscopic methods (dispersive Raman spectroscopy and Fourier transform infrared spectroscopy (FT-IR)) in the analysis of the structure of historical cellulose textiles.

2 Materials and methods

2.1 Textile samples

Textile samples for the analysis were obtained from 14 different historical textile objects stored in Slovene museums, different religious institutions or were under conservation at the Restoration Centre of the Institute for the Protection of Cultural Heritage of Slovenia (IPCHS). The historical textile objects originate from different historical periods from the 16th century or later. The analyzed textile objects are listed in Table 1 and presented in Table 2. Figure 1 presents an example of infection on one of the infected historical artefacts. Textile objects were made from different cellulosic fibers, which were identified by optical microscopy as described in our previous work [16]. The objects were selected according to their appearance: objects with visible mycelium growth or uncommon stains appearing like fungal spots were selected. The samples for the analysis were taken from historical objects in form of small pieces of fabrics or single threads according

Table 1: List of the selected historical objects with their description, source institution (and for paintings also storage institution), dating, material, and information about fungal infection in the upper rows non-infected objects are listed and in lower rows the infected

Sample label	Object description	Dating	Institution	Material	Fungal infection
MKS03	cloth, partly embroidered with metal threads	unknown	Slovene Museum of Christianity	cotton	no
PMP02	embroidered tablecloth	½ 20th cent.	Ptuj Regional Museum	flax	no
PMP05	leather belt with textile lining	½ 20th cent.	Ptuj Regional Museum	cotton	no
RCS04	painting on canvas	end of 17 th cent.	IPCHS[a)] (Convent)	flax and hemp	no
RCS06	painting on canvas	1st decade of 18th cent.	IPCHS[a)] (Convent)	flax	no
RCS07	painting on canvas	1582–1584	IPCHS[a)] (Provost church)	flax	no
RCS08	painting on canvas	unknown	IPCHS[a)] (Convent)	hemp and flax	no
MKS02	painting on canvas with a paper patch on the back	unknown	Slovene Museum of Christianity	flax	yes
MKS04	painting on canvas	unknown	Slovene Museum of Christianity	flax	yes
PMP03	underwear	unknown	Ptuj Regional Museum	cotton	yes
RCS01	painting on canvas	½ 19th cent.	IPCHS[a)] (Succursal church)	flax	yes
RCS05	painting on canvas	1729	IPCHS[a)] (Monastery)	flax	yes
RCS09	painting on canvas	17th cent.	IPCHS[a)] (Cathedral)	flax	yes
RCS14	painting on canvas	1821	IPCHS[a)] (Parish church)	flax	yes

[a)]IPCHS = the Institute for the Protection of Cultural Heritage of Slovenia

to the conservators and restaurateurs code [2]. The current storage conditions of all analyzed objects are listed in our previous work [2]. Environmental conditions in the past, which had influence on properties of objects, are not known.

2.2 Isolation and identification of fungi

The historical samples were analyzed for possible fungal contamination [2]. The sampling for the fungi was performed with areas of the material that we supposed could be infected by fungi (e.g. unusual stains, mycelium like spots etc.).

The fungi were sampled from the selected objects by rubbing with a sterile cotton swab that was either soaked in physiological solution (0.9% [w/v] NaCl), or was dry, in the cases of more sensitive objects. The fungi were isolated from these swabs by subsequent inoculation onto malt extract agar medium with the added antibiotic chloramphenicol (50 mg/l), to prevent bacterial growth. The plates were incubated at 25 °C for up to 21 days. Pure cultures of the fungi were obtained from the primary isolation plates by the further culturing of selected colonies with different morphologies. All of the isolated

Table 2: Photographs of all analyzed historical objects and close-up captures of spots which might be infected by fungi (first and second column – infected historical objects; third and fourth column – non-infected historical objects)

fungi are stored in the Microbiological Culture Collection EX of the Department of Biology, Biotechnical Faculty, University of Ljubljana (www.ex-genebank.com).

The fungi in the fungal isolates were identified according to their macromorphological and micromorphological characteristics, and using genus/species-specific molecular markers, according to

taxonomic standards. For the fungal DNA isolation, the strains were grown on malt extract agar medium for 7 days. Their DNA was extracted according to Gerrits van den Ende and de Hoog [22], by mechanical lysis of *ca*. 1 cm^2 of their mycelia.

Figure 1: An example of infection spot on the infected historical artefact (MKS 02)

For the purpose of the research, contemporary cotton and flax fabrics were analyzed using the same testing conditions and procedures as in the case of historic samples (see chapter 2.2). The reference materials were not bleached and were unsized to resemble the historical materials. Reference fabrics with the mixed content of hemp and flax were not available to us to directly compare historical textiles made of hemp/ flax mixture.

2.2 FT-Raman spectroscopy method

For the FT-Raman analysis, Bruker multiRam instrument was used. The instrument is equipped with cryo-cooled Ge detector, Nd-YAG laser with a wavelength of 1064 nm with a line width of ~ 5 cm^{-1} to 10 cm^{-1}, and a resolution of 4 cm^{-1}. Raman spectrometer was calibrated each day before use. The applied laser intensity varied between 30 mW and 150 mW. The number of accumulated scans varied between 100 and 5000. Raw fibers or pieces of textiles were used without additional sample preparation and put under the FT-Raman microscope. The surface area of the analysis was approximately 20 μm in diameter. Several areas, selected randomly, were analyzed on each historical as well as reference sample. By comparison of reference and historical samples' spectra structural changes in historical objects were determined.

All spectra are shown in the range between 150 cm^{-1} and 2000 cm^{-1}. Lower wavenumbers would not be reasonable due to high fluorescence in this region, as observed from obtained the spectra. Spectra were baseline-corrected to give clearer results and better visual comparison.

The ratios I^{1121}/I^{1096} [20] and I^{380}/I^{1096} [23] were calculated for all the samples (where bands were clearly visible). Bands are typical of symmetrical vibrations of glycoside bonds (1120 cm^{-1}), asymmetrical vibrations of glycoside bonds (1096 cm^{-1}) and CCC vibrations of glycoside ring (380 cm^{-1}) [24]. The ratios were selected as the most often occurring and proved as reliable for cellulose crystallinity determination in the available literature. The first ratio has proved to be stable and reliable in several articles (as confirmed by Jähn and co-workers [25]). For the second ratio Agarwal and co-workers [23] have proved that the bands at 380 cm^{-1} and 1096 cm^{-1} are significantly affected by cellulose crystallinity modification and that this ratio generated excellent regression (R2 = 0.992) and showed good sensitivity to crystallinity change.

Heights of the bands were measured using OPUS software. Band heights were measured from a selected baseline in the spectrum as shown in Figure 2.

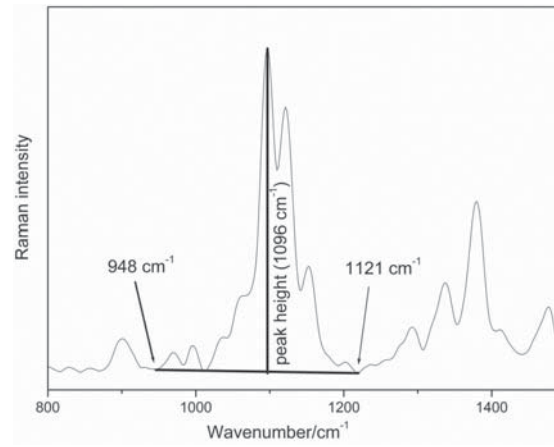

Figure 2: Baseline selection and peak height measurement for quantitative analyses

3 Results and discussion

As it can be seen from the Table 1, three of the selected historical specimens were made of cotton (MKS03, PMP03, and PMP05), nine objects were made of flax, and two were mixed, made of flax in

the warp direction and hemp in the weft (RSC04 and RCS08). The textile materials were identified by optical microscopy as described in our previous work [16].

3.1 FT- Raman analysis of the cotton samples

Two of the analyzed cotton samples turned out not to be infected by fungi. Infection with fungi was confirmed on one sampled underwear (PMP03, Tables 1 and 2) [2]. FT- Raman spectra of different quality were obtained from the cotton specimen.

Two different spectra were obtained from the specimens taken from the infected underwear (PMP03) sample (Figure 3). This fact leads us to the conclusion that the degree of deterioration is not uniform over the whole sample and depends mostly on the fungal contamination and activity. As it can be seen in the Figure 3a, spectrum b resembles contemporary cotton (spectrum a) to a great extent. The band heights are decreased. However, the ratio between them remained similar to those of reference spectra, as confirmed also by quantitative analyses (Table 3). Decreased band heights can be a consequence of luminescent background due to surface dirt or fungi [20]. It can be concluded that no severe deterioration occurred in this area of the sample. In the case of the spectrum c (Figure 3a), structural changes of the cotton fibers could be clearly observed when compared to reference spectra of the cotton (spectrum a). Some bands in the spectrum c decreased relative to other when compared to the reference spectrum. The decrease of the band at 380 cm^{-1}, typical of vibrations of glycoside ring [24], is a sign of decreased crystallinity of the cellulose [23]. The decrease of the band at 437 cm^{-1}, typical of glucose rings vibrations [24, 26], is a sign of cellulose degradation [26]. Additionally, the bands at 1096 cm^{-1} and 1120 cm^{-1}, typical of asymmetric and symmetric β-glycosidic linkages respectively [24], decreased strongly relative to the reference spectrum. This is a sign of a hydrolytic fission of the glycosidic bonds [27]. The decrease of the intensities occurred at the bands between 1250 cm^{-1} and 1450 cm^{-1}, typical mainly of CH_2 vibrations, as well as HCC, HCO, and COH bending, all indicating cellulose deterioration [20, 28]. On the basis of the above-mentioned results, it can be concluded that cotton fabric infected with fungi is subjected to depolymerization and the decrease of crystallinity. The deterioration takes place only in the infected spots.

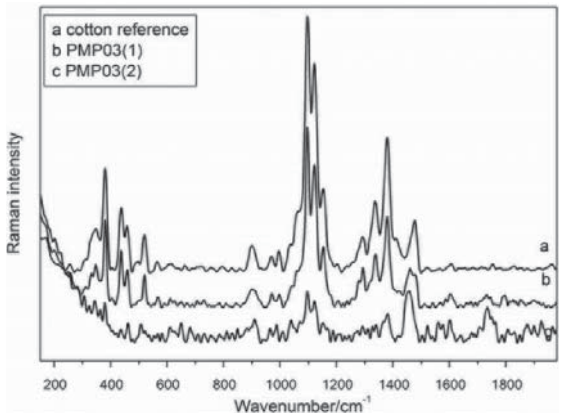

Figure 3a: Comparison of two different spectra form infected cotton object (PMP03; spectra b and c) with cotton reference (spectrum a)

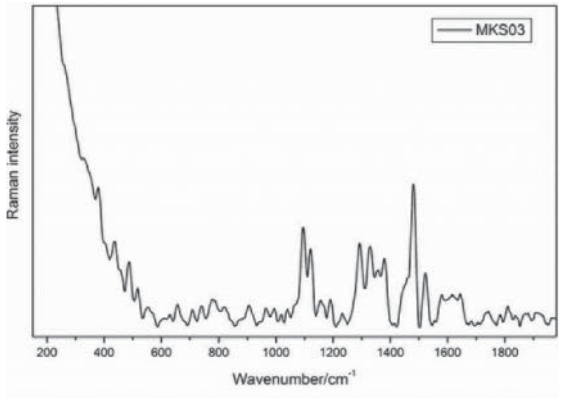

Figure 3b: Spectrum MKS03, showing poorly resolved bands and unidentified bands (around 1500 cm^{-1})

The spectra of belt lining made of cotton (PMP05) did not show any changes in typical cellulose features, only a strong luminescent background because of which a clear analysis of its supermolecular structure was not possible. Luminescence is usually a consequence of severe deterioration or presence of dirt or fungal hyphae on the surface of the analyzed objects [20]. Since the object was not subjected to fungal deterioration, the strong luminescence was probably a consequence of deterioration caused by aging and surface dirt. According to FTIR spectroscopy results obtained previously [16], it has been discovered that the crystallinity of the sample was higher compared to the reference sample, as observed by decreasing of the band at 900 cm^{-1} and the presence of a strong band 1280 cm^{-1}. Higher crystallinity could be a consequence of the deterioration of the amorphous regions caused by aging [29].

The spectra of the third cotton specimen (MKS03) exhibits very low intensity. Since the objects were not infected by fungi and the bands are very low, severe deterioration of the cellulose can be assumed. Additionally, a strong decrease of the bands at 1337 cm^{-1} and 1380 cm^{-1} is a sign of cellulose deterioration. Changes in the structure could have been caused by different environmental factors, e.g. light, as well as fluctuations in humidity and temperature.

The comparison of the state of preservation of the three investigated cotton samples shows that fungi did not cause more severe deterioration than environmental impacts. Processing and environmental impacts of the past decades, which could be of crucial importance for the state of preservation of each object, are unknown to us. However, even in time of sampling, most objects were not kept under the most appropriate conditions (relative humidity 40 to 65% and temperature 16 to 18 °C [30]) as described in our previous article [2].

Intensity ratios of the selected spectral bands were calculated for cotton historical objects and for cotton reference (Table 3). For both analyzed objects, the ratio I^{1121}/I^{1096} decreased, as was expected according to the literature [20, 31]. The ratio in the spectrum of the non-infected object (MKS03) also showed a small decrease relative to the ratio in the reference spectrum of cotton. It can be concluded that non-infected structure of the cotton also changed during aging. The differences in values of different areas (4b and 4c) of the infected object (PMP03) are a consequence with natural processes in fibers and fungal growth which do not affect all the areas equally. Comparing both ratios of cotton samples, it can be seen that in both cases the highest crystallinity ratio exhibits the sample PMP03_4b[a)] which is followed by the sample PMP03_4c[a)]. The lowest crystallinity ratio exhibits the sample MKS03. The degree of crystallinity is a function of many interconnected processes to which a textile material is subjected during its life.

Table 3: Intensity ratios I^{1121}/I^{1096} and I^{380}/I^{1096} for the cotton samples

Sample	I^{1121}/I^{1096}	I^{380}/I^{1096}
cotton reference	0.82	0.33
MKS03	0.77	0.27
PMP03_4b[a)]	0.81	0.43
PMP03_4c[a)]	0.79	0.38

[a)]Infected objects

The ratio I^{380}/I^{1096} was suggested by Agarwal and coworkers [23] to be the most appropriate to determine the cellulose crystallinity. It shows different tendency than the ratio I^{1121}/I^{1096}. According to the ratio I^{380}/I^{1096}, the crystallinity decreased in the sample MKS03 and increased in the sample PMP03 compared to the reference sample. On the basis of the presented results, it can be concluded that aging decreased the crystallinity ratio I^{380}/I^{1096} and fungal infection increased it. This could be explained by faster deterioration of amorphous regions compared to crystalline when subjected to fungal infection and by the fact that the amorphous/crystalline ratio is changing. The ratio I^{1121}/I^{1096} remains relatively similar in all tested samples. This is to be expected, since both the 1121 cm^{-1} and 1096 cm^{-1} bands are assignable to the β-glycosidic COC vibration of cellulose [20].

3.2 FT- Raman analysis of the bast fibers samples

Nine of the analyzed fabrics were made of flax fibers, and two of a mixture of flax and hemp fibers. One sample was taken from an embroidered tablecloth and the rest were taken from painting canvases, most of which are still kept in churches or cloisters, whereas two are kept in a museum in improper conditions with too high relative humidity and fluctuating temperature [2]. Neither of the two samples with mixed composition was infected by fungi. On the other hand, six of nine samples made from pure flax were infected by different fungal species (Tables 1 and 2). Spectra of both samples with mixed fibers had a strong luminescent background, which prevented us to make any conclusions regarding their supermolecular structure. The reason for bad quality is the presence of hemp, as it contains many non-cellulosic substances (e.g. lignin, hemicellulose, pectin, etc.) which, according to Agarwal, cause luminescent background [18].

At FT-Raman spectrum of non-infected flax sample taken from the embroidered tablecloth, (PMP02) a relatively strong band at 457 cm^{-1} (Figure 4, spectrum b), compared to the band at 435 cm^{-1}, appeared which is typical of ring vibrations [20]. This is a sign of relatively high crystallinity [26]. The same is true for the intensive band at 520 cm^{-1}, typical of glycoside links [19, 20]. A relative increase of the band at 1120 cm^{-1} regarding the band at 1096 cm^{-1} is also seen, which is again a sign of more organized structure in cellulose fibers [27]. However, according

to Kovur et al., it could also be a consequence of cellulose degradation and remaining of non-cellulosic compounds (lignin, hemicelluloses) [32]. The latter is, in this case, less probable since the absence of the band at 1276 cm^{-1} signifies the absence of lignin [33]. Therefore, it can be concluded that during the aging process the amorphous regions deteriorated and only the crystalline regions remained. The band at 780 cm^{-1} in Figure 4, spectrum d (RCS07) is most probably due to lignin [34].

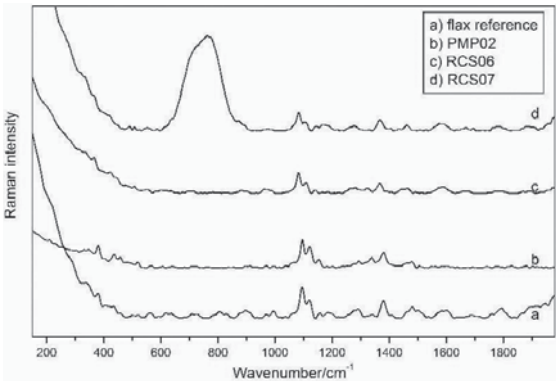

Figure 4: Comparison of non-infected flax objects PMP02 (spectrum b), RCS06 (spectrum c) and RCS07 (spectrum d) with flax reference (spectrum a)

According to the FT-Raman spectra of non-infected specimens of two paintings treated at the Restoration Centre of the IPCHS (RCS06 and RCS07, Figure 4, spectra c and d), it can be seen that not only biodeterioration is the cause of luminescence. The older painting from the 16th century (RCS07) has the more intensive luminescent background and consequently weaker bands, especially in the region between 300 cm^{-1} and 600 cm^{-1}, which makes the evaluation of its structure difficult. On the other hand, the spectra of younger painting from the beginning of the 18th century (RCS06) show relatively well-resolved bands despite moderate luminescent background. The decrease of the band at 1380 cm^{-1} is a sign of cellulose depolymerization [28]. This band decreased at spectra of both objects. Additionally, the ratio between 1120 cm^{-1} and 1096 cm^{-1} bands also decreased, indicating the degradation of cellulose [27]. The cellulose degradation is probably the main reason for low spectra quality.

Six of the investigated linen fabrics were infected by fungi (Tables 1 and 2). All of the infected investigated objects were painting canvases. Two of them were from the Slovene Museum of Christianity and all others were from different religious institutions, treated at the Restoration Centre of the IPCHS.

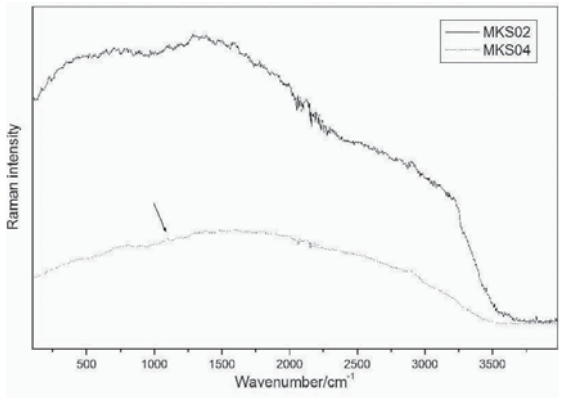

Figure 5: Spectra MKS02 and MKS04 showing an intensive background with only slightly visible main bands around 1100 cm^{-1} (arrow)

The spectrum of one of the two paintings from the Museum of Christianity (MKS02, Figure 5, solid spectrum) had a strong luminescent background and no spectral bands could be observed. Therefore, no estimation of its structure was possible by FT-Raman spectroscopy. At spectra of the other painting from the same museum (MKS04, Figure 5, dotted spectrum), which is approximately one century older, the background is strong. However, weak bands of the cellulose could still have been observed. However, most of the bands are difficult to interpret. Therefore the structure of cellulose could not be estimated properly. This example shows, that the higher age of the sample is not necessary the cause of stronger deterioration. Since the history of neither object is familiar to us, no further conclusions can be drawn about what caused faster deterioration of the later produced textile.

Figure 6 represents a comparison of biodeteriorated flax objects sampled during the conservation processes at IPCHS: RCS01 (spectrum a), RCS05 (spectrum b), RCS08 (spectrum c), RCS09 (spectrum d), RCS14 (spectrum e) with flax reference (spectrum f). The most severely and visibly infected (of all the investigated objects) was the painting from a succursal church, dating from the first half of the 19th century (RCS01). The mycelium growth was visible with a naked eye on the whole back side (Table 2). The FT-Raman spectra of the sample RCS01 (Figure 6, spectrum a) exhibited too strong background

and no spectral bands could be observed. The reason for the strong background is the presence of fungal hyphae as proposed by Edwards and co-authors [20] or severe deterioration of the cellulose, as confirmed by FTIR spectroscopy [1].

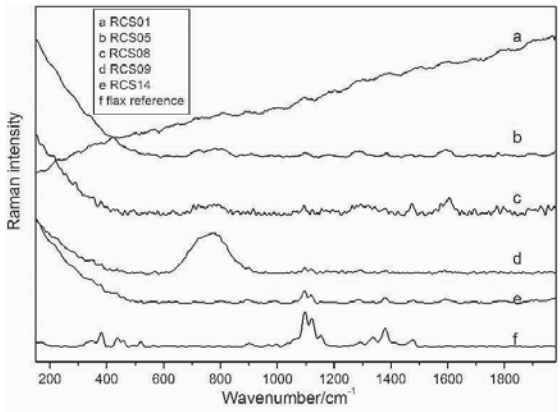

Figure 6: Comparison of biodeteriorated flax objects RCS01 (spectrum a), RCS05 (spectrum b), RCS08 (spectrum c), RCS09 (spectrum d), and RCS14 (spectrum e) with flax reference (spectrum f)

The strong luminescent background can be seen also in some other samples as well (Figure 6, spectra b, c and d). At the spectrum of sample RCS05 from the Franciscan monastery, dating from 1729 (Figure 6, spectrum b), only the strongest bands in the spectrum are visible, therefore the structural determination is difficult. In the region around 1100 cm^{-1}, only a broad band with the peak at 1096 cm^{-1} could be observed (Figure 6, spectrum b), with only a slight shoulder towards 1120 cm^{-1}. According to the FT-Raman spectra of sample RCS05, it can be concluded that the fibers are severely deteriorated and the glycoside vibrations are weak.

In the FT-Raman spectrum (Figure 6, spectrum d) of the painting from the Ljubljana cathedral (RCS09), which was painted in the 17th century, the background was strong as well. However, the most characteristic features of cellulose could still be observed. The disappearance of the band at 995 cm^{-1} and the decrease in intensities of the bands at 1096 cm^{-1}, 1120 cm^{-1}, and 1380 cm^{-1} are a sign of cellulose deterioration [27]. The disappearance of the band at 1480 cm^{-1} is a sign of crystallinity decrease [20]. It can be concluded on the basis of all these findings that the fibers are severely deteriorated and the crystallinity content in the fibers has decreased.

In the FT-Raman spectrum (Figure 6, spectrum e) of the infected sample RCS14, the background is rather intensive. However, the bands could still be distinguished relatively clearly. Several differences could be observed compared to contemporary reference spectra. Decreased intensities were observed at bands at 1096 cm^{-1}, 1120 cm^{-1}, 1380 cm^{-1} and 1480 cm^{-1} indicating cellulose deterioration and the decrease of crystallinity [35, 36].

At the FT-Raman spectrum of the sample RCS08 (Figure 6, spectrum c), all the bands are very weak. Thus, it is difficult to compare visually with reference spectra. All the main bands are visible. Their ratios, however, are difficult to interpret.

The features were less visible and more difficult to interpret in all FT-Raman spectra of flax samples than at cotton samples spectra. The most probable cause for luminescent background masking spectral bands is the presence of lignin and other non-cellulosic features, which are present in bast fibers and absent in cotton. However, when comparing the results of infected and non-infected objects, it seems, that fungi influence the cellulose structure that it becomes more crystalline and the ageing itself to become more amorphous. Due the small number of the samples this cannot be seen as rule, but could be explained that the enzymes can more easily degrade amorphous structures, whereas (mainly) physical influences during ageing influence crystalline structure.

Table 4: Intensity ratios for flax fibers

Sample	I^{1121}/I^{1096}	I^{380}/I^{1096}
Flax reference	0.57	0.16
PMP02	0.75	0.35
RCS05[a)]	0.26	0.05
RCS06	0.53	0.23
RCS07	0.42	0.06
RCS08	0.58	0.18
RCS09[a)]	0.59	0.39
RCS14[a)]	0.61	0.17

[a)]Infected objects

In Table 4, the calculated intensity ratios of flax samples are presented. It can be seen that neither aging nor fungal infection causes the same crystallinity changes in all the cases. An increase or a decrease of the ratios are not directly connected to fungal deterioration. The degree of crystallinity is a

function of many interconnected processes to which a textile material is subjected during its life. The reason for this is unique influences of physical environmental factors (light, relative humidity, temperature) and of different fungal species to a specific investigated object.

3.3 Comparison of FT-Raman, dispersive Raman, and FTIR methods

Selected samples were analyzed using FT-Raman spectroscopy method. The same samples were previously analyzed also with the dispersive Raman and FT-IR spectrometers [11, 12]. Especially with dispersive Raman spectrometer we met with several difficulties, since fluorescence masked spectral bands [17]. Raman spectrometers give information about skeletal structure of the polymers [28], whereas infrared spectra base more on functional groups' vibrations [37]. FT-Raman spectroscopy was invented as an upgrade of dispersive Raman spectroscopy, to reduce the luminescence [21]. The aim of presented work is also to test the applicability of this analytical method in the field of historical materials especially for their analysis, restoration and conservation.

Obtained FT-Raman spectra were analyzed and compared to dispersive Raman spectra and FT-IR spectra. Figure 7a represents a comparison of FT-Raman spectrum of the sample RCS14 (solid line) to dispersive Raman spectrum of the same specimen (dotted line). In FT-Raman spectra, several minor bands can be observed. They are hidden in the case of dispersive Raman spectra by fluorescent background (Figure 7a).

Comparing the FT-Raman and dispersive Raman spectroscopy methods and their results it can be clearly seen that additional information could be gathered from the FT-Raman spectra when compared to dispersive Raman spectra. Additionally, the scanning time for FT-Raman spectra is shorter, since samples need no or only little signal quenching whereas dispersive Raman spectra sometimes needed several hours of signal quenching to obtain informative spectra. Therefore if one has a choice the use of FT-Raman spectroscopy would be advised for the analysis of historical textiles analyses.

Figure 7b shows FTIR spectra of the same specimen (RCS14). In FTIR spectra, all peaks and details can be clearly seen and well resolved. However, the main vibrations which are seen on FTIR spectra are vibrations of functional groups whereas Raman spectroscopy shows more clearly the cellulose backbone structure vibrations [28]. Therefore FTIR and Raman spectroscopy and their results are complementary. In FT-IR spectrum of the sample RCS14 no significant changes were observed, when compared to contemporary reference flax spectra in one spot, but the other one shows some changes in the cellulose vibrations regions (1300 to 1400 cm^{-1} and 1200 do 1000 cm^{-1}), showing cellulose deterioration and crystallinity decrease [38, 39, 40]. FT-Raman spectra as well show decrease of certain bonds (as mentioned above), also indicating cellulose deterioration and the decrease of crystallinity [27, 28]. Since FT-IR spectra are easy and quick to obtain, although not without problem, especially when working in transmission mode [16], it will remain the preferred method for the authors.

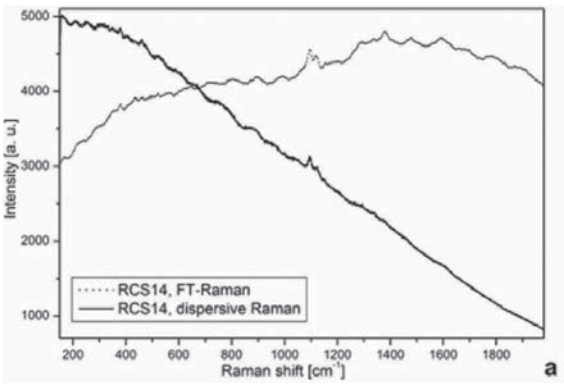

Figure 7a: Comparison of FT-Raman spectrum of the sample RCS14 (dotted line) to dispersive Raman spectrum of the same specimen (solid line)

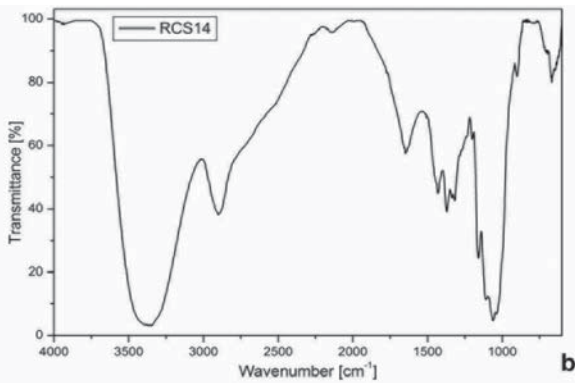

Figure 7b: FTIR spectrum of the sample RCS14

4 Conclusion

FT-Raman spectroscopy has proved to be a useful tool for investigation and analysis of cellulose historical textile objects and fiber supermolecular structure for cotton and in most cases for bast fibers. In the case when cellulose fibers contain many non-cellulosic substances, as it is in the case of hemp fibers, or are subjected to severe deterioration, a strong luminescent background appears which masks spectral bands and prevents the analysis of the cellulose fiber supermolecular structure. Compared to dispersive Raman spectroscopy, FT-Raman spectroscopy enables clearer spectra with more visible spectral bands and with less luminescence which leads to more accurately interpreted supermolecular structure of cellulose fibers. To obtain even more precise information about the supermolecular structure of investigated materials combining FT-Raman method with other analytical methods (especially FT-IR spectroscopy) is highly recommended.

The FT-Raman analysis also clearly confirmed the fact that the physical and biological factors cause severe deterioration of cotton and flax fibers as a consequence of fungi attack or other, especially physical, deteriorating factors (e. g. light and humidity). The results show relatively more intensive changes at infected objects compared to non-infected. This confirms the prediction that the supermolecular structure of cellulose fibers change more at objects subjected to fungal infection than at those which were not infected by fungi and were only only infected by the physical environmental factors. This is confirmed especially for cotton fibers. Other cellulosic fibers (bast fibres) exhibit too high luminescence to be reliably analysed.

Acknowledgements

The authors would like to thank Ingalill Nystrom and the Department for Conservation of the University of Gothenburg, Sweden, for giving us the possibility to use the FT-Raman equipment at their institution. We would also like to thank the Slovene Museum of Christianity, Ptuj, the Regional Museum and the Department for Easel Paintings of the Restoration Centre of the IPCHS for providing the sampling objects.

References

1. SFILIGOJ SMOLE, Majda, HRIBERNIK, Silvo, STANA-KLEINSCHEK, Karin, KREŽE, Tatjana. Plant fibres for textile and technical applications. In *Advances in Agrophysical Research* [edited by Stanisław Grundas], [online]. InTech [accessed 10. 10. 2017]. Available on World Wide Web: <https://www.intechopen.com/books/advances-in-agrophysical-research/plant-fibres-for- textile-and-technical-applications>.
2. KAVKLER, Katja, GUNDE-CIMERMAN, Nina, ZALAR, Polona, DEMŠAR, Andrej. Fungal contamination of textile objects preserved in Slovene museums and religious institutions. *International Biodeterioration & Biodegradation*, 2015, **97**, 51–59, doi: 10.1016/j.ibiod.2014.09.020.
3. ZOTTI, M., FERRONI, A., CALVINI, P. Mycological and FTIR analysis of biotic foxing on paper substrates [online]. *ITOG,* 2010 [accessed 8. 4. 2010]. Available on World Wide Web: <www.itog-ve.org/contenuto/foxing/pagine/E_Cont03.htm>.
4. VALENTIN, N. Microbial contamination in museum collections: organic materials. In *Molecular biology and cultural heritage. Proceedings of the International Congress on Molecular Biology and Cultural Heritage, 4-7 March 2003, Sevilla, Spain*. Edited by C. Saiz-Jimenez. Lisse, The Netherlands : Routledge, 2003, pp. 85–92.
5. SEVES, Annamaria, ROMANÒ, Maria, MAIFRENI, Tullia, SORA, Silvio, CIFERRI, Orio. The microbial degradation of silk: a laboratory investigation. *International Biodeterioration & Biodegradation*, 1998, **42**(4), 203–211, doi: 10. 1016/S0964-8305(98)00050-X.
6. TOMŠIČ, Brigita, SIMONČIČ, Barbara, OREL, Boris, ČERNE, Lidija, FORTE TAVČER, Petra, ZORKO, Mateja, JERMAN, Ivan, VILČNIK, Aljaž, KOVAČ, Janez. Sol-gel coating of cellulose fibres with antimicrobial and repellent properties. *Journal of sol-gel science and technology*, 2008, **47**(1), 44–57, doi: 10.1007/s10971-008-1732-1.
7. SIVARAMANAN, Sivakumaran. Biodeterioration of cotton by cellulolytic fungi. *International Journal of Science and Research*, 2013, **2**(12), 62–67, doi: 10.13140/2.1.5181.6961.

8. SEVES, Annamaria, ROMANÒ, Maria, MAIFRENI, Tullia, SEVES, Alberto, SCICOLONE, Giovanna, SORA, Silvio, CIFERRI, Orio. A laboratory investigation of the microbial degradation of cultural heritage. In *Of microbes and art: the role of microbial communities in the degradation and protection of cultural heritage*. Edited by O. Ciferri, P. Tiano, G. Mastromei. New York : Kluwer Academic/Plenum Publishers, 2000, pp. 121–133.
9. MONTEGUT, D., INDICTOR, N., KOESTLER, R. J. Fungal deterioration of cellulosic textiles: a review. *International Biodeterioration*, 1991, **28**(1–4), 209–226, doi: 10.1016/0265-3036(91)90043-Q.
10. CHAKRAVARTY, T., BOSE, R. G., BASU, S. N. Fungi growing on jute fabrics deteriorating under weather exposure and in storage. *Applied and Environmental Microbiology*, 1962, **10**(5), 441–447.
11. MARSH, P. B., BOLLENBACHER, K., BUTLER, M. L., RAPER, K. B. The fungi concerned in fiber deterioration II: their abbility to decompose cellulose. *Textile Research Journal*, 1949, **19**(8), 462–484, doi: 10.1177/004051754901900803.
12. ABDEL-KAREEM, Omar, ALFAISAL, R. Treatment, conservation and restoration of the Bedouin dyed textiles in the museum of Jordanian heritage. *Mediterranean Archaeology and Archaeometry*, 2010, **10**(1), 25–36.
13. CAPODICASA, Serena, FEDI, Stefano, PORCELLI, Anna Maria, ZANNONI, Davide. The microbial community dwelling on a biodeteriorated 16th century painting as revealed by T-RFLP analysis. *International Biodeterioration & Biodegradation*, 2010, **64**(8), 727–733, doi: 10.1016/j.ibiod.2010.08.006.
14. PEACOCK, E. E. Biodegradation and characterization of water-degraded archaeological textiles created for conservation research. *International Biodetrioration & Biodegradation*, 1996, **38**(1), 49–59, doi: 10.1016/S0964-8305(96)00023-6.
15. TOMŠIČ, Brigita, SIMONČIČ, Barbara, OREL, Boris, VILČNIK, Aljaž, SPREIZER, Helena. Biodegradability of cellulose fabric modified by imidazolidinone. *Carbohydrate Polymers*, 2007, **69**, 478–488, doi: 10.1016/j.carbpol.2007.01.003.
16. KAVKLER, Katja, GUNDE-CIMERMAN, Nina, ZALAR, Polona, DEMŠAR, Andrej. FTIR spectroscopy of biodegraded historical textiles. *Polymer Degradation and Stability*, 2011, **96**(4), 574–580, doi: 10.1016/j.polymdegradstab. 2010.12.016.
17. KAVKLER, Katja, DEMŠAR, Andrej. Examination of cellulose textile fibres in historical objects by micro-Raman spectroscopy. *Spectrochimica Acta Part A*, 2011, **78**(2), 740–746, doi: 10.1016/j.saa.2010.12.006.
18. AGARWAL, Umesh P. An overview of Raman spectroscopy as applied to lignocellulosic materials. In *Advances in lignocellulosic characterization*. Edited by Diimitris S. Argyropoulos. Atlanta : Tappi, 1999, pp. 201–225.
19. EDWARDS, H. G. M., WYETH, Paul. Case study: Ancient textile fibres. In *Raman spectroscopy in archaeology and art history*. Edited by Howell G. M. Edwards and John M. Chalmers. Cambridge : Royal Society of Chemistry, 2005, pp. 304–324.
20. EDWARDS, H. G. M., ELLIS, E., FARWELL, D. W., JANAWAY, R. C. Preliminary study of the application of Fourier transform Raman spectroscopy to the analysis of degraded archaeological linen textiles. *Journal of Raman Spectroscopy*, 1996, **27**(9), 663–669, doi: 10.1002/(SICI)1097-4555(199609)27:9<663::AID-JRS11>3.0.CO;2-E.
21. HIRSCHFELD, T., CHASE, B. FT-Raman spectroscopy: Development and justification. *Applied Spectroscopy*, 1986, **40**(2), 133–137, doi: 10.1366/0003702864509538.
22. GERRITS van den ENDE, Bert, DE HOOG, Sybren. Variability and molecular diagnostics of the neurotropic species *Cladophialophora bantiana*. *Studdies in Mycology*, 1999, **43**, 151–162.
23. AGARWAL, Umesh P., REINER, Richard S., RALPH, Sally A. Cellulose I crystallinity determination using FT-Raman spectroscopy: univariate and multivariate methods. *Cellulose*, 2010, **17**(4), 721–733.
24. EDWARDS, H. G. M., FARWELL, D. W., WEBSTER, D. FT Raman microscopy of untreated natural plant fibres. *Spectrochimica Acta Part A*, 1997, **53**(13), 2383–2392, doi: 10.1016/S1386-1425(97)00178-9.
25. JÄHN, A., SCHRÖDER, M.W., FÜTING, M., SCHENZEL, K., DIEPENBROCK, W. Characterization of alkali treated flax fibres by means of FT Raman spectroscopy and environmental scanning electron microscopy. *Spectrochimica*

Acta Part A, 2002, **58**(10) 2271–2279, doi: 10.1016/S1386-1425(01)00697-7.

26. PETROU, M., EDWARDS, H. G. M., JANAWAY, R. C., THOMPSON, G. B., WILSON, A. S. Fourier-transform Raman spectroscopic study of a Neolithic waterlogged wood assemblage. *Analytical and Bioanalytical Chemistry*, 2009, **395**(7), 2131–2138, doi: 10.1007/s00216-009-3178-x.
27. EDWARDS, Howell G. M., NIKHASSAN, Nik F., FARWELL, Dennis W., GARSIDE, P., WYETH, P. Raman spectroscopic analysis of a unique linen artefact: the HMS Victory Trafalgar sail. *Journal of Raman Spectroscopy*, 2006, **37**(10), 1193–1200, doi: 10.1002/jrs.1609.
28. CAO, Yu, SHEN, Deyan, LU, Yonglai, HUANG, Yong. A Raman-scattering study on the net orientation of biomacromolecules in the outer epidermal walls of mature wheat stems (*Triticum aestivum*). *Annals of Botany*, 2006, **97**(6), 1091–1094, doi: 10.1093/aob/mcl059.
29. GAWRON, J., SZCZĘSNA, M., ZIELENKIEWICZ, T., GOŁOFIT, T. Cellulose crystallinity index examination in oak wood originated from antique woodwork. *Drewno*, 2012, **55**(188), 109–114.
30. ILEC, Eva. Tekstil, *Priročnik: Muzejska konzervatorska in restavratorska dejavnost* [online]. Skupnost muzejev Slovenije [accessed 19. 01. 2018]. Available on World Wide Web: http://www.sms-muzeji.si/udatoteke/publikacija/netpdf/3-6.pdf.
31. TOMŠIČ, Brigita, SIMONČIČ, Barbara, VINCE, Jelica, OREL, Boris, VILČNIK, Aljaž. FIR, Mojca, ŠURCA VUK, Angela, JOVANOVSKI, Vasko. The use of ATR IR spectroscopy in the study of structural changes of the cellulose fibres. *Tekstilec*, 2007, **50**(1–3), 3–15.
32. KOVUR KUMAR, Siva, SCHENZEL, Karla C., GRIMM, Eckhard, DIEPENBROCK, Wulf. characterization of refined hemp fibres using NIR FT Raman micro spectroscopy and environmental scanning electron microscopy. *Bioresources*, 2008, **3**(4), 1081–1091, doi: 10.15376/biores.3.4.1081-1091.
33. STEVANIC SRNDOVIC, Jasna. *Interactions between wood polymers in wood cell walls and cellulose/hemicellulose biocomposites* : *doctoral thesis*, Chalmers University of Technology, Göteborg, Sweden, 2011.
34. De GUSSEM, Kris. *Optimisation of Raman spectroscopy for the analysis of Basidiomycota: spores, latex and mycelium : doctoral thesis*, Universiteit Gent, Faculteit Wetenschappen, 2007, p. 154.
35. AGARWAL, U. P., RENIER, R. S., RALPH, S. A. Determination of cellulose I crystallinity by FT-Raman spectroscopy. In *Proceedings of the 15th International Symposium on Wood, Fiber, and Pulping Chemistry.* Oslo, Norway (June 15-18, 2009), p. 4.
36. SCHENZEL, Karla, FISCHER, Steffen. Application of FT Raman spectroscopy for the characterization of cellulose. *Lenzinger Berichte*, 2004, **83**, 64–70.
37. DERRICK, Michele R., STULIK, Dusan C., LANDRY, James M. *Infrared spectroscopy in conservation science. Scientific tools for conservation*. Los Angeles : The Getty Conservation Institute, 1999.
38. PRONIEWICZ, L. M., PALUSKIEWICZ, C., WESEŁUCHA-BIRCZYŃSKA, A., BERAŃSKI, A., KONIECZNA, A. FT-IR and FT-Raman study of hydrothermally degradated cellulose. *Journal of Molecular Structure*, 2001, **596**, 163–169, doi: 10.1016/S0022-2860(01)00706-2.
39. CAO, Q., ZHU, S., PAN, N., ZHU, Y., TU, H. Characterization of archaeological cotton (*G. herbaceum*) fibers from Yingpan. *Technical Briefs in Historic Archaeology*, 2009, **4**, 18–28.
40. CARRILLO, F., COLOM, X., SUÑOL, J. J., SAURINA, J. Structural FTIR analysis and thermal characterisation of lyocell and viscose-type fibres. *European Polymer Journal*, 2004, **40**, 2229–2234, doi: 10.1016/j.eurpolymj.2004.05.003.

Sukhvir Singh
Amity University, Amity School of Fashion Design and Technology, Gurgaon, Haryana - 122413, India

Effect of MJS Spinning Variables on Yarn Quality

Vpliv nastavitve procesnih parametrov MJS curkovnega predilnika na kakovost preje

Original Scientific Article/*Izvirni znanstveni članek*
Received/*Prispelo* 03-2018 • Accepted/*Sprejeto* 06-2018

Abstract

Air-jet spinning variables play a significant role in determining MJS (Murata Jet Spinner) yarn structure and quality. This research work is an attempt to highlight the effect of a few imperative MJS spinning parameters on yarn quality characteristics. In order to investigate the effect of the MJS spinning speed, first-nozzle pressure and feed ratio on resultant yarn quality parameters, a Box-Behnken experimental design for three factors and three levels was adopted for research design and sample preparation. An analysis of variance (ANOVA) was performed to test the statistical significance of all effects.
Keywords: spinning speed, first-nozzle pressure, feed ratio, air-jet yarn

Izvleček

Procesni parametri curkovnega predenja imajo pomemben vpliv na strukturo in kakovost preje, izdelane na curkovnem predilniku MJS Murata. Raziskava se osredinja na vplive nekaterih pomembnih parametrov MJS Murata curkovnega predenja na lastnosti preje. Priprava vzorcev za proučitev vplivov hitrosti predenja, tlaka v prvi šobi in dovajalnega razmerja na kakovost končne preje je temeljila na eksperimentalnemu načrtu po Box-Behnkenu za tri faktorje in tri stopnje. Z analizo variance (ANOVA) je bila preizkušena statistična pomembnost vseh učinkov.
Ključne besede: hitrost predenja, tlak v prvi šobi, dovajalno razmerje, curkovna preja

1 Introduction

The effect of MJS spinning variables on yarn quality has been studied by many researchers in the past. It has been demonstrated in air-jet spinning machines that yarn tensile properties improve with an increase in delivery speed and first-nozzle pressure up to a certain limit, but that yarn quality deteriorates due to an increase in imperfection levels [1–3].Yarn hairiness increases with an increase in spinning speed due to a reduced number of wrapper fibres, which become inadequate for binding all protruding fibres [4–6]. It has been reported that an increase in first-nozzle pressure significantly improves MJS yarn tenacity and breaking elongation [7]. The number of core fibres decreases, while wrapper, wild and wrapper-wild fibres increase with an increase in first-nozzle pressure. First-nozzle pressure has a significant effect on yarn evenness due to the increased concentration of mass in a very short length on account of an increasing number of wrapper fibres [8–9]. It is believed that the yarn uniformity will improve with an increased feed ratio. The optimum value was found to be 0.98 (ratio of the surface speed of the delivery roller to the surface speed of the front roller). It has been reported that fibre orientation improves with an increase in feed ratio [10–11]. MJS yarn flexural rigidity and abrasion resistance improve with an increase in feed ratio [11–13].

In order to study the effect of scrutinised MJS spinning variables on viscose yarn quality, spinning speed, first-nozzle pressure and feed ratio were taken into account. For this purpose, draw-frame sliver was processed precisely on a MJS machine during sample preparation.

Corresponding author/*Korespondenčni avtor:*
Sukhvir Singh
E-mail: ssingh8@ggn.amity.edu

2 Materials and methods

2.1 Material

Air-jet spun viscose yarns of 14.76 tex were produced from 51 mm fibre length and 1.5 denier fibre fineness, taking into account a fibre density of 1.52 g/cm^3 Drawn viscose sliver hank of 3.28k tex was processed on a Murata air-jet spinner 802 machine for the preparation of yarn samples.

Preparation of yarn samples and experimental plan

In order to investigate the effect of MJS spinning variables on yarn quality parameters, a three-factor and three-level Box-Behnken experimental design technique was adopted for research design and the optimisation of the number of standard runs of manufactured yarn samples. The Box-Behnken design for three variables, together with the actual values of variables corresponding to the coded levels, is presented in Table 1 and Table 2 respectively. The most influential MJS spinning parameters, such as spinning speed, first-nozzle pressure and feed ratio, were shortlisted and taken into account as independent parameters to monitor their effect on dependent parameters, such as yarn unevenness and imperfections. The numerical values of each independent parameter were scrutinised in such a way that the difference between the low-to-middle and middle-to-high values remains constant, as seen in Table 2. An appropriate randomisation and replication technique was taken into account during sample preparation for an effective statistical analysis.

Conditioning of sample

The yarn sample was conditioned under standard atmospheric conditions, in a tropical atmosphere of 27 ± 2 °C and 65 ± 2% relative humidity, while the number of readings was determined according to the variation in the sample in order to achieve a 95% confidence interval.

2.2 Methods

Design of experiment

Table 1 and Table 2

Statistical analysis

The effect of the independent MJS spinning variables were statistically investigated using an ANOVA at a 95% confidence interval using statistical software. The independent factors taken into account were spinning speed, first-nozzle pressure and feed ratio to check for any statistically significance.

Yarn testing

Adequate numbers of yarn samples were tested taken into account a coefficient of variation. Yarn evenness and total imperfections, including thick +50%, thin –50% and neps +200%, were measured on a Star Evenness Tester, while maintaining a yarn speed of 50 m/min. Yarn hairiness was measured using a ZWEIGLE G565 instrument. An Instron tensile tester was used to test 20 samples per run of the single yarn strength and elongation percentage at break. Testing gauge length was kept at 500 mm at a 200 mm/min extension rate. Flexural rigidity was calculated using Owen's ring-loop method [14].

Table 1: Box-Behnken design for three variables

Standard runs	1	2	3	4	5	6	7	8	9	10	11	12	13	14	15
Spinning speed	–1	1	–1	1	–1	1	–1	1	0	0	0	0	0	0	0
First-nozzle pressure	–1	–1	1	1	0	0	0	0	–1	1	–1	1	0	0	0
Feed ratio	0	0	0	0	–1	–1	1	1	–1	–1	1	1	0	0	0

Table 2: Actual values of variables corresponding to the coded levels

Variables	–1	0	+1
Spinning speed [m/min]	150	170	190
First-nozzle pressure [kg/cm^2]	2	2.5	3
Feed ratio	0.96	0.97	0.98

3 Results and discussion

Table 3: Box-Behnken sample design, together with variables and their corresponding responses

Runs	Variables			Responses				
	Spinning speed [m/min]	First-nozzle pressure [kg/cm^2]	Feed ratio	U [%]	Total imperfections	Tenacity [g/tex]	Flexural rigidity [g·cm^2×10^{-3}]	Hairiness [S3hairs/ 100 m]
1	–1	–1	0	12.29	200	8.81	1.59	130
2	1	–1	0	14.10	304	9.38	2.58	155
3	–1	1	0	13.02	424	9.71	1.87	86
4	1	1	0	15.20	488	9.67	3.65	127
5	–1	0	–1	12.80	400	8.51	1.55	110
6	1	0	–1	14.50	520	7.77	2.62	155
7	–1	0	1	12.90	304	9.73	1.89	112
8	1	0	1	14.50	376	10.31	2.9	152
9	0	–1	–1	13.10	272	6.72	1.92	170
10	0	1	–1	14.20	544	9.31	2.15	121
11	0	–1	1	12.62	208	9.35	2.39	175
12	0	1	1	13.60	408	9.98	2.44	123
13	0	0	0	12.46	216	6.41	1.5	154
14	0	0	0	12.56	228	6.69	1.54	149
15	0	0	0	12.61	240	6.92	1.57	145

Table 4: ANOVA of MJS yarn quality parameters

Spinning variables	Effects				
	U [%]	Total Imperfections	Tenacity [g/tex]	Flexural rigidity [g·cm^2×10^{-3}]	Hairiness
Spinning speed [m/min]	0.00[a)], s [b)]	0.00, s	0.00, s	0.00, s	0.00, s
First-nozzle pressure	0.00, s	0.00, s	0.00, s	0.00, s	0.00, s
Feed ratio	0.00, s	0.00, s	0.00, s	0.03, s	0.62, ns[c)]

[a)] p-value

[b)] significant if $p < 0.05$ at a 95% confidence interval

[c)] ns- not significant if $p > 0.05$

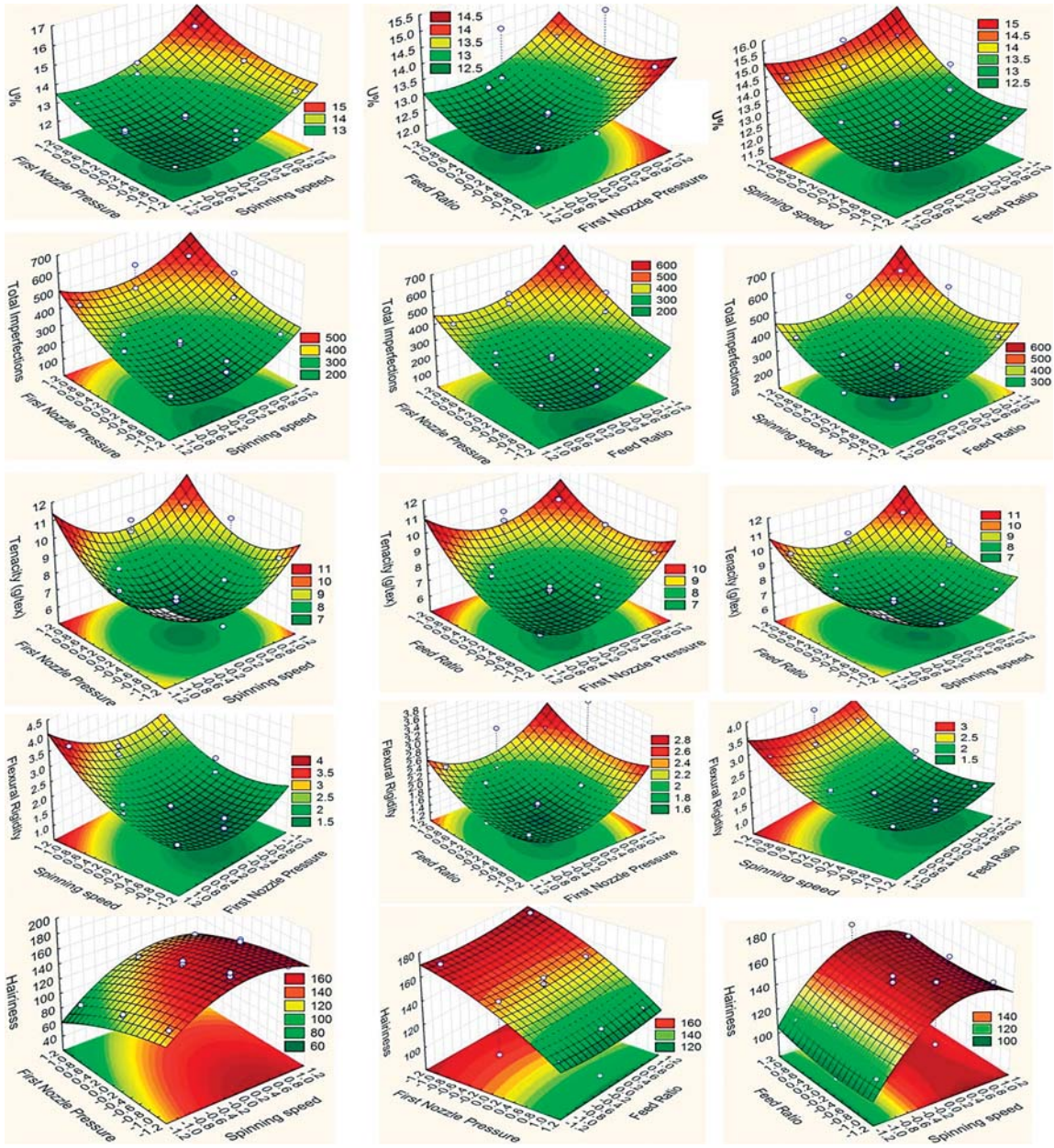

Figure 1: Effect of spinning variables on MJS yarn quality parameters

3.1 Effect of spinning speed on MJS yarn quality

At a high spinning speed, the air flow at the front roller nip causes the edge fibres to move away from the main bundle of fibres and increase the proportion of wrapper fibres. For this reason, yarn hairiness increases with an increase in spinning speed from 150 m/min to 190 m/min. Yarn unevenness increased slightly from 150 m/min to 170 m/min, while a further increase in spinning speed resulted in an increased number of imperfections in yarn, and thus, contributes to a deterioration in yarn quality, as seen in high level of unevenness. The interpretation of the experimental results shown in figure 1 reveals that yarn strength improves with an increase in spinning speed from 170 m/min to 190 m/min, but that yarn unevenness and total imperfections also increase. Yarn tenacity and flexural rigidity also increase slightly at a higher spinning speed due to the presence of more wrapper fibres and a compact yarn structure. Analysis of variance confirms the experimental findings.

3.2 Effect of first-nozzle pressure on MJS yarn quality

First-nozzle pressure has a significant effect on yarn structure, and due to an increased concentration of mass in a very short length as the result of an increasing number of wrapper fibres at a higher first-nozzle pressure. Thus, yarn hairiness decreases with an increase in first-nozzle pressure. It was observed that yarn unevenness and the total number of imperfections increases with an increase in first-nozzle pressure. Moreover, an increase in first-nozzle pressure will lead to an increase in yarn tenacity, while increased flexural rigidity may be due to the presence of an increased number of wrapper fibres.

3.3 Effect of feed ratio on MJS yarn quality

It was observed that there is no significant change in yarn quality characteristics with a change in the feed ratio from 0.96 to 0.98. However, the twist level of the yarn increases at a lower feed ratio, resulting in a harsher yarn.

4 Conclusion

It was observed that the spinning speed and first-nozzle pressure have a significant effect on MJS yarn quality parameters, while the feed ratio has a marginal effect on yarn quality parameters. The experimental results demonstrate that both unevenness and total imperfection increase with an increase in spinning speed and first-nozzle pressure. This study shows that an increase in spinning speed results in an increase in yarn hairiness, while the latter decreases with an increase in first-nozzle pressure. The effect of spinning variables on yarn tenacity and flexural rigidity was found to be marginal.

References

1. TYAGI, Gajendra Kumar, SALHOTRA, K. R. Influence of process parameters on characteristics of MJS yarns. *Indian Journal of Fibre& Textile Research,* 1996, **21**(3), 184-188.
2. CHASMAWALA, Rasesh J., HANSEN, Steven M., JAYARAMAN, Sundaresan. Structure and properties of air-jet spun yarns. 1990, *Textile Research Journal*, 1990,**60**(2), 61-69,doi: 10.1177/004051759006000201.
3. GROSBERG, P., OXENHAM, W., MIAO, M. The insertion of 'twist' into yarns by means of air-jets. Part 1: An experimental study of air-jet spinning. *Journal of Textile Institute* 1987, **78**(3),189203-,doi: 10.1080/00405008708658245.
4. LAWRENCE, Carl A., BAQUI, M. A. Effects of machine variables on structure and properties of air-jet fasciated yarns. *Textile Research Journal,* 1991, **61**(3),123-130, doi: 10.1177/004051759106100301.
5. ARTZET, P., DALLMANN, H. Opportunities for processing cotton by the air-spinning process. *MelliandTextilberichte,* 1989, **70**(5)3, 18-324.
6. TYAGI, Gajendra Kumar, SHAW, S. Performance characteristics of viscose ring and air-jet spun yarns as a consequence of draw frame speed and its preparatory process. *Indian Journal of Fibre& Textile Research,* 2012, **37**(4), 337-342.
7. PUNJ, S. K., MUKHOPADHYAY, A., BISWAS, J. Effect of machine variables on MJS P/V yarn properties. *Indian Textile Journal,* 1996, **106**(11), 34-36.
8. PUNJ, S. K., ISHTIAQUE, S. M., DHINGRA, L.K. Influence of spinning conditions on structure and properties of polyester-viscose blended MJS yarns. *Indian Journal of Fibre& Textile Research*, 1997, **22**(2), 73-83.
9. PUNJ, S. K., MOITRA, K., BEHERA, B.K. Effect of some machine variables on structure and properties of polyester-viscose air-jet spun yarn. *Indian Journal of Fibre& Textile Research*, 1998, **23**(2), 85-93.
10. PUNJ, S. K., MUKHOPADHYAY, Arunangshu, SAHA, R. N. Air-jet spinning of acrylic. *Textile Asia,* 1996, **27**(5), 53-56.
11. KATO, Hisaaki. Development of MJS yarns. *Journal of the Textile Machinery Society of Japan,* 1986, **32**(4), 95-102, doi: 10.4188/jte1955.32.95.
12. TYAGI, Gajendra Kumar, . Effect of spinning conditions on characteristics of polyester-viscose MJS core yarns. *Indian Journal of Fibre& Textile Research,* 2006, **31**(4), 515-520.
13. TYAGI, Gajendra Kumar, KAUSHIK, R.C.D., SALHOTRA, K. R. Properties of OE rotor and MJS yarns spun at high spinning speed. *Indian Journal of Fibre& Textile Research,* 1997, **22**(1), 8-12.
14. OWEN, J. D., RIDING, G. The weighted-ring stiffness tests. *Journal of Textile Institute Transactions,* 1964, **55**(8), 414-417, doi: 10.1080/19447026408662420.

Jana Banner, Maria Dautzenberg, Theresa Feldhans, Julia Hofmann, Pia Plümer, Andrea Ehrmann
Bielefeld University of Applied Sciences, Faculty of Engineering and Mathematics, Interaktion 1,
33619 Bielefeld, Germany

Water Resistance and Morphology of Electrospun Gelatine Blended with Citric Acid and Coconut Oil

Vodoodpornost in morfologija elektropredene želatine, mešane s citronsko kislino in kokosovim oljem

Original Scientific Article/*Izvirni znanstveni članek*
Received/*Prispelo* 04-2018 • Accepted/*Sprejeto* 06-2018

Abstract

Bio-polymer gelatine can be found in a broad variety of applications, mostly in the food industry. Moreover, it is used in the encapsulation of active pharmaceutical ingredients. In electrospinning, it is used for drug release, but can also strongly influence the morphologies of nanofiber mats when blended with other polymers. In a recent project, we studied the influence of adding citric acid and coconut oil to gelatine electrospinning solutions. While the former can be used to modify gelatine nanofiber diameters and create diverse morphologies between the fibres and sprayed droplets of different shapes, the latter results in an electrospraying process and additionally increases water resistance, suggesting a possible use of the combination for tailored drug release.
Keywords: nanofiber mat, water resistance, electrospraying

Izvleček

Biopolimerno želatino uporabljajo na številnih področjih, še posebno v živilski industriji, pa tudi pri kapsuliranju aktivnih farmakoloških sestavin. Pri elektropredenju jo uporabljajo za sproščanje zdravil. Ko jo mešajo z drugimi polimeri, pa lahko pomembno vpliva na morfologijo nanovlaknatih kopren. V nedavnem projektu sta bila preučevana vpliva dodatka citronske kisline in kokosovega olja k raztopljeni želatini za potrebe elektropredenja. Medtem ko se citronska kislina lahko uporabi za spreminjanje premera nanovlaken iz želatine in ustvarjanje različne morfologije med vlakni in razpršenimi kapljicami različnih oblik, pa povzroči kokosovo olje elektrorazprševanje in dodatno poveča vodoodpornost, kar kaže na možno uporabo kombinacije za načrtovano sproščanje zdravil.
Ključne besede: nanovlaknata koprena, vodoodpornost, elektrorazprševanje

1 Introduction

Gelatine belongs to bio-polymers which are often electrospun to create nanofiber mats for diverse purposes. Gelatine nanofibers can be used to mimic an extra-cellular matrix [1, 2] and are therefore expected to provide good growth and proliferation conditions for cells. Gelatine is known to bind cell surfaces via fibronectin binding better than native collagen [3]. However, gelatine has a disadvantage since it is water-soluble, which makes crosslinking after the electrospinning necessary, e.g. with a heat-treatment in the presence of different other chemicals [4, 5], addition of diverse acids [6] or toxic materials, such as glutaraldehyde [8].

Another possibility is using gelatine blended with other polymers. Blending silk fibroin with gelatine, for example, resulted in an increased nanofiber diameter and hydrophobicity, while the mechanical properties decreased [8]. Testing diverse PAN/bio-polymer blends, gelatine was found to be the only bio-polymer which significantly increased the PAN fibre diameters, an effect which survived wetting the samples although no cross-linking step

Corresponding author/*Korespondenčna avtorica:*
Prof. Dr. Dr. Andrea Ehrmann
E-mail: andrea.ehrmann@fh-bielefeld.de

was included [9]. Similarly, large fibre diameters could not be gained by modifying spinning and solution parameters of pure PAN [10]. Electrospinning PVA/gelatine blends was used to create scaffolds with modified hydrophobicity and morphology [11]. Similar results were found in ethyl cellulose/gelatine blends, which could be tailored between hydrophobic and hydrophilic properties, showing tuneable water stability [12]. Zein/gelatine blends were found to show high crystallinity, resulting in the preservation of a porous 3D structure gained by electrospinning, which was not possible in pure gelatine or pure zein nanofibers [13].

Blended with cellulose acetate, gelatine loaded with gabapentin was found to significantly increase injury regeneration in rats [14]. Similarly, gelatine-coated poly(butylene succinate) nanofiber mats could be used to immobilize thrombin, a haemostat, resulting in shorter haemostasis times and less blood loss than commercial gelatine sponges when tested in a rat liver model [15].

In the research, apart from some pre-tests with respect to pure gelatine, we examined the influence of citric acid on water resistance and morphology of pure gelatine fibres. This acid was shown to increase water stability of collagen/PEO nanofibers [16], of gelatine scaffolds which were not produced by electrospinning [17], and of electrospun native collagen fibres [18]. It must be mentioned that according to the literature, the bio-polymer which should be crosslinked and the citric acid need to be incubated for several hours and should afterwards be electrospun from the solution containing a high ratio of ethanol or similar solvents [19]. The latter was not possible in the electrospinning machine used in this project. Thus, our experiments aim at investigating whether the electrospinning process itself can replace the incubation process due to the large forces and high dynamics working during nanofiber formation. Electrospinning both materials together without former incubation has, to the best of our knowledge, not been reported before in the scientific literature and therefore represents a new approach to create water resistant gelatine nanofiber mats. If working, it would allow creating waterproof gelatine nanofiber mats without the necessity of using toxic cross-linkers afterwards, which could lead to the use of gelatine nanofiber mats for medical or biotechnological applications.

Additionally, the influence of coconut oil – which is known to work as a plasticizer [20] – was tested. Coconut oil also shows good antibacterial, anti-inflammatory and anti-viral properties [21, 22]. Electrospinning blends of gelatine and coconut oil were not found in the literature either, and might not only increase the possible application of such electrospun nanofiber due to combining the intrinsic medical properties of both materials, but may also stabilize gelatine to increase its water resistance.

2 Materials and methods

For electrospinning, a needleless electrospinning machine "Nanospider Lab" from Elmarco (Czech Republic) was used. The spinning parameters were as follows: temperature in the spinning chamber (21 ± 1) °C, relative humidity 33%, carriage speed 75–150 mm/s, substrate speed 0 mm/min, electrode distance 175–220 mm, electrode-substrate distance 50 mm, high voltage 70–75 kV between the lower electrode and the grounded upper electrode, and nozzle diameter 0.6–0.9 mm, depending on the viscosity of the spinning solutions. A polypropylene (PP) substrate (from Elmarco) was used as the substrate during electrospinning. A sketch of the electrospinning machine is shown in Figure 1.

Figure 1: Electrospinning setup in "Nanospider Lab"

Gelatine powder was purchased from Abtei (Germany), coconut oil from BioWise (Germany). The following spinning solutions were prepared from these materials, using aq. dest. as a solvent (all fractions are given as weight percentage, all spinning solutions besides the one with coconut oil had room temperature during electrospinning):

- G1: 35% gelatine,
- G1b: 35 wt.-% gelatine, boiling the solution and cooling down before spinning,
- G2b: 40 wt.-% gelatine, boiling the solution and cooling down before spinning,
- GCA1: 33 wt.-% gelatine + 3 wt.-% citric acid (solid),

– GCA2: 31 wt.-% gelatine + 14 wt.-% citric acid (solid),
– GCA3: 27 wt.-% gelatine + 24 wt.-% citric acid (solid),
– GCA4: 24 wt.-% gelatine + 33 wt.-% citric acid (solid),
– GCO: 26 wt.-% gelatine + 26 wt.-% coconut oil (heated to ~ 40 °C before spinning to reduce viscosity).

An optical examination of nanofiber mats was performed using a confocal laser scanning microscope (CLSM) VK-9000 (Keyence, Germany) with a nominal magnification of 2000×. All scale bars have the dimension of 10 μm.
Water resistance tests were performed by immersing the nanofiber mats completely into water for 1 min and letting them dry at room temperature afterwards.
Fibre diameters were measured on 10 fibres per image using ImageJ 1.51j8 (National Institutes of Health, USA).

3 Results and discussion

The first experiments aimed at investigating the influence of boiling the gelatine solution on the nanofiber mat morphology, as compared to its working at room temperature. Figure 2 depicts nanofiber mats, prepared from the solutions G1 and G1b, spun at the voltage of 70 kV. The images show that, on the one hand, the fibres became thinner after boiling the solution, and on the other hand, spherical agglomerates were formed. Thinner fibres can be explained by the reduction of gel-building abilities of gelatine when it is boiled. Both changes in the nanofiber mat morphology are not desired; the relatively thick gelatine nanofibers are often preferable for the application in cell growth, compared to the thinner ones.
Consequently, in the next test, a slightly higher concentration of gelatine was used to prepare a solution which had to be boiled again before the spinning to slightly reduce the viscosity and thus support the spinning process. Higher concentrations often result in thicker fibres, as investigations of other polymers have shown [10,23]. Figure 3 depicts the results of this experiment. Unfortunately, in this way only relatively few, chaotically arranged nanofibers were produced, which after the spinning duration of 35 min merely covered the thick substrate fibres, without creating a visible nanofiber mat.

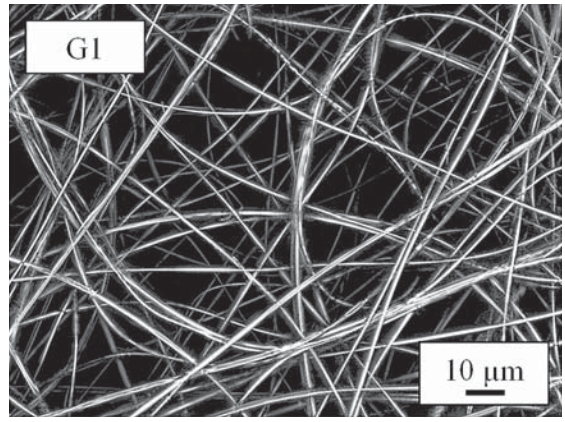

a

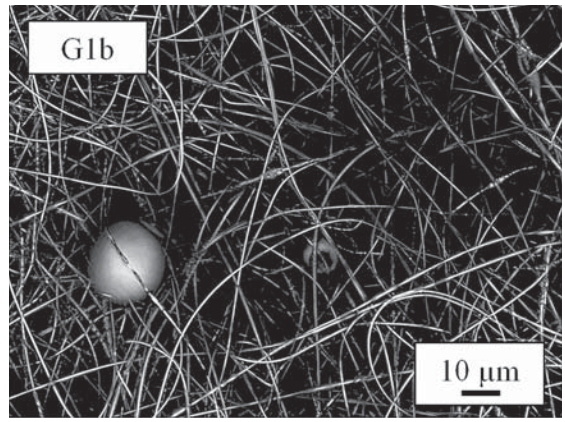

b

Figure 2: Nanofiber mat, created from solutions with 35% gelatine, prepared at room temperature (left panel, diameters (770 ± 210) nm) and after boiling, respectively (right panel, diameters (440 ± 130) nm)

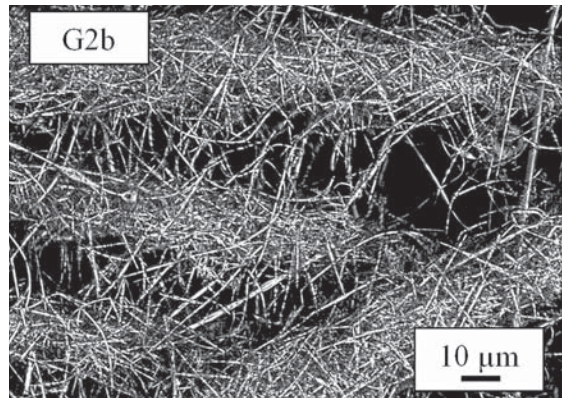

Figure 3: Nanofiber mat, created from solution with 40% gelatine, prepared after boiling (diameters (580 ± 140) nm)

Since former experiments in our group revealed a similar trend to significantly higher spinnability for slightly lower gelatine concentrations, the experiments with gelatine/citric acid blends were performed with reduced gelatine concentrations and without boiling.

The results are depicted in Figure 4. While sample GCA1, containing the highest gelatine and the lowest citric acid concentration, resulted in a mat of nanofibers with reduced diameters, increasing the citric acid concentration and at the same time decreasing the amount of gelatine resulted in electrospraying instead of electrospinning, with strongly changed droplet morphologies between spiky arrangements of very short nanofibers (GCA2) and smooth drops in a broad variety of diameters (GCA4). This finding can be explained by the well-known suppression of the gelling properties of gelatine in the presence of acids. The most interesting structure, however, is visible in sample GCA3. Here, a relatively thick coating on substrate fibres can be recognized, on top of which a labyrinth-like structure is revealed, looking like a strongly cross-linked net of thick gelatine fibres. It should be mentioned that the width of these features is approx. 1.5–2 μm, i.e. thicker than the nanofibers gained for sample GCA1 with the diameters in the range of 600–900 nm.

Unfortunately, the tests of water resistance of these nanofiber mats showed that all electrosprayed or electrospun structures were completely washed off of the substrate. The same occurred at all tests to increase water resistance by spraying citric acid onto pure gelatine fibre mats or vapour coating the electrospun gelatine mats with citric acid. It does not seem to be possible to increase water resistance of gelatine nanofiber mats in this way. Apparently, the incubation step mentioned in the literature cannot be replaced by the electrospinning process itself.

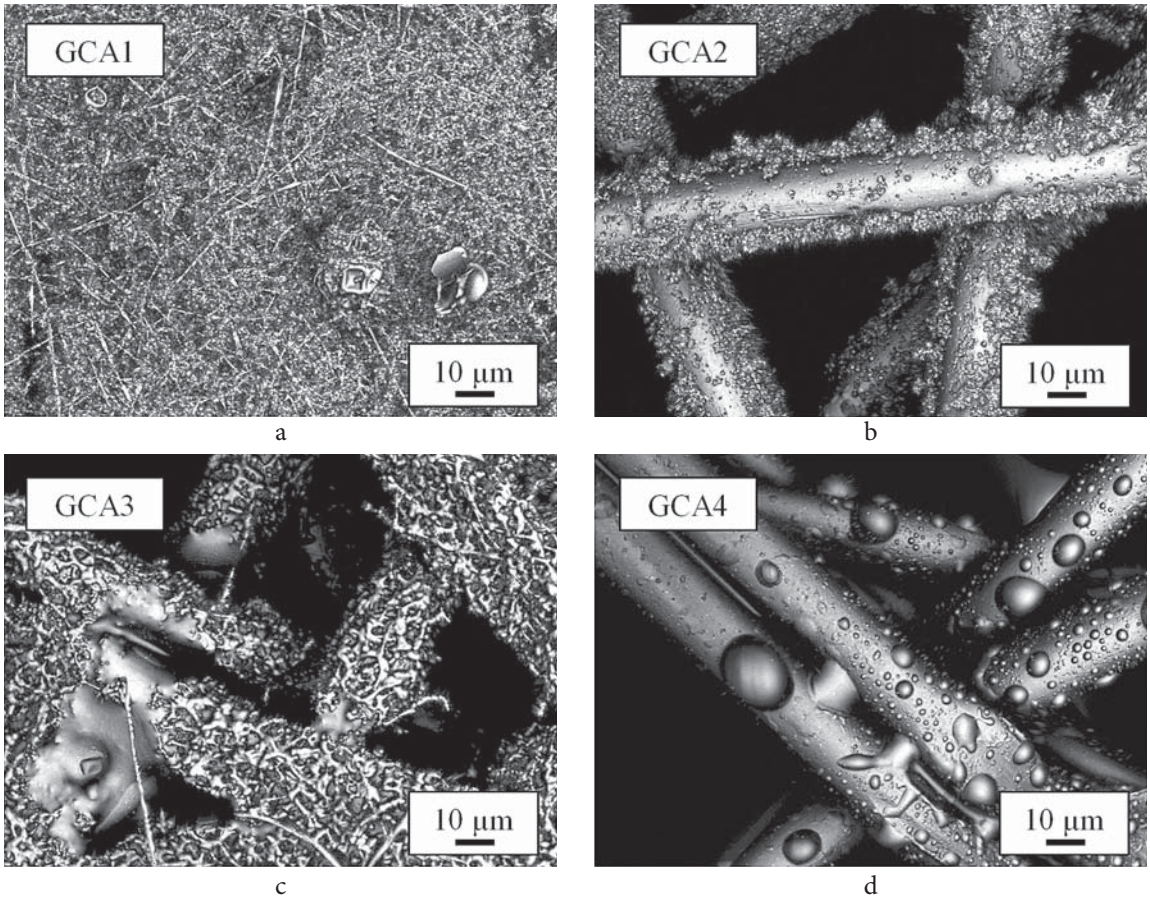

Figure 4: Nanofiber mats and electrosprayed samples GS1–GS4, prepared combining gelatine and citric acid, using carriage speed of 75 mm/s, electrode distance of 200 mm and high voltage of 75 kV

Finally, an experiment was performed combining gelatine with coconut oil. The solution could only be spun in a relatively warm state, i.e. for a limited time of approx. 30 min after heating the solution and putting it into the spinning equipment. The results of the electrospinning process and of wetting the sample afterwards are depicted in Figure 5.

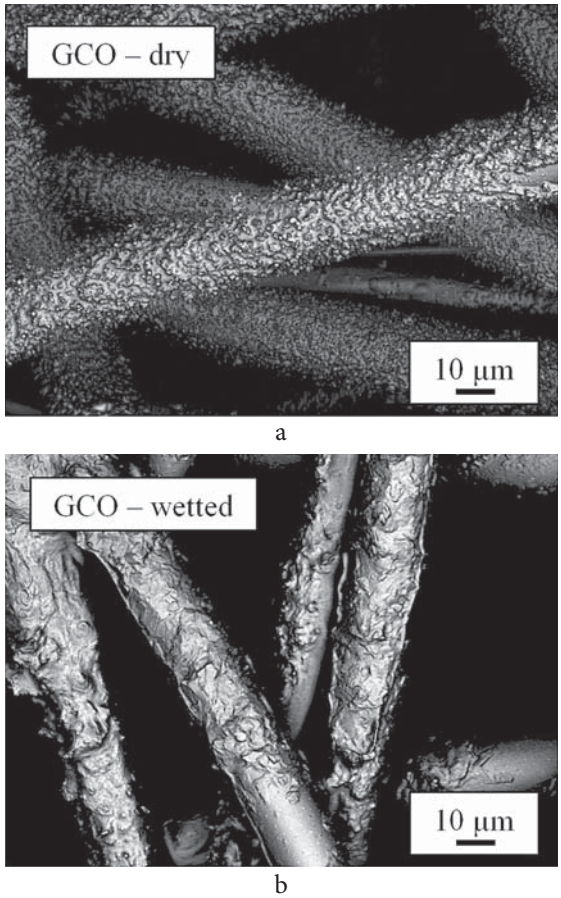

Figure 5: Electrosprayed samples GCO, prepared from warm gelatine/coconut oil solution, using carriage speed of 75 mm/s, electrode distance of 200 mm and high voltage of 75 kV

Figure 5 again shows an electrosprayed coating of the support nonwoven with another morphology than the other samples. Typically, electrospraying results in single, round dots, such as for sample GCA4. A similar structure, however, can be created by electrospraying poloxamer/dextran blends [24].
Opposite to the tests with gelatine/citric acid, which aimed at increasing water resistance compared to pure gelatine, adding coconut oil could indeed reduce the water solubility of the gelatine spray-coating. As depicted in Figure 5 (right panel), the surface morphology clearly changed after wetting the sample with a drop of water which dried on the fabric at room temperature, not washing off the coating. This finding is consistent with former experiments on casein, for which water stability could be significantly increased by adding wax or paraffin oil to the spinning solution [25]. We assume that this reduction of water solubility can be attributed to closing small pores in the coating, thus reducing the contact area between gelatine and water [26]. This suggests further experiments with different gelatine : coconut oil ratios to create nanofibers which may also show increased water resistance, making them suitable for a slow release of medical drugs etc.

4 Conclusion and outlook

To conclude, this study shows that citric acid can be used to modify the nanofiber mat morphology and create not only thinner fibres than with pure gelatine, but also different sprayed structures, including a labyrinth-like surface. Coconut oil, on the other hand, has indeed increased the water resistance of the resulting electrosprayed coatings.
Future research will concentrate on combining both features, i.e. creation of nanofiber mats or labyrinth-like coatings with increased water resistance, possibly also using the combination of coconut oil and citric acid to enable the use of such materials for drug delivery and similar applications where a large surface : volume ratio of nanofibers should be combined with slow dissolving in aqueous environments.

References

1. SROUJI, Samer, KIZHNER, Tali, SUSS-TOBI, E., LIVNE, E., ZUSSMAN, Eyal. 3-D Nanofibrous electrospun multilayered construct is an alternative ECM mimicking scaffold. *Journal of Materials Science: Materials in Medicine*, 2008, **19**(3), 1249–1255, doi: 10.1007/s10856-007-3218-z.
2. NAGHIBZADEH, Majid, ADABI, Mahdi. Evaluation of effective electrospinning parameters controlling gelatin nanofibers diameter via modelling artificial neural networks. *Fibers and Polymers*, 2014, **15**(4), 767–777.

3. PANKOV, Roumen, YAMADA, Kenneth M. Fibronectin at a glance. *Journal of Cell Science*, 2002, **115**, 3861–3863, doi: 10.1242/jcs.00059.
4. MINCHEVA, Rosica, MANOLOVA, Nevena, PANEVA, Dilyana, RASHKOV, Iliya. Preparation of polyelectrolyte-containing nanofibers by electrospinning in the presence of a non-ionogenic water-soluble polymer. *Journal of Bioactive and Compatible Polymers*, 2005, **20**(5), 419–435, doi: 10.1177/0883911505057447.
5. NAGHIBZADEH, Majid, FIROOZI, Saman, NODOUSHAN, Fatemeh Sadeghian, ADABI, Mohsen, KHORADMEHR, Arezoo, FESAHAT, Farzaneh, ESNAASHARI, Seyedeh Sara, KHOSRAVANI, Masood, ADABI, Mandi, TAVAKOL, Shima, PAZOKI-ROROUDI, Hamidreza, ADEL, Moein, ZAHMATKESHAN, Masoumeh. Application of electrospun gelatin nanofibers in tissue engineering. *Biointerface Research in Applied Chemistry*, 2018, **8**(1), 3048–3052.
6. CHOMACHAYI, Masoud Dadras, SOLOUK, Atefeh, AKBARI, Somaye, SADEGHI, Davoud, MIRAHMADI, Fereshteh, MIRZADEH, Hamid. Electrospun nanofibers comprising of silk fibroin/gelatin for drug delivery applications: Thyme essential oil and doxycycline monohydrate release study. *Journal of Biomedical Materials Research Part A*, 2018, **106**(4), 1092–1103, doi: 10.1002/jbm.a.36303.
7. TAVASSOLI-KAFRANI, Elham, GOLI, Sayed Amir Hossein, FATHI, Milad. Fabrication and characterization of electrospun gelatin nanofibers crosslinked with oxidized phenolic compounds. *International Journal of Biological Macromolecules*, 2017, **103**, 1062–1068, doi: 10.1016/j.ijbiomac.2017.05.152.
8. LAHA, Anindita, YADAV, Shital, MAJUMDAR, Saptarshi, SHARMA, Chandra S. In-vitro release study of hydrophobic drug using electrospun cross-linked gelatin nanofibers. *Biochemical Engineering Journal*, 2016, **105**, 481–488, doi: 10.1016/j.bej.2015.11.001.
9. WEHLAGE, Daria, BÖTTJER, Robin, GROTHE, Timo, EHRMANN, Andrea. Electrospinning water-soluble/insoluble polymer blends. *AIMS Materials Science*, 2018, **5**(2), 190–200, doi: 10.3934/matersci.2018.2.190.
10. GROTHE, Timo, WEHLAGE, Daria, BÖHM, Tobias, REMCHE, Alexander, EHRMANN, Andrea. Needleless Electrospinning of PAN Nanofiber Mats. *Tekstilec*, 2017, **60**(4), 290–295, doi: 10.14502/Tekstilec2017.60.290-295.
11. PEREZ-PUYANA, Victor, JIMENEZ-ROSADO, Mercedes, ROMERO, A., GUERRERO, Antonio. Development of PVA/gelatin nanofibrous scaffolds for Tissue Engineering via electrospinning. *Materials Research Express*, 2018, **5**(3), 035401, doi: 10.1088/2053-1591/aab164.
12. LIU, Yuyu, DENG, Lingli, ZHANG, Cen, FENG, Fengqin, ZHANG, Hui. Tunable physical properties of ethylcellulose/gelatin composite nanofibers by electrospinning. *Journal of Agricultural and Food Chemistry*, 2018, **66**(8), 1907–1915, doi: 10.1021/acs.jafc.7b06038.
13. DENG, Lingli, ZHANG, Xi, LI, Yang, QUE, Fei, KANG, Xuefan, LIU, Yuyu, FENG, Fengqin, ZHANG, Hui. Characterization of gelatin/zein nanofibers by hybrid electrospinning. *Food Hydrocolloids*, 2018, **75**, 72–80, doi: 10.1016/j.foodhyd.2017.09.011.
14. FARZAMFAR, Saeed, NASERI-NOSAR, Mahdi, VAEZ, Ahmad, ESMAEILPOUR, Farshid, EHTERAMI, Arian, SAHRAPEYMA, Hamed, SAMADIAN, Hadi, HAMIDIEH, Amir-Ali, GHORBANI, Sadegh, GOODARZI, Arash, AZIMI, Arian, SALEHI, Majid. Neural tissue regeneration by a gabapentin-loaded cellulose acetate/gelatin wet-electrospun scaffold. *Cellulose*, 2018, **25**(2), 1229–1238, doi: 10.1007/s10570-017-1632-z.
15. CHENG, Hui-Hui, XIONG, Jiang, XIE, Zhi-Ning, ZHU, Ya-Ting, LIU, Yu-Man, WU, Zhong-Yin, YU, Jian, GUO, Zhao-Xia. Thrombin-loaded Poly(butylene succinate)-based electrospun membranes for rapid hemostatic application. *Macromolecular Materials and Engineering*, 2018, **303**(2), 1700395, doi: 10.1002/mame.201700395.
16. GAO, Jing, GUO, Huiwen, ZHAO, Linshuang, ZHAO, Xinzhe, WANG, Lu. Water-stability and biological behavior of electrospun collagen/PEO fibers by environmental friendly crosslinking. *Fibers and Polymers*, 2017, **18**(8), 1496–1503, doi: 10.1007/s12221-017-7319-0.
17. JIANG, Qiuran, XU, Helan, CAI, Shaobo, YANG, Yiqi. Ultrafine fibrous gelatin scaffolds with deep cell infiltration mimicking 3D ECMs for soft tissue repair. *Journal of Materials Science: Materials in Medicine*, 2014, **25**(7), 1789–1800, doi: 10.1007/s10856-014-5208-2.

18. JIANG, Qiuran, REDDY, Narendra, ZHANG, Simeng, ROSCIOLI, Nicholas, YANG, Yiqi. Water-stable electrospun collagen fibers from a non-toxic solvent and crosslinking system. *Journal of Biomedical Materials Research Part A*, 2013, **101**(5), 1237–1247, doi: 10.1002/jbm.a.34422.
19. JIANG, Qiuran, REDDY, Narendra, YANG, Yiqi. Cytocompatible cross-linking of electrospun zein fibers for the development of water-stable tissue engineering scaffolds. *Acta Biomaterialia*, 2010, **6**(10), 4042–4051, doi: 10.1016/J.ACTBIO.2010.04.024.
20. CHAVEZ GUTIERREZ, Miguel, DEL CARMEN NUNEZ-SANTIAGO, Maria, ROMERO-BASTIDA, Claudia Andrea, MARTINEZ-BUSTOS, Fernando. Effects of coconut oil concentration as a plasticizer and Yucca schidigera extract as a surfactant in the preparation of extruded corn starch films. *Starch – Stärke*, 2014, **66**(11–12), 1079–1088, doi: 10.1002/star.201400062.
21. EL-NAGGAR, Mehrez E., SHAFIE, Shaarawy A. El., HEBEISH, A. Development of antimicrobial medical cotton fabrics using synthesized nanoemulsion of reactive cyclodextrin hosted coconut oil inclusion complex. *Fibers and Polymers*, 2017, **18**(8), 1486–1495, doi: 10.1007/s12221-017-7390-6.
22. MUKTAR, Muhammad Zulhemi, ROSE, Laili Che, AMIN, Khairul Anuar Mat. Formulation and optimization of virgin coconut oil with Tween-80 incorporated in gellan gum hydrogel. In *3rd Electronic and Green Materials International Conference 2017 : AIP Conference Proceedings*. Krabi, Thailand, 2017, **1885**, 020044-1, doi: 10.1063/1.5002238.
23. SABANTINA, Lilia, MIRASOL, José Rodríguez, CORDERO, Tomás, FINSTERBUSCH, Karin, EHRMANN, Andrea. Investigation of needleless electrospun pan nanofiber mats. *AIP Conference Proceedings*, 2018, **1952**, 020085, doi: 10.1063/1.5032047.
24. BÖTTJER, Robin, GROTHE, Timo, WEHLAGE, Daria, EHRMANN, Andrea. Electrospraying poloxamer/(bio-)polymer blends using a needleless electrospinning machine. *Journal of Textiles and Fibrous Materials*, 2018, **1**, 1–7, doi: 10.1177/2515221117743079.
25. BIER, Marie Carolin, KOHN, Sophia, STIERAND, Antonia, GRIMMELSMANN, Nils, HOMBURG, Sarah Vanessa, RATTENHOLL, Anke, EHRMANN, Andrea. Investigation of eco-friendly casein fibre production methods. *IOP Conf. Series: Materials Science and Engineering*, 2017, **254**, 192004, doi: 10.1088/1757-899X/254/19/192004.
26. LAI, Huey-Min PADUA, Graciela W. Properties and microstructure of plasticized zein films. *Cereal Chemistry*, 1997, **74**, 771–775, doi: 10.1094/CCHEM.1997.74.6.771.

Jelena Vasiljević[1], Marija Čolović[2], Ivan Jerman[2], Barbara Simončič[1]
[1]University of Ljubljana, Faculty of Natural Sciences and Engineering, Aškerčeva 12, 1000 Ljubljana, Slovenia
[2]National Institute of Chemistry, Hajdrihova 19, 1000 Ljubljana, Slovenia

Recent Advances in Production of Flame Retardant Polyamide 6 Filament Yarns

Najsodobnejše raziskave na področju proizvodnje ognjevarnih poliamidnih 6 filamentnih prej

Scientific Review/*Pregledni znanstveni članek*
Received/*Prispelo* 06-2018 • Accepted/*Sprejeto* 06-2018

Abstract

Polyamide 6 is one of the key engineering polymers with excellent mechanical properties and resistance which enable its global production and wide use in the industrial and domestic plastic manufacturing. Polyamide 6 also represents an important raw material for the production of technical filament yarns. However, an important drawback associated with the flammability of PA6 fibres has not been resolved yet. This paper reviews the most common halogen-free flame retardant additives for polyamide 6, their mode of action as well as different strategies for the incorporation of flame retardant additives in the production process of flame ratardant polyamide 6 fibres. The most recent research and patents on this topic are critically discussed.
Keywords: textile, bulk polymers, flame retardancy, flame retardant additives, production strategies

Izvleček

Poliamid 6 je eden ključnih inženirskih polimerov z odličnimi mehanskimi lastnostmi in visoko odpornostjo, ki omogoča njegovo široko uporabo pri proizvodnji industrijskih in gospodinjskih plastičnih mas. Poliamid 6 predstavlja tudi pomembno surovino za proizvodnjo filamentnih prej za tehnične namene. Vendar pa pomembna pomanjkljivost, povezana z vnetljivostjo poliamidnih 6 vlaken, še ni bila odpravljena. Članek vključuje pregled najpogosteje uporabljenih ne-halogenih ognjevarnih aditivov za poliamid 6, njihovega načina delovanja in različnih pristopov za vgradnjo ognjevarnih aditivov v proizvodnem procesu ognjevarnih vlaken iz poliamida 6. Predstavljena je kritična razprava o najsodobnejših raziskavah in patentih na področju.
Ključne besede: tekstilije, plastične mase, ognjevarnost, ognjevarna sredstva, proizvodne strategije

1 Introduction

Polyamide 6 (PA6) is one of the key engineering polymers with excellent mechanical properties and resistance which enable its global production and wide use in the industrial and domestic plastic manufacturing. Excellent processing properties, low moulding shrinkage and simple and low cost processing on one hand as well as its toughness, high tensile strength, abrasion and creep resistance on the other hand enabled PA6 to become one of the most important raw materials in the production of textile fibres for technical applications, such as technical clothing, carpets and carpet paddings, fabrics for furniture upholstery, transport seats, floor coverings and air bags [1]. Whereas PA6 plastics represent the largest segment of the global polyamide market, the PA6 textile fibre application segment is the fastest growing [2]. Furthermore, PA6 has an exceptional feature, i.e., its chemical recyclability back to monomer ε-caprolactam, which classifies PA6 as a "sustainable polymer"

Corresponding author/*Korespondenčna avtorica:*
Assist dr. Jelena Vasiljević
E-mail: jelena.vasiljevic@ntf.uni-lj.si

and, consequently, dramatically enhances its reusability and added value [3].

Despite the widespread use of PA6 in various economic areas, a problem associated with the flammability of PA6 fibres has not been solved yet. Specifically, a very hazardous drawback of PA6 is its inherent flammability, which can lead to rapid burning with an intensive flammable melt-dripping and a release of toxic smoke, which may present a great risk and danger for lives and material goods. Despite the rather successful production of flame retardant (FR) PA6 moulding plastic materials, the development of FR PA6 textile fibres remains a challenging scientific problem, and commercially available FR PA6 textile fibres still do not exist [4].

Much effort has been put into the production of FR PA6 fibres during the last decades [4–8]. For effective FR action, it is crucial that the FR additive matches the processing and pyrolysis specifics of PA6. Accordingly, the FR additive needs to be thermally stable and non-volatile at the processing temperatures of PA6 composites and filaments. The thermal stability and mode of action of the FR additive must match those of PA6 during pyrolysis, during which the mostly volatile cyclic monomer ε-caprolactam, alkyl cyanides and ammonia are produced, leaving no charred residue in the condensed phase [9]. According to the literature, FR loadings higher than 15 wt% are required to achieve an effective FR action in the PA6 bulk polymers [4], but these high loadings are unacceptable for the textile fibres because of their impaired spinnability and tensile properties. These represent the most important limitations in the production of FR PA6 fibres in comparison with PA6 bulk polymers. Furthermore, compared to bulk plastic, the lightweight PA6 textile fibres and fabrics have an open structure with a much higher surface, which intensifies the burning rate.

2 Structures of FR additives and their mode of action

Although halogenated FR additives are very effective and have been some of the most important FR additives for PA6 over the decades, they have been prohibited as substances of Very High Concern (REACH SVCH), and due to their persistence, bioaccumulation and high toxicity (PBT), there is a gap in the market for FR additives. The most intensively investigated halogen-free FR additives for PA6 include phosphorus (P)- and nitrogen (N)-based FRs, inorganic hydroxides and different nanoparticles [4–8, 10–12]. The most common FRs for PA6 are summarised in Table 1, and some of them are presented in Figure 1.

FR mechanisms and modes of action depend on the chemical structures of the FR additives as well as the structure and thermal decomposition pathway of the polymers. Accordingly, FR additives act chemically and/or physically in the gas phase and/or in the condensed phase (Figure 2) [4–8, 10–12]. It is known that the same FR additive can provide different flame retardancy for different polymers. In general, P-based FR additives are active in both the condensed phase and the gas phase depending on the oxidation state of the P atom [67]. According to the condensed-phase mode of action, phosphorous compounds, i.e., phosphates and phosphonates, promote char formation by influencing the decomposition pathway of the polymers. If this reaction is accompanied by the release of water, the combustive vapours are also diluted. According to the gas-phase mechanism, phosphorous compounds, i.e., phosphinates and phosphine oxides, decompose to radical scavengers, which terminate the oxidative radical chain reactions in the combustion cycle. In the case of PA6, the gas phase contributes more to flame retardancy than char formation because the polymer chain scission, which occurs during thermal decomposition, leads to the generation of ε-caprolactam and other volatiles from the shorter chain fragments, and very little char residue is formed. Therefore, char-promoting phosphorous FRs alone are not enough to be effective in PA6. In contrast, the gas phase active P-based FR additives are of great importance for the protection of PA6. Specifically, phosphorous radicals in the flame, i.e., HPO_2·, PO·, PO_2· and HPO·, can scavenge H· and OH· radicals that propagate fuel combustion. This leads to a reduction in concentrations of H· and OH· radicals and the quenching of the flame.

Among N-based FR additives, MeCy has special importance since it is considered as one of the most effective FR additives for aliphatic polyamides [68]. MeCy exhibits a strong condensed-phase mode of action; however, it is also active in the gaseous phase [18]. At higher temperatures, MeCy undergoes

Table 1: The most common halogen-free FR additives for PA6

FR-active chemical element or group	Chemical structure	Reference
Phosphorous	6-((6-oxidodibenzo[c,e][1,2]-oxaphosphinine-6-yl) methoxy)dibenzo[c,e][1,2]-oxaphosphinine-6-oxide) (Di-DOPO-MeO)	[13]
Nitrogen	ammonium sulfamate (AS)	[14–17]
	melamine cyanurate (MeCy)	[18–27]
Phosphorous, nitrogen	ammonium polyphosphate (APP)	[28]
	melamine polyphosphate (MPP)	[29–32]
	6-(2-(4,6-diamino-1,3,5-triazin-2-yl)ethyl)dibenzo[c,e] [1,2]oxaphosphinine-6-oxide (DTE-DOPO)	[33]
	6, 60-(ethane-1,2-diylbis(azanediyl))bis(dibenzo[c,e] [1,2]-oxaphosphinine-6-oxide) (Di-DOPO-EDA)	[13]
	9,10-dihydro-9-oxa-10-phosphaphenanthrene-10-oxide-based diepoxide (DEP)	[34, 35]
	cyclotriphosphazene	[36–38]
Phosphorous, aluminium	aluminium dialkylphosphinate (AlPi)	[16, 28–31, 33, [38–46]
	aluminium hypophosphite	[41, 42, 47]
Phosphorous, boron	boron phosphate	[44, 48, 49]
Phosphorous, silicon	9,10-dihydro-9-oxa-10-phosphaphenanthrene-10-oxide-functionalised triethoxysilane (SiDOPO)	[50, 51]
	diethylphosphatoethyltriethoxysilane (SiP)	52
Boron	zinc borate	44, 53
Group II or III hydroxides	alumina monohydrate, AlO(OH)	[4, 54, 55]
	magnesium hydroxide, $Mg(OH)_2$	[55, 56]
Silicon	tetraethoxysilane	[52]
Aluminium, silicon	pristine clays (bentonite, kaolinite, zeolite), pristine nanoclays (halloysite nanotubes)	[14, 27, 57–60]
	organically modified nanoclays (montmorillonite (MMT))	[30, 31,61,62]
Carbon	carbon nanotubes (CNTs)	[63–66]

endothermic decomposition to melamine and cyanuric acid. Melamine partially sublimes at approximately 350 °C, which is accompanied by a significant absorption of energy. In the condensed phase, melamine undergoes endothermic self-condensation with the release of ammonia, which volatilises and dilutes the fuel gases that support combustion. MeCy also decreases the thermal stability of PA6 and catalyses the chain scission of PA6 macromolecules to oligomeric segments, which are less flammable than caprolactam. The chain scission also decreases the melt viscosity and accelerates melt flow and dripping. Because the melt drips remove heat from the polymer matrix, the phenomenon of flame self-extinguishment occurs. MeCy also promotes the formation of a cross-linked structure in the self-condensation reaction with the generated oligomers. This promotes the formation of a closed char layer.

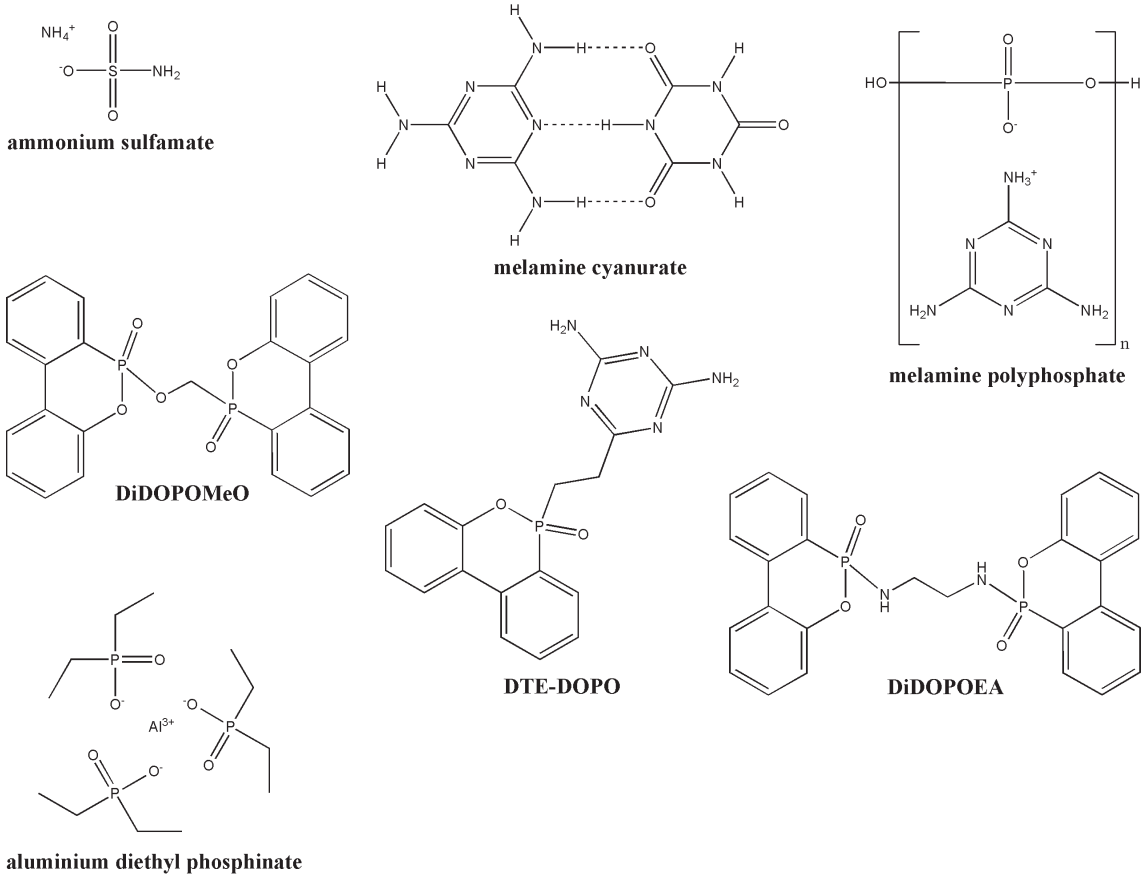

Figure 1: Chemical structures of some representative FR additives for PA6

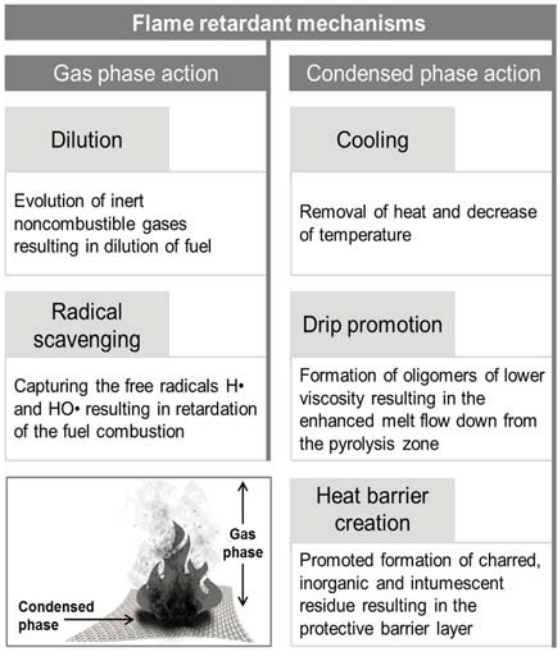

Figure 2: Flame retardant mechanisms of FR additives

MPP, as a representative of the P/N-based FR additives, was developed as a char former in the intumescent FR action. The latter is characterised by swelling and expanding at temperatures higher than critical temperature, leading to the formation of a foamed cellular charred layer [4, 9, 69]. In the intumescent FR formulations, MPP acts as an acid source because the release of phosphoric acid promotes the creation of a carbonaceous shield on the polymer surface, which acts as a heat-barrier and physically prevents contact between the polymer and the flame and hinders the flow of oxygen and heat to the polymer surface. As an acid source, ammonium phosphate, ammonium polyphosphate or AS can also be used [8]. For effective intumescent FR action, the acid source-containing FR additives are usually combined with the carbon source-containing additives, for instance, pentaerythritol, as well as a blowing agent, mostly melamine or guanidine, which releases non-combustible gases.

The FR action of inorganic hydroxides, such as AlO(OH) and $Mg(OH)_2$, involves heat sink and heat-barrier effects [8, 54, 56]. At temperatures between 340–350 °C and above 300–320 °C, boehmite and magnesium hydroxide, respectively, undergo endothermic decomposition (absorbing heat) in which free water is produced. This results in the cooling of the polymer and the diluting of the combustive gas mixture by the release of the vapours. The water release could also enhance the decomposition of PA6. In addition, a mineral layer formed on the polymer surface acts as a barrier that prevents contact between the heat and the polymer.

Silica as well as different clays exhibit the heat-barrier FR effect. They contribute to the formation of a reinforced insulating charred layer, which acts as a heat and gas barrier and protects the polymer against thermal oxidation and mass loss during combustion [30, 61, 70]. The presence of the protective layer increases the thermal stability of PA6 and significantly reduces the heat release rate during combustion relative to pristine PA6, suggesting improved fire behaviour. Additionally, smoke obscuration is significantly lowered in the presence of clays. Well-dispersed particles of clay can act as nucleating sites for bubble formation in the residue during the decomposition process, leading to an expanded carbonized material composed of a large bubble covering the residue. The gases trapped under the bubble insulate the surface of the polymer [30].

The FR mechanism of CNTs differs from that of clays [63]. It is assumed that CNTs act as inert fillers that do not significantly influence the thermal decomposition behaviour of PA6. The presence of CNTs in the PA6 composite increases the time to ignition and decreases the heat release rate but does not significantly lower the total heat release in comparison to pristine PA6. The reason for the increase in the time to ignition is attributed to the improved thermal conductivity or the increased melt viscosity of the composite. A decreased heat release rate caused by the CNTs in the composite would indicate a reduction in flammability. However, on the contrary, during ignition, the CNTs form a thermally stable interconnected network structure, which fixes the molten material in the pyrolysis zone and prevents melt-dripping. This results in the increase in the composite burning intensity. Since CNTs subsequently decompose in the thermo-oxidative reaction, no charred residue is created during the thermal decomposition of the PA6 composite.

3 Strategies for the production of FR PA6 fibres

The most common strategy for the production of FR PA6 fibres includes the use of the melt-compounded PA6/FR composites in the melt-spinning process [71]. However, there are several drawbacks in the fibre production process when using the "melt-compounding approach" related to the agglomeration of FR additives in the PA6 matrix [26, 32]. Specifically, the high melt reactivity of PA6 and its poor compatibility with FRs due to the strong intermolecular hydrogen bonds between the polymer chains cause the agglomeration of FR additive species. This results in the non-uniformly dispersed and low-dispersed micro-sized FR additive particles in the PA6 matrix. The flame-retardant action of the FR molecules entrapped in the micro-sized agglomerates is inhibited because of the inability of the entrapped FR molecules to actively participate in the flame retarding action. The flame retarding action occurs at the nanoscopic level. In the case of the micro-sized aggregates, only the outermost molecules can efficiently participate in the flame retarding action. Thus, in the case of the aggregated FRs, increased weight percent loading of the FR additive is unavoidable for efficient flame retardancy. Furthermore, the micro-sized FR agglomerates impair the spinnability of the PA6 composite filaments since they cause clogging of the filters and spinnerets at higher FR additive loadings. The agglomerates also significantly impair the physical and mechanical properties of the fibres. Consequently, the loading of FR additives that are acceptable for the continuous melt-spinning process provides only a poor FR effect. To solve these problems, three main approaches in the production process of FR PA6 fibres have been introduced: (i) preparation of the melt-compounded PA6/FR composites with the incorporation of FR nanoparticles as well as FR mixtures with a synergistic action, (ii) *in situ* polymerisation of ε-caprolactam in the presence of the FR additives, and (iii) synthesis of PA6 copolymers with the incorporation of reactive FR co-monomers.

3.1 Melt-compounded PA6/FR composites with the incorporation of nanoparticles and synergistic FR mixtures

The incorporation of nanoclays into the PA6 composite fibres was first reported by Bourbigot et al. [61], who prepared a PA6 nanocomposite with 5 wt%

Cloisite 30B (Southern Clay Products Inc., USA), which is organically modified montmorillonite. The composite masterbatch was used in a melt-spinning process for the production of multifilament yarn, which was afterwards knitted into knit fabric. Flame retardancy was evaluated in terms of cone calorimetric analysis. The results show that the presence of nanoclay reduced the heat release rate by 40% and significantly lowered smoke obscuration in comparison with the pristine PA6 fabric. However, the flame spread test was not carried out.

Onder et al. [62] also used two types of nanoclays, i.e., a commercially available organically modified montmorillonite, SA682640 (Sigma-Aldrich, UK), and a self-produced organoclay, and melt spun PA6 nanocomposite monofilaments comprising varying amounts of the organoclay ranging between 0.5 and 5 wt%. The results of the thermogravimetric (TG) analysis reveal that the presence of both nanoclays considerably improves the thermal stability of the nanocomposite structures, which is caused by the shift of their mass loss to higher temperatures by 25 to 33 °C. In addition to improved thermal properties, the mechanical properties of the PA6 composite yarns met the requirements of many textile applications.

Dogan and Bayramli [49] investigated the influence of boron phosphate (BPO_4) particles of spherical shapes with diameters of approximately 200 nm on the thermal and mechanical properties of the PA6 fibres. They mixed the PA6 pellets with the BPO_4 powder to prepare composites with 3 wt% and 10 wt% BPO_4 from which monofilament fibres were melt spun. The flame retardancy of the fibres was investigated by TG analysis and micro-combustion calorimetry. The results show that the presence of BPO_4 slightly reduced the thermal stability of the PA6 composite fibres, which was caused by the decrease in the maximum decomposition temperature of PA6, reducing the total heat release and increasing the amount of char residue. The latter phenomenon was more susceptible at higher BPO_4 concentrations. The incorporation of BPO_4 deteriorated the mechanical properties of the PA6 composite fibres, resulting in a decrease in the Young's modulus, stress at break and elongation of break. The deterioration of the mechanical properties increased with the increase in BPO_4 concentration.

Coquelle et al. [15] prepared PA6 composite monofilament fibres with the addition of 3 wt%, 5 wt%, 7 wt% and 10 wt% of AS (Sigma-Aldrich, Germany) as the FR additive. The results of the TG and a pyrolysis combustion flow calorimetric analyses show that 7 wt% AS reduced the peak of heat release rate by 30 % due to the combined gas and condense phases action of AS. However, fibres containing 7 wt% of AS were spinnable but were very brittle, therefore lower AS loadings were recommended for the production of PA6/AS fibres for the textile applications.

Sun et al. [32] studied the influence of MPP in the form of the commercial product, Melapur 200 (BASF, Germany), and halloysite nanotubes (Sigma-Aldrich, Germany) on the flammability and thermal stability of PA6 composites as well as the spinnability of PA6 composite fibres. To assure good spinnability, the total amount of FR additives was fixed at 12 wt% with different ratios of both MMP and halloysite nanotubes. The flame-retardant properties of the PA6 composites, but not of the composite fibres, were characterised by the limiting oxygen index (LOI) test, UL 94 vertical burning test and cone calorimetry. The results show that the presence of all the FR additive mixtures increased the LOI values of the composites but did not significantly improved the UL 94 test ratings, which remained at the V2 level. The increase in the wt% ratio of halloysite nanotubes in the FR mixture delayed the time to ignition, decreased the heat release rate and increased the char residue. These results confirm the existence of FR synergism between MPP and halloysite nanotubes in PA6.

Horrocks et al. [16] produced PA6/FR composite multifilament yarns by using 2 wt% organically modified montmorillonite nanoclay (NC), Cloisite 25A (Southern Clay Products Inc., USA), together with two types of FR formulations: the vapour phase active micro-sized particles of AlPi, Exolit OP935 (Clariant, Switzerland), at 10 wt%; and the condensed-phase intumescent active mixture of AS (Sigma-Aldrich, UK) and dipentaerythritol (DP) (Fisher Scientific, UK) at 2.5 wt% and 1 wt%, respectively. All the yarns had acceptable tensile properties and were knitted into knit fabrics. This paper is the first to report the burning and extinguishing behaviour of the knit fabrics using the vertical flame spread test. Since not all fabrics burned the entire length, the respective burn lengths, the time to burn that length (or extinguishment time), the rate of flame spread and the average number of molten drops were recorded for each fabric. The results

showed that the presence of NC with AlPi in the PA6 composite fabric sample impaired the flame retardant activity of AlPi, which resulted in increases in the total burning time and the burn length compared to fabric samples with only AlPi. The PA6/AlPi/NC fabric sample did not show any tendency to self-extinguish. In contrast, the presence of NC with the AS/DP mixture in the PA6 composite fabric further decreased the self-extinction time from 31 s to approximately 23 s and the burn length compared to that of the AS/DP mixture, which confirmed the compatibility of the FR additives. However, the authors addressed the water solubility of ammonium sulphamate as a possible limitation regarding the wash durability of these fibres.

Šehić et al. [27] investigated the influence of two FR mixtures consisting of MeCy, Mastertek (Campine, Belgium) and AlPi, Exolit OP931 (Clariant, Switzerland), MeCy and sodium aluminosilicate (SASi), and Zeolite ZP–4A TSR (Silkem, Slovenia) at different weight ratios on the flammability, thermal behaviour and mechanical properties of PA6 composite yarns produced by melt-spinning. The results of the UL-94 vertical burning test indicate that, within the V2 rating, the incorporation of the MeCy+SASi mixture significantly decreased the after-flame time of the PA6/FR yarns relative to pristine PA6, indicating an improvement of the flame retardant properties. The MeCy+SASi mixture also enhanced the thermo-oxidative stability of the PA6/FR yarns compared to when MeCy was the only component, suggesting that the additive has a slightly synergistic effect with the 8 wt% MeCy and 2 wt% SASi mixture. In contrast, the performance of the MeCy+AlPi mixture was antagonistic, irrespective to their concentrations. The tensile properties of the studied PA6/FR composite filament yarns were not significantly deteriorated, and these yarns could be appropriate for knitting into the knit fabrics. There results confirmed the Horrocks's observations that silica-based FR additives improved the FR action of condensed-phase active FR additives but not the gas-phase active aluminium dialkylphosphinate.

3.2 In situ polymerization of ε-caprolactam in the presence of FR additives

There is little research that reports on the in situ polymerisation of ε-caprolactam in the presence of FR additives [20, 21, 23, 24, 26, 72, 73]. However, the in situ polymerisation of ε-caprolactam in the presence of additives is advantageous over the melt-compounding method as it enables the production of PA6 nanocomposites with nanodispersed additives [33–38]. According to our knowledge, Alfonso et al. [74] were the first to report results regarding the in situ polymerisation of ε-caprolactam in the presence of FR additives. They found that, contrary to MeCy and APP, which strongly inhibit polymerisation, red P and magnesium oxide do not have an adverse effect on kinetics or thermodynamics and enhance fire performance by the thorough distribution of the additives. According to the preparation method introduced by Wu et al. [21], Li et al. [26] synthesised melamine/adipic acid salt and cyanuric acid/hexane diamine salt and used them in the in situ polymerisation of ε-caprolactam. The obtained results for the bulk nanocomposite confirmed the formation of uniformly dispersed MeCy nanoparticles in the PA6 matrix [21]. This nanocomposite showed superior flame retardancy and significantly less deterioration of the mechanical properties compared to the composite prepared by the common melt-compounding of PA6 with commercial MeCy. The PA6/MeCy composites were pelleted and melt spun into the FR composite filament yarns [26]. Unfortunately, the flame retardant performance of the knitted fabrics was discussed only qualitatively.

3.3 Synthesis of PA6 copolymers with the incorporation of FR reactive comonomers

In recent years, a new approach for the preparation of FR PA6 fibres has been developed based on the introduction of 9,10-dihydro-9-oxa-10-phosphaphenanthrene-10-oxide DOPO-based reactive co-monomers during the melt polycondensation of ε-caprolactam [75, 76]. This approach was inspired by the synthesis procedure of a DOPO-containing co-polyester [77–79], which was commercialised as the DOPO-based FR reactive additive, Ukanol ES, and a co-polyester, Ukanol ES-CoPET (Schill+Seilacher GmbH, Germany). Accordingly, DOPO was first reacted with itaconic acid to prepare a phosphorus-containing di-acid, 9,10-dihydro-10-[2,3-di(hydroxycarbonyl)propyl]- 10-phosphaphenanthrene-10-oxide (DDP) (Figure 3). In the second step, DDP was reacted with a diamine to form a salt containing an amidogen and a carboxyl group at each end. The salt was then mixed

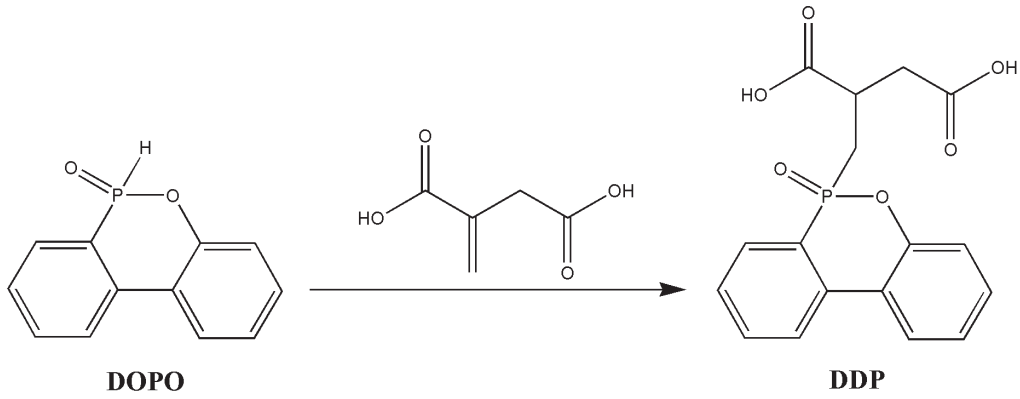

Figure 3: Preparation of DDP

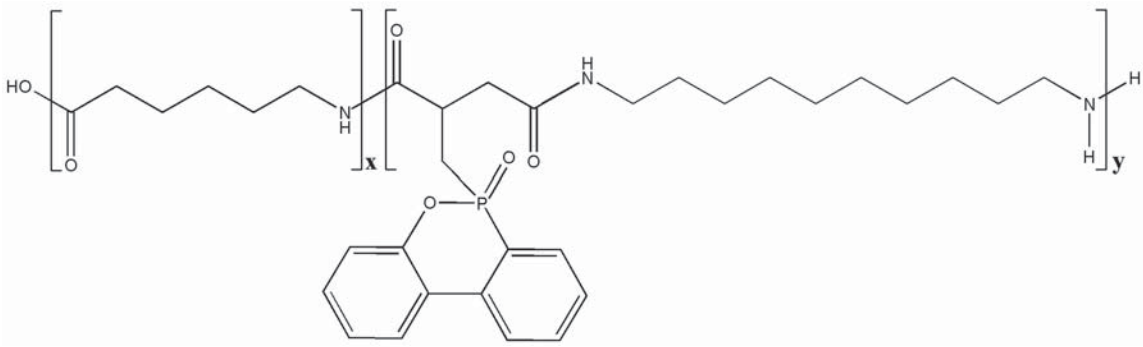

Figure 4: Chemical structure of PA6/DDP copolymer

with ε-caprolactam, and the polymerisation process was carried out under the appropriate conditions. The synthesised FR PA6 includes polyamide chain segments and DOPO-based FR chain segments of different weight ratios (Figure 4).

According to this procedure, Liu et al. [76] prepared the PA6/DDP composites containing 2 wt% to 5 wt% DDP, and their thermal stability and flame retardancy were determined by thermogravimetry, the UL 94 test and cone calorimetry. To study the mechanical properties as well as flame retardancy using the vertical burning test, filament fibres and knit fabric samples were prepared. The results show that the introduction of DDP decreased the initial temperature of the composite decomposition and simultaneously increased its thermal oxidative stability. The presence of 5 wt% DDP decreased the total heat release during combustion and significantly increased the LOI value in comparison with pristine PA6. The results of the vertical burning test show that the after-flame time of the knit fabric samples decreased when the concentration of DDP increased and that 5 wt% DDP was enough to preserve the self-extinguishment of the melt drops and reach the LOI value of 28.4 for the fabric. The incorporation of DDP decreased the tenacity at break of the fibres, but it still met the requirements of textiles.

4 Conclusion

Since halogenated FR additives have been prohibited due to health and environmental concerns, phosphorus (P) and nitrogen (N) based FRs, inorganic hydroxides as well as nanoparticles have been established for PA6. Among them, AlPi, MeCy, AS and DOPO derivatives alone or in combination with nanoclays have been mainly used. FR additives were incorporated into the polymer matrix by mixing FR additives with PA6 pellets in the process of the preparation of melt-compounded PA6/FR composites prior to the melt-spinning of PA6 composite fibres or by introducing FR additives during the polymerisation of ε-caprolactam. Whereas the *in situ* polymerisation was characterised for the MeCy incorporation, the

reactive DOPO derivatives were included as comonomers in the synthesis of PA6 copolymers. The latter approach is the most promising and will therefore provide important research challenges in the future. It represents a powerful tool for highlighting the flame retardant mechanisms of the nanodispersed FRs in the PA6 matrix and how these mechanisms function in the open high surface structure textile materials. This knowledge will provide the missing blocks to the current state of the art. Development of the flame retardant PA6 nanocomposite also provides very important solution for the lowering FR additive loadings in the bulk polymers, which will increase their sustainability.

Acknowledgement

This work was supported by the Slovenian Research Agency, Slovenia (Program P2-0213, Program P2-0393 and I0-0026 Infrastructural Centre RIC UL NTF).

References

1. RICHARDS, A.F. Nylon fibres. In *Synthetic fibres: nylon, polyester, acrylic, polyolefin*. Edited by J. E. McIntyre. Cambridge : Woodhead Publishing, 2005, pp. 20–94.
2. Market research report: Polyamide market by application (engineering plastics, fiber), type (PA 6, PA 66, bio-based & specialty polyamides), and region (Asia-Pacific, North America, Europe, Middle East & Africa, South America) - Global forecast to 2021 [online] [accessed 19. 06. 2018]. Available on World Wide Web: <https://www.giiresearch.com/report/mama270202-polyamide-market-by-type-polyamide-6-polyamide-6-6.html>.
3. Circular economy: Implementation of the circular economy action plan [online] [accessed 19. 06. 2018]. Available on World Wide Web: <http://ec.europa.eu/environment/circular-economy/index_en.htm>.
4. WEIL, E. D., LEVCHIK S. V. *Flame retardants for plastics and textiles: Practical applications* (Second edition), Munich : Hanser, 2016.
5. LEVCHIK, S. V., LEVCHIK, G. F., BALABANOVICH, A. I., CAMINO, G., COSTA, L. Mechanistic study of combustion performance and thermal decomposition behaviour of nylon 6 with added halogen-free fire retardants. *Polymer Degradation and Stability*, 1996, **54**(2–3), 217–222, doi: 10.1016/S0141-3910(96)00046-8.
6. HORROCKS, A. R., KANDOLA, B. K., DAVIES, P. J., ZHANG, S., PADBURY, S. A. Developments in flame retardant textiles – a review. *Polymer Degradation and Stability*, 2005, **88**(1), 3–12, doi: 10.1016/j.polymdegradstab.2003.10.024.
7. HORROCKS, A. R. Technical fibres for heat and flame protection. In *Handbook of technical textiles: Technical textile applications*. Edited by A. R. Horrocks, S. C. Anand, Cambridge : Woodhead Publishing, 2016.
8. *Update on flame retardant textiles: State of the art, environmental issues and innovative solutions*. Edited by Alongi, J., Horrocks, A. R., Carosio, F., Malucelli, G. Shawbury : Smithers Rapra Technology, 2013.
9. LEVCHIK, S. V., WEIL, E. D., LEWIN, M. Thermal decomposition of aliphatic nylons. *Polymer International*, 1999, **48**, 532–557; doi: 10.1002/(SICI)1097-0126(199907)48:7<532::AID-PI214>3.0.CO;2-R.
10. *Fire retardant materials*. Edited by A. R. Horrocks, D. Price. Cambridge : Woodhead Publishing, 2001.
11. LEVCHIK, Sergei V., WEIL, Edward D. A review of recent progress in phosphorus-based flame retardants. *Journal of Fire Sciences*, 2006, **24**, 345–364, doi: 10.1177/0734904106068426.
12. van der VEEN, Ike, de BOER, Jacob. Phosphorus flame retardants: Properties, production, environmental occurrence, toxicity and analysis. *Chemosphere*, 2012, **88**(10), 1119–1153, doi: 10.1016/j.chemosphere.2012.03.067.
13. BUCZKO, A., STELZIG, T., BOMMER, L., RENTSCH, D., HENECZKOWSKI, M., GAAN, S. Bridged DOPO derivatives as flame retardants for PA6. *Polymer Degradation and Stability*, 2014, **107**, 158–165, doi: 10.1016/j.polymdegradstab.2014.05.017.
14. DAHIYA, J. B., KANDOLA, B. K., SITPALAN, A., HORROCKS, A. R. Effects of nanoparticles on the flame retardancy of the ammonium sulphamate-dipentaerythritol flame-retardant system in polyamide 6. *Polymers for Advanced Technologies*, 2013, **24**(4), 398–406, doi: 10.1002/pat.3095.
15. COQUELLE, M., DUQUESNE, S., CASETTA, M., SUN, J., ZHANG, S., BOURBIGOT, S. Investigation of decomposition pathway of polyamide

6/ammonium sulfamate fibers. *Polymer Degradation and Stability*, 2014, **106**, 150–157, doi: 10.1016/j.polymdegradstab.2014.02.007.

16. HORROCKS, R., SITPALAN, A., ZHOU, C., KANDOLA, B. K. Flame retardant polyamide fibres: The challenge of minimising flame retardant additive content with added nanoclays. *Polymers*, 2016, **8**(8), 288, doi: 10.3390/polym 8080288.
17. XIANG, Hengxue, LI, Lili, CHEN, Wei, YU, Senlong, SUN, Bin, ZHU, Meifang. Flame retardancy of polyamide 6 hybrid fibers: Combined effects of α-zirconium phosphate and ammonium sulfamate. *Progress in Natural Science: Materials International*, 2017, **27**(3), 369–373, doi: 10.1016/j.pnsc.2017.04.013.
18. GIJSMAN, P., STEENBAKKERS, R., FURST, C., KERSJES, J. Differences in the flame retardant mechanism of melamine cyanurate in polyamide 6 and polyamide 66. *Polymer Degradation and Stability*, 2002, **78**(2), 219–224, doi: 10.1016/S0141-3910(02)00136-2.
19. CHEN, Y., WANG, Q., YAN, W., TANG, H. Preparation of flame retardant polyamide 6 composite with melamine cyanurate nanoparticles in situ formed in extrusion process. *Polymer Degradation and Stability*, 2006, **91**(11), 2632–2643, doi: 10.1016/j.polymdegradstab.2006.05.002.
20. WU, Z.-Y., XU, W., XIA, J. K., LIU, Y.-C., WU, Q.-X., XU, W.-J. Flame retardant polyamide 6 by in situ polymerisation of ε-caprolactam in the presence of melamine derivatives. *Chinese Chemical Letters*, 2008, **19**(2), 241–244, doi: 10.1016/j.cclet.2007.12.012.
21. WU, Z. Y., XU, W., LIU, Y. C., XIA, J. K., WU, Q. X., XU, W. J. Preparation and characterisation of flame-retardant melamine cyanurate/polyamide 6 nanocomposites by *in situ* polymerisation. *Journal of Applied Polymer Science*, 2009, **113**(4), 2109–2116, doi: 10.1002/app.30022.
22. ISBASAR, C., HACALOGLU, J. Investigation of thermal degradation characteristics of polyamide-6 containing melamine or melamine cyanurate via direct pyrolysis mass spectrometry. *Journal of Analytical and Applied Pyrolysis*, 2012, **98**, 221–230, doi: 10.1016/j.jaap.2012.09.002.
23. MU, Jun Qian, YANG, Yi, PENG, Zhi Han. Preparation and characterization of a novel flame retarded mca-pa6 resin by *in situ* polymerization. *Advanced Materials Research*, 2012, **399-401**, 444-448, doi: 10.4028/www.scientific.net/AMR.399-401.444.
24. SHA, K., HU, Y. L., WANG, Y. H., XIAO, R. Preparation and flame retardant polyamide 6/melamine cyanurate via *in situ* polymerisation and its characterisation. *Materials Research Innovations*, 2014, **18**, S4-843–S4-847, doi: 10.1179/1432891714Z.000000000804.
25. TANG, S., QIAN, L., QIU, Y., SUN, N. The effect of morphology on the flame-retardant behaviors of melamine cyanurate in PA6 composites. *Journal of Applied Polymer Science*, 2014, **131**(15), 40558, doi: 10.1002/app.40558.
26. LI, Y., LIN, Y., SHA, K., XIAO, R. Preparation and characterisation of flame retardant melamine cyanurate/polyamide 6 composite fibres via *in situ* polymerisation. *Textile Research Journal*, 2017, **87**(5), 561–569, doi: 10.1177/0040517516632478.
27. ŠEHIĆ, Alisa, VASILJEVIĆ, Jelena, JORDANOV, Igor, DEMŠAR, Andrej, MEDVED, Jožef, JERMAN, Ivan, ČOLOVIĆ, Marija, HEWITT, Fiona, HULL, T. Richard, SIMONČIČ, Barbara. Influence of N-, P- and Si-based flame retardant mixtures on flammability, thermal behavior and mechanical properties of PA6 composite fibers. *Fibres and Polymers*, 2018, Accepted Article doi: 10.1007/s12221-000-0000-0.
28. HORROCKS, A. R., KANDOLA, B., MILNES, G. J., SITPALAN, A., HADIMANI, R. L. The potential for ultrasound to improve nanoparticle dispersion and increase flame resistance in fibre-forming polymers. *Polymer Degradation and Stability*, 2012, **97**(12), 2511–2523, doi: 10.1016/j.polymdegradstab.2012.07.003.
29. BRAUN, U., BAHR, H., SCHARTEL, B. Fire retardancy effect of aluminium phosphinate and melamine polyphosphate in glass fibre reinforced polyamide 6. *e-Polymers*, 2010, **10**(1), 443–456, doi: 10.1515/epoly.2010.10.1.443.
30. SAMYN, F., BOURBIGOT, S. Protection mechanism of a flame retarded PA6 nanocomposite, *Journal of Fire Sciences*, 2013, **32**(3), 241–256, doi: 10.1177/0734904113510685.
31. SAMYN, F., BOURBIGOT, S. Thermal decomposition of flame retarded formulations PA6/aluminium phosphinate/melamine polyphosphate/organomodified clay: Interactions between the constituents? *Polymer Degradation and Stability*, 2012, **97**(11), 2217–2230, doi: 10.1016/j.polymdegradstab.2012.08.004.

32. SUN, J., GU, X., ZHANG, S., COQUELLE, M., BOURBIGOT, S., DUQUESNE, S., CASETTA, M. Effects of melamine polyphosphate and halloysite nanotubes on the flammability and thermal behaviour of polyamide 6. *Polymers for Advanced Technologies*, 2014, **25**(12), 1552–1559, doi: 10.1002/pat.3400.
33. BUTNARU, Irina, FERNÁNDEZ-RONCO, María P., CZECH-POLAK, Justyna, HENECZKOWSKI, Maciej, BRUMA, Maria, GAAN, Sabyasachi. Effect of meltable triazine-dopo additive on rheological, mechanical, and flammability properties of PA6. *Polymers*, 2015, **7**(8), 1541–1563, doi: 10.3390/polym7081469.
34. WIRASAPUTRA, Alvianto, ZHENG, Lijun, LIU, Shumei, YUAN, Yanchao, ZHAO, Jianqing. High-performance flame-retarded polyamide-6 composite fabricated by chain extension. *Macromolecular materials and Engineering*, 2016, **301**(5), 614–624, doi: 10.1002/mame.201500357.
35. CAI, Jianan, WIRASAPUTRA, Alvianto, ZHU, Yaming, LIU, Shumei, ZHOU, Yubin, ZHANG, Chunhua, ZHAO, Jianqing. The flame retardancy and rheological properties of PA6/MCA modified by DOPO-based chain extender. *RSC Advances*, 2017, **7**, 19593–19603, doi: 10.1039/C6RA28293H.
36. SUN, J., GU, X., ZHANG, S., COQUELLE, M., BOURBIGOT, S., DUQUESNE, S., CASETTA, M. Improving the flame retardancy of polyamide 6 by incorporating hexachlorocyclotriphosphazene modified MWNT. *Polymers for Advanced Technologies*, 2014, **25**(10), 1099–1107, doi: 10.1002/pat.3358.
37. HÖHNE, Carl-Christoph, WENDEL, Rainer, KÄBISCH, Bert, ANDERS, Thorsten, HENNING, Frank, KROKE, Edwin. Hexaphenoxycyclotriphosphazene as FR for CFR anionic PA6 via T-RTM: a study of mechanical and thermal properties. *Fire and Materials*, 2017, **41**(4), 291–306, doi: 10.1002/fam.2375.
38. XU, Miao-Jun, LIU, Chuan, MA, Kun, LENG, Yang, LI, Bin. Effect of surface chemical modification for aluminum hypophosphite with hexa-(4-aldehyde-phenoxy)-cyclotriphosphazene onthe fire retardancy, water resistance, andthermal properties for polyamide 6. *Polymers Advanced Technologies*, 2017, **28**(11), 1382–1395, doi: 10.1002/pat.4015.
39. LIN, G. P., CHEN, L. I., WANG, X. L., JIAN, R. K., ZHAO, B., WANG, Y. Z. Aluminum hydroxymethylphosphinate and melamine pyrophosphate: synergistic flame retardance and smoke suppression for glass fiber reinforced polyamide 6. *Industrial & Engineering Chemistry Research*, 2013, **52**(44), 15613–15620, doi: 10.1021/ie402396x.
40. SEEFELDT, H., DUEMICHENB, E., BRAUN, U. Flame retardancy of glass fiber reinforced high temperature polyamide by use of aluminium diethylphosphinate: thermal and thermo-oxidative effects. *Polymer International*, 2013, **62**(11), 1608–1616, doi: 10.1002/pi.4497.
41. ZHAO, B., CHEN, L., LONG, J. W., CHEN, H. B., WANG, Y. Z. Alumunium hypophosphite versus alkyl-substituted phosphinate in polyamide 6: flame retardance, thermal degradation and pyrolysis behaviour. *Industrial & Engineering Chemistry Research*, 2013, **52**(8), 2875–2886, doi: 10.1021/ie303446s.
42. ZHAO, B., CHEN, L., LONG, J. W., JIAN, R. K., WANG, Y. Z. Synergistic effect between aluminum hypophosphite and alkyl-substituted phosphinate in flame-retarded polyamide 6. *Industrial & Engineering Chemistry Research*, 2013, **52**(48), 17162–17170, doi: 10.1021/ie4009056.
43. HORROCKS, A. R., SMART, G., KANDOLA, B., PRICE, D. Zinc stannate interactions with flame retardants in polyamides; Part 2: Potential synergies with non-halogen-containing flame retardants in polyamide 6 (PA6). *Polymer Degradation and Stability*, 2012, **97**(4), 645–652, doi: 10.1016/j.polymdegradstab.2012.01.004.
44. DOGAN, E. Bayramli. The flame retardant effect of aluminum phosphinate in combination with zinc borate, borophosphate, and nanoclay in polyamide-6. *Fire and Materials*, 2014, 38(1), 92–99, doi: 10.1002/fam.2165.
45. KAYNAK, Cevdet, POLAT, Osman. Influences of nanoclays on the flame retardancy of fiber-filled and unfilled polyamide-6 with and without aluminium diethylphosphinate. *Journal of Fire Sciences*, 2015, 33(2), 87–112, doi: 10.1177/0734904114555961.
46. MA, Kun, LI, Bin, XU, Miaojun. Simultaneously improving the flame retardancy and mechanical properties for polyamide 6/aluminum diethylphosphinate composites by incorporating of 1,3,5-triglycidyl isocyanurate. *Polymers*

Advanced Technologies, 2018, **29**(3), 1068–1077, doi: 10.1002/pat.4218.

47. GE, H., TANG, G., HU, W.Z., WANG, B. B., PAN, Y., SONG, L., HU, Y. Aluminum hypophosphite microencapsulated to improve its safety and application to flame retardant polyamide 6. *Journal of Hazardous Materials*, 2015, **294**, 186–194, doi: 10.1016/j.jhazmat.2015.04.002.
48. DOGAN, M., BAYRAMLI, E. Effect of boron-containing materials on the flammability and thermal degradation of polyamide 6 composites containing melamine. *Journal of Applied Polymer Science*, 2010, **118**(5), 2722–2727, doi: 10.1002/app.32637.
49. DOGAN, M., BAYRAMLI, E. Effect of boron phosphate on the mechanical, thermal and fire retardant properties of polypropylene and polyamide-6 fibers. *Fibers and Polymers*, 2013, **14**(10), 1595–1601, doi: 10.1007/s12221-013-1595-0.
50. SAHYOUN, J., BOUNOR-LEGARÉ, V., FERRY, L., SONNIER, R., Da CRUZ-BOISSON, F., MELIS, F., BONHOMMÉ, A., CASSAGNAU, P. Synthesis of a new organophosphorous alkoxysilane precursor and its effect on the thermal and fire behavior of a PA66/PA6 copolymer. *European Polymer Journal*, 2015, **66**, 352–366, doi: 10.1016/j.eurpolymj.2015.02.036.
51. LI, Maolin, ZHONG, Yuhua, WANG, Zheng, FISCHER, Andreas, RANFT, Florian, DRUMMER, Dietmar, WU, Wei. Flame retarding mechanism of Polyamide 6 with phosphorus-nitrogen flame retardant and DOPO derivatives. *Journal of Applied Polymer Science*, 2016, **133**(6), 42932 DOI: 10.1002/APP.42932.
52. NIEUWENHUYSE, P., BOUNOR-LEGARÉ, V., BARDOLLET, P. Phosphorylated silica/polyamide 6 nanocomposites synthesis by in situ sol-gel method in molten conditions: Impact on the fire-retardancy. *Polymer Degradation and Stability*, 2013, **98**(12), 2635–2644, doi: 10.1016/j.polymdegradstab.2013.09.027.
53. SI, Gaojie, LI, Duxin, YOU, Yilan, HU, Xi. Investigation of the influence of red phosphorus, expansible graphite and zinc borate on flame retardancy and wear performance of glass fiber reinforced PA6 composites. *Polymer Composites*, 2017, **38**(10), 2090–2097, doi: 10.1002/pc.23781.
54. HULL, T. R., WITKOWSKI, A., HOLLINGBERY, L. Fire retardant action of mineral fillers. *Polymer Degradation and Stability*, 2011, **96**(8), 1462–1469, doi: 10.1016/j.polymdegradstab.2011.05.006.
55. LI, Minghui, CUI, Huijuan, LI, Qunying, ZHANG, Qian. Thermally conductive and flame retardant polyamide 6 composites. *Journal of Reinforced Plastics and Composites*, 2016, **35**(5), 435–444, doi: 10.1177/0731684415618538.
56. CASETTA, M., MICHAUX, G., OHL, B., DUQUESNE, S., BOURBIGOT, S. Key role of magnesium hydroxide surface treatment in the flame retardancy of glass fiber reinforced polyamide 6. *Polymer Degradation and Stability*, 2018, **148**, 95–103, doi: 10.1016/j.polymdegradstab.2018.01.007.
57. BATISTELLA, M. A, SONNIER, R., OTAZAGHINE, B., PETTER, C. O., LOPEZ-CUESTA J.-M. Interactions between kaolinite and phosphinate-based flame retardant in Polyamide 6. *Applied Clay Science*, 2018, **157**, 248–256, doi: 10.1016/j.clay.2018.02.021.
58. DEMIR, H., ARKIS, E., BALKOSE, D., ULKU, S. Synergistic effect of natural zeolites on flame retardant additives. *Polymer Degradation and Stability*, 2005, **89**(3), 478–483, doi: 10.1016/j.polymdegradstab.2005.01.028.
59. MARNEY, D. C. O., RUSSELL, L. J., WU, D. Y., NGUYEN, T., CRAMM, D., RIGOPOULOS, N., WRIGHT, N., GREAVES, M. The suitability of halloysite nanotubes as a fire retardant for nylon 6. *Polymer Degradation and Stability*, 2008, **93**(1), 1971–1978, doi: 10.1016/j.polymdegradstab.2008.06.018.
60. LI, L., WU, Z., JIANG, S., ZHANG, S., LU, S., CHEN, W., SUN, B., ZHU, M. Effect of halloysite nanotubes on thermal and flame properties of polyamide 6/melamine cyanurate composites. *Polymer Composites*, 2015, **36**(5), 892–896, doi: 10.1002/pc.23008.
61. BOURBIGOT, S., DEVAUX, E., FLAMBARD, X., FLAMBARD, X. Flammability of polyamide-6 /clay hybrid nanocomposite textiles. *Polymer Degradation and Stability*, 2002, **75**(2), 397–402, doi: 10.1016/S0141-3910(01)00245-2.
62. ONDER, E., SARIER, N., ERSOY, M. S. The manufacturing of polyamide– and polypropylene–organoclay nanocomposite filaments and their suitability for textile applications. *Thermochimica Acta*, 2012, **543**, 37–58, doi: 10.1016/j.tca.2012.05.002.
63. SCHARTEL, B., PÖTSCHKE, P., KNOLL, U., ABDEL-GOAD, M. Fire behaviour of polyamide 6/multiwall carbon nanotube nanocomposites.

European Polymer Journal, 2005, **41**(5) 1061–1070, doi: 10.1016/j.eurpolymj.2004.11.023.

64. LI, Juan, TONG, Lifang, FANG, Zhengping, GU, Aijuan, XU, Zhongbin. Thermal degradation behavior of multi-walled carbon nanotubes/polyamide 6 composites. *Polymer Degradation and Stability*, 2006, **91**(9), 2046–2052 doi: 10.1016/j.polymdegradstab.2006.02.001.
65. SCAFFARO, R., MAIO, A., TITO, A. C. High performance PA6/CNTs nanohybrid fibers prepared in the melt. *Composites Science and Technology*, 2012, **72**(15), 1918–1923, doi: 10.1016/j.compscitech.2012.08.010.
66. KHUN, Nay Win, CHENG, Henry Kuo Feng, LI, Lin, LIU, Erjia. Thermal, mechanical and tribological properties of polyamide 6 matrix composites containing different carbon nanofillers. *Journal of Polymer Engineering*, 2015, **35**(4), 367–376, doi: 10.1515/polyeng-2013-0241.
67. VELENCOSO, Maria M., BATTIG, Alexander, MARKWART, Jens C., SCHARTEL, Bernhard, WURM, Frederik R. Molecular firefighting – how modern phosphorus chemistry can help solve the flame retardancy task. *Angewandte Chemie*, 2018, Accepted Article, doi: 10.1002/anie.201711735.
68. WEIL, E. D., LEVCHIK, S. V. Flame retardants in commercial use or development for textiles. *Journal of Fire sciences*, 2008, **26**, 243–281, doi: 10.1177/0734904108089485.
69. BOURBIGOT, Serge, DUKUESNE, Sophie. Intumescence and nanocomposites: a novel route for flame-retarding polymeric materials. In *Flame retardant polymer nanocomposites*. Edited by Alexander B. Morgan, Charles A. Wilkie. New Jersy : John Wiley & Sons, 2007, pp. 131–162.
70. GILMAN, Jefrey W. Flame retardant mechanism of polymer-clay nanocomposites. In *Flame retardant polymer nanocomposites*. Edited by Alexander B. Morgan, Charles A. Wilkie. New Jersy : John Wiley & Sons, 2007, pp. 67–87.
71. *Manufactured fibre technology*. Edited by V. B. Gupta, V. K. Kothari. Dordrecht : Springer Science & Business Media, 2012.
72. XIAO, Ru; SHA, Kai; CHEN, Xin; CHEN, Jizong, GU, Liqin, WANG, Huaping, LI, Xilin, ZHENG, Xiaoting, HUANG, Jianhua, CAO, Xiaoyu, QIAO, Jiaxin, LI, Yue, TANG, Youhao, LIN, *Huagang. MCA flame-resistant polyamide 6 fibers and preparation method thereof. CN patent, no. CN104294392 (A). 2015-01-21*.
73. LIANG, Weidong, XIAO, Ru, QIAO, Jiaxin, CHEN, Xin, CHEN, Jizong, LI, Xilin, SHA, Kai, HU, Yulong, LIU, Peng, LIU, Ke, TANG, Youhao, TAO, Lei. *Preparation method of flame-retarded polyamide 6 fiber. CN patent, no. CN104499076 (A). 2015-04-08*.
74. ALFONSO, Giovanni Carlo, COSTA, Giovanna, PASOLINI, Massimo, RUSSO, Saverio, BALLISTRERI, Alberto, MONTAUDO, Giorgio, PUGLISI, Concetto. Flame-resistant polycaproamide by anionic polymerization of ε-caprolactam in the presence of suitable flame-retardant agents. *Journal of Applied Polymer Science*, 1986, **31**(5), 1373–1382, doi: 10.1002/app.1986.070310521.
75. XIAO, Ru, LIU, Ke, LI, Yuanyuan, LI, Taotao, WANG, Huaping. *Flame-retarded polyamide 6 and preparation method thereof. CN patent, no. CN106675007 (A). 2017-05-17*.
76. LIU, Ke, LI, Yuanyuan, TAO, Lei, XIAO, Ru. Preparation and characterization of polyamide 6 fibre based on a phosphorus-containing flame retardant. *RSC Advances*, 2018, **8**, 9261–9271, doi: 10.1039/C7RA13228J.
77. SEIJI, Endo, TAKAO, Kashihara, AKITADA, Osako, TATSUHIKO, Shizuki, TADASHI, Ikegami. *Neue phosphor-enthaltende verbindungen. DE patent, no. DE2646218 (A1). 1977-04-28*.
78. CHANG, Shinn-Jen, CHANG, Feng-Chih. Characterizations for blends of phosphorus-containing copolyester with poly(ethylene terephthalate). *Polymer Engineering and Science*, 1998, **38**(9), 1471–1481, doi: 10.1002/pen.10318.
79. CHEN, Hong-Bing, ZHANG, Yi, CHEN, Li, SHAO, Zhu-Bao, LIU, Ya, WANG, Yu-Zhong. novel inherently flame-retardant poly(trimethylene terephthalate) copolyester with the phosphorus-containing linking pendent group. *Industrial & Engineering Chemistry Research*, 2010, **49**(15), 7052–7059, doi: 10.1021/ie1006917.

SHORT INSTRUCTIONS FOR AUTHORS OF SCIENTIFIC ARTICLES

Scientific articles categories:

- **Original scientific article** is the first publication of original research results in such a form that the research can be repeated and conclusions verified. Scientific information must be demonstrated in such a way that the results are obtained with the same accuracy or within the limits of experimental errors as stated by the author, and that the accuracy of analyses the results are based on can be verified. An original scientific article is designed according to the IMRAD scheme (Introduction, Methods, Results and Discussion) for experimental research or in a descriptive way for descriptive scientific fields, where observations are given in a simple chronological order.
- **Review article** presents an overview of most recent works in a specific field with the purpose of summarizing, analysing, evaluating or synthesizing information that has already been published. This type of article brings new syntheses, new ideas and theories, and even new scientific examples. No scheme is prescribed for review article.
- **Short scientific article** is original scientific article where some elements of the IMRAD scheme have been omitted. It is a short report about finished original scientific work or work which is still in progress. Letters to the editor of scientific journals and short scientific notes are included in this category as well.

Language: The manuscript of submitted articles should be written in UK English and it is the authors responsibility to ensure the quality of the language.

Manuscript length: The manuscript should not exceed 30,000 characters without spacing.

Article submission: The texts should be submitted only in their electronic form in the format *.doc (or *docx) and in the format *.pdf (made in the computer program Adobe Acrobat) to the address: tekstilec@a.ntf.uni-lj.si. The name of the document should contain the date (year-month-day) and the surname of the corresponding author, e.g. 20140125Novak.docx. The articles proposed for a review need to have their figures and tables included in the text. The article can also be submitted through a cloud-based file transfer service, e.g. "WeTransfer" (www.wetransfer.com).

Publication requirements: All submitted articles are professionally, terminologically and editorially reviewed in accordance with the general professional and journalistic standards of the journal Tekstilec. Articles are reviewed by one or more reviewers and are accepted for publication on the basis of a positive review. If reviewers are not unanimous, the editorial board decides on further proceedings. The authors can propose to the editorial board the names of reviewers, whereas the editorial board then accepts or rejects the proposal. The reviewers' comments are sent to authors for them to complete and correct their manuscripts. The author is held fully responsible for the content of their work. Before the author sends their work for publication, they need to settle the issue on the content publication in line with the rules of the business or institution, respectively, they work at. When submitting the article, the authors have to fill in and sign the Copyright Statement (www.tekstilec.si), and send a copy to the editors by e-mail. They should keep the original for their own personal reference. The author commits themselves in the Copyright Statement that the manuscript they are submitting for publication in Tekstilec was not sent to any other journal for publication. When the work is going to be published depends on whether the manuscript meets the publication requirements and on the time reference the author is going to return the required changes or corrections to the editors.

Copyright corrections: The editors are going to send computer printouts for proofreading and correcting. It is the author's responsibility to proofread the article and send corrections as soon as possible. However, no greater changes or amendments to the text are allowed at this point.

Colour print: Colour print is performed only when this is necessary from the viewpoint of information comprehension, and upon agreement with the author and the editorial board.

More information on: www.tekstilec.si

POSODABLJAMO PRIHODNOST

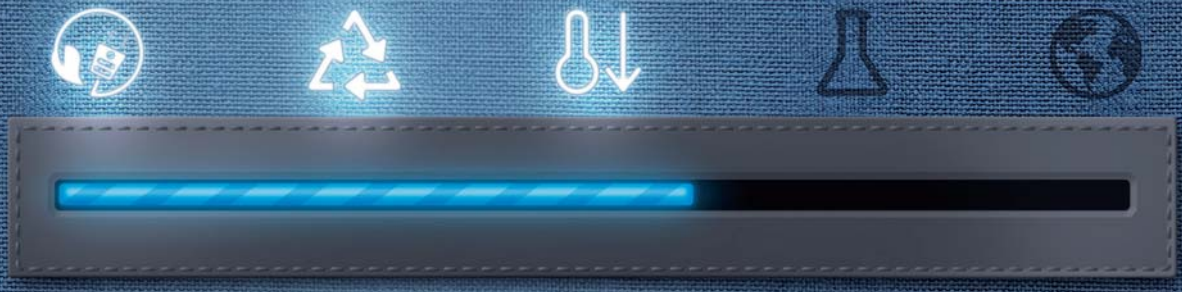

MANJ JE VEČ

NIZEK VPLIV • VISOKA PRODUKTIVNOST •
INOVATIVNE TEHNOLOGIJE ZA PRALNICE PRIHODNOSTI

EXPOdetergo INTERNATIONAL

18. mednarodna razstava opreme, storitev,izdelkov in dodatkov za pranje, likanje in čiščenje tkanin in podobnih izdelkov

FIERA MILANO | 19.-22. OKTOBER 2018.

**Ne zamudite priložnosti.
Rezervirajte svojo vstopnico na
www.expodetergo.com**

EXPO Detergo
T. +39 02 3931.4120 • F. +39 02 3931.5160
expo@expodetergo.com

Fiera Milano
T. +39 02 4997.6053 - 6241 • F. +39 02 4997.6252
expodetergo@fieramilano.it

FIERA MILANO